THEORY OF OPTICAL HANLE EFFECT IN ATOMIC BEAMS AND IN CAVITIES UNDER ARBITRARY PUMPING CONDITIONS

A Thesis
submitted to the
UNIVERSITY OF HYDERABAD
for the Degree of
DOCTOR OF PHILOSOPHY

By

P. ANANTHA LAKSHMI

School of Physics
UNIVERSITY OF HYDERABAD
HYDERABAD, INDIA

August, 1983

This is to state that I, P. ANANTHA LAKSHMI have carried out the research embodied in the present thesis for the full period prescribed under Ph.D. Ordinances of the University under the supervision of Professor G.S. Agarwal.

I declare to the best of my knowledge that no part of this thesis was earlier submitted for the award of research degree of any University.

P. Anantha Lakshmi

AUGUST 1983 (P. ANANTHA LAKSHMI)

G S Agarwal 6.8.83

(Signature of the Supervisor)

D E A N
School of Physic
University of Hyder
Hyderabad - 500 1

ACKNOWLEDGMENTS

I am deeply indebted to my Supervisor, Professor G.S. Agarwal for his guidance and constant encouragement during my research. His patience and understanding have gone a long way in helping me complete this thesis.

I am grateful to Professor A.K. Bhatnagar, Dean, School of Physics for making the facilities of the school available to me. I would also like to thank Dr. S. Chaturvedi and Dr. Ragini Saxena.

My sincere thanks go to Mr. P. Chandra Prakash Reddy for painstakingly typing the manuscript of this thesis.

Finally, I wish to thank the Council of Scientific and Industrial Research for the award of a research fellowship during the tenure of which this work was carried out.

P. Anantha Lakshmi

P. ANANTHA LAKSHMI

TO MY PARENTS

ABSTRACT

This thesis is devoted to the development of the quantum theory of optical Hanle effect. Various questions regarding the intensities, fluorescence spectra, cooperative behaviour of atoms, squeezing properties of the states of the scattered radiation field, excited state coherences under different conditions of excitation are analyzed in great detail.

Chapter I introduces the problem with its previous history and outlines the need and relevance of the present analysis.

Chapter II contains a general formulation of the problem for obtaining the density matrix equations, the fluorescence intensities and expressions for the fluorescence spectra, in terms of the atomic density matrix elements and atomic correlation functions.

In chapter III, a quantum statistical theory of optical Hanle effect for arbitrary intensities and bandwidth of the pump laser field is developed. The excited and ground-state level shifts caused by another light field with appropriate polarization are taken into account by using Bogoliubov-Mitropolsky's method of time averaging. The laser fluctuations are

treated exactly by adopting the phase-diffusion model of the pump laser. The analytical and numerical results for the fluorescence signals are presented for a variety of excitations. A comparison with recent works of Kaftandjian, Klein and Hanle is made. The case of a very broadband excitation under saturation conditions is analyzed and the results for signals in different directions and for different polarizations are obtained. For completeness, the effect of laser bandwidth on the magnetic field Hanle signals is also examined.

In chapter IV, the studies of chapter III are extended to investigate the spectral features of the signals in the optical Hanle system, with respect to the various directions of observation and the polarization of the emitted and the exciting radiation. The asymmetries in the spectra are found to be critically dependent on each of these parameters.

In chapter V, the cooperative behaviour of atoms has been examined to study the possible existence of multistable behaviour in the optical Hanle geometry. The collective behaviour of atoms contained in a cavity which can have two modes of excitation with different polarizations under the pumping by a linearly polarized electric field is studied. The transmission characte-

ristics for such a situation are obtained. In the special case when the intensities of both the cavity field modes are identical, the system is found to exhibit bistable behaviour.

In chapter VI, the quantum statistical properties of the states of radiation scattered by an atomic system under resonant excitation is investigated. In particular, the squeezing properties of the radiation field are investigated. Analytical expression for the second factorial moment of the photon counting distribution, which is a measure of the squeezing of the states is obtained. It is found that squeezing of the scattered radiation field states, i.e., negative value of the quantity $S(T) \equiv \langle n^{[2]} \rangle - \langle n \rangle^2$, persists for very short intervals of the counting time in most cases.

Finally, in chapter VII, the creation of coherence among excited states, not connected by a dipole transition, is discussed. Analytical results are presented which show how a complete coherence could result by using strong fields. The role of the coherence associated with pump laser in creating the excited state coherence is investigated in detail.

CONTENTS

CHAPTER I

INTRODUCTION

From the beginning of this century, experiments using resonance radiation and resonance fluorescence[1-5] have been largely responsible for our increasing understanding of excited atoms and their interaction with radiation. In the 1920's the polarization of resonance fluorescence from atoms subjected to external magnetic fields[2,6] and subsequently to external electric fields was studied in detail by Hanle[6] and used to measure the

radiative atomic lifetimes. The physical basis of such phenomena is found in the splitting of the m-state degeneracy by an externally applied field. More recently Brossel and Kastler[5] pointed out that polarized resonance radiation could be used to produce and detect differences in populations of the Zeeman substates of both ground and excited levels of atoms. Following these suggestions, the techniques of magnetic resonance were widely applied to the study of bulk samples of free atoms. These experiments enabled detailed information about the Zeeman and hyperfine structure of excited and ground states of atoms to be obtained, together with measurements of radiative lifetimes and interatomic collisional relaxation rates[1-15]. The techniques of magnetic depolarization of resonance fluorescence known as the Hanle effect, magnetic optical double resonance and optical pumping of metastable and ground state atoms cover an important area in the field of atomic physics. Thus, in the usual Hanle effect, the properties of the magnetic sublevels are studied by preparing the system in a coherent superposition of the Zeeman sublevels and by observing the fluorescence from such a coherent superposition as a function of the magnetic field. The coherent superposition[11,16,17] can be obtained either by using a broadband source or a monochromatic pump. With broadband excitation and magnetic field scanning, the Hanle effect has

been extensively studied and applied to lifetimes and radiative relaxation rate measurements for atomic and molecular species[18-25]. The use of laser sources for the coherent excitation of the Zeeman sublevels has recently led to the observation of strongly modified level crossing curves. The modifications are related to the high power density (nonlinear effects) and the monochromaticity of the laser light. It was found that the linewidth of the observed signal is critically dependent on the nature of the exciting source [11,16] viz., its strength, detuning, bandwidth etc.

Several variations[18-25] of the Hanle effect have been proposed and used in the high resolution spectroscopic work. For instance, it was shown that the modulated pump field leads to fluorescence variation that immediately yields not only the relaxation parameters but also the excited state splittings[18-22]. A novel variation[23,24] of the Hanle experiment, namely, the electric analog of the magnetic Hanle effect, involves the use of a suitably polarized electric field to lift the degeneracy of the excited states i.e., each energy level is shifted by a different amount due to Stark shifts[26-28]. The technique of lifting the degeneracy of the excited states by means of the ac Stark effect,

produced by a strong off-resonant laser beam[23-25] (whose intensity and detuning can be varied) is known as the optical Hanle effect. It is to be noted that the strong off-resonant laser field with appropriate polarization is applied in addition to the pump field, which pumps the atoms to the excited states. The intensity of the fluorescence signal is now observed as a function of the intensity or frequency of the powerful off-resonant laser beam. For the case when this second laser was circularly polarized, it was found by Kaftandjian et al.[23] that the zero-field level crossings occur in the same manner as in the magnetic field Hanle effect. Further experimental investigations of the optical Hanle effect have been performed by Kaftandjian et al.[29,30] with a barium atomic beam resonantly excited by a weak linearly polarized laser beam both for monochromatic as well as broadband cases. They have observed absorption and dispersion - shaped level crossing resonances, both for monochromatic and broadband excitations, by varying the power of the strong nonresonant laser beam which induces the Stark splitting.

This thesis is devoted to the development of a general theory of optical Hanle effect and to a study of the various aspects of this effect. In chapter II, we present a general formulation for the fluorescence

signals, fluorescence spectra of the optical Hanle effect which will be used in subsequent chapters to study special cases depending on the geometry of the system and the nature of transitions.

In chapter III, a quantum statistical theory[31-35] of the optical Hanle effect, which is valid for arbitrary intensities and bandwidths of the pump field, is developed. The excited and ground state level-shifts which are caused by the off-resonant laser field with appropriate polarization are directly included in the theory by the method of time averaging[36-37]. The laser fluctuations are treated exactly by using the phase diffusion model for the pump laser[38,39]. The analytical and numerical results for the fluorescence intensities are presented for a wide variety of geometrical arrangements. The results obtained here in the limiting case are in agreement with those of Kaftandjian, Klein and Hanle[23,24,29,30]. An exact analysis for the case of a very broadband excitation under saturation conditions is also given and the results for signals in various directions and for different polarizations are obtained. The results obtained here are in agreement with the experimental observations of optical Hanle signals in monochromatic and broadband fields reported by Delsart et al.[25,29,30]. The experiments of Delsart et al. have been done under the condi-

tion when saturation effects are not important.

The fluorescence spectra emitted by a multilevel atomic system have been studied in literature ~~both~~ for monochromatic as well as broadband excitations[41-52]. Recently Kornblith and Eberly[46] have studied the spectral dependence on the direction of observation for the magnetic field Hanle situation. Since, in the optical Hanle effect, there is a considerable selectivity of the Zeeman sublevels depending upon the polarization of the nonresonant electric field, it is worthwhile to carry out a detailed analysis, both experimentally and theoretically of the fluorescence signals produced in such a case.

In chapter IV, numerical results for the fluorescence spectra for a variety of excitations both for the weak field as well as the strong field case are presented. For the strong field case, the spectra are found to exhibit a seven-peaked structure. We have also presented analytical expressions for the fluorescence spectra, in the presence of collisions, to second order in the field strengths. The asymmetries of the spectra are found to be strongly dependent on the system parameters such as relaxation rates, field strengths etc.

In view of the growing interest in the study of the cooperative behaviour of atoms which resulted in new and interesting phenomena such as optical multistability[53-68] etc., one would like to understand the behaviour of the optical Hanle system contained in a cavity. Therefore, in chapter V, the behaviour of a collection of atoms contained in a cavity which can have two modes of excitation with different polarizations under pumping by a linearly polarized electric field is studied. The transmission characteristics of the cavity field for such a situation are obtained. In the special case when the intensities of both the cavity modes are identical, the system is found to exhibit bistable behaviour.

Having obtained detailed information on different aspects of the atomic system, we now investigate the properties of the states of the radiation field scattered by such a system.[69-78] Information on the states of the scattered radiation field can be obtained by studying the higher order correlation functions of the scattered electric field, in addition to the usual second order correlation functions. This can experimentally be accomplished by the photon counting measurements[75]. The Photon counting techniques enable one to obtain informa-

tion on such properties of the states of the scattered radiation field, such as squeezing[69,70,75]. Squeezed coherent states have recently become important in the study of quantum limits on a measurement process[73]. Recently, Mandel[75] has shown that the quantity $S(T) \equiv \langle n^{[2]} \rangle - \langle n \rangle^2$ related to the second factorial moment $\langle n^{[2]} \rangle$ of the photon counting distribution for a superposition of the external coherent radiation and the radiation scattered by a two level atom exhibits squeezing of the scattered radiation. Therefore, for the purpose of observing squeezing in the scattered radiation, one has to mix external coherent radiation with the radiation scattered by the atom and study the photon statistics of this mixed radiation. In chapter VI, the properties of the photon counting distribution for arbitrary counting intervals, produced by a mixture of an external coherent radiation and the radiation scattered by an atomic system are investigated. Such properties reflect in an important way on the squeezing characteristics[69,70,75] and the anomalous correlators[74] of the scattered radiation.

Excited state coherence was seen to be very significant in the determination of signals in various directions and therefore one has to find out the conditions under which maximum possible coherence can be achieved. This

question is also very important in connection with the quantum beats[79-86] which arise solely due to a nonzero coherence in the excited states. Therefore, in chapter VII, we study how the excitation of atoms and molecules by intense laser fields could lead to strong coherence between the excited states. The calculations are done for a three level system consisting of two excited states $|1\rangle$ and $|2\rangle$ which are not connected through a dipole transition but are connected to the ground state $|3\rangle$ by dipole transitions. This is the most common three level scheme used in the description of quantum beats[79-86] and Hanle experiments[16]. The transition amplitudes corresponding to the dipole transitions between the pairs of levels $|1\rangle$, $|3\rangle$ and $|2\rangle$, $|3\rangle$ interfere to produce beats provided that there is a nonzero coherence between the excited states initially. We found that the coherence between the two excited states is very strong when both the exciting fields are of the same order.

CHAPTER II

THE OPTICAL HANLE EFFECT - GENERAL FORMULATION

In this chapter we develop a quantum statistical theory of optical Hanle effect and study different aspects of the optical Hanle effect such as the intensities of the fluorescent light and the fluorescence spectra emitted by the atomic system in various directions for different geometries of the system. The atomic sample is contained in a cell and interacts with a circularly polarized nonresonant electric field which induces the ac Stark

shift and lifts the degeneracy of the excited states. At low pressures and small atomic densities, the interaction of the atoms amongst themselves may be neglected so that, in effect, one needs to consider the interaction of a single, isolated atom with the external laser fields. An intense, plane polarized laser beam (which we will hereafter refer to as pump) leads to the atomic transitions between the non-degenerate ground state and the sublevels of the excited states. The atomic system interacts with the vacuum of the radiation field and emits radiation spontaneously. Here, a general formulation for the fluorescence radiation emitted by the multilevel atomic system interacting with strong laser fields is given and special cases are studied in subsequent chapters depending upon the geometry of the experiment and the nature of the transitions. The total Hamiltonian for the atomic system interacting with the radiation fields is given and the equations of motion for the reduced density operator for the atomic system are presented. A relationship between the fluorescence intensity and the atomic density matrix elements is developed.

2.1 The Hamiltonian

The total Hamiltonian for the atom and the radiation field in the presence of an external field is

$$H = H_A + H_R + H_c(t) + H_{AR} + H_{ext}(t) \qquad (2.1.1)$$

where $H_A(H_R)$ is the unperturbed Hamiltonian for the atom (vacuum of the radiation field), $H_c(t)$ is the interaction Hamiltonian describing the interaction of the atom and the circularly polarized electric field and H_{AR} ($H_{ext}(t)$) is the interaction Hamiltonian describing the interaction between the atom and the vacuum of the radiation field (external laser field).

If the energy of the eigen state $|m\rangle$ is denoted by E_m and the atomic operator by a subscripted A, then we have

$$H_A = \sum_m E_m A_{mm} ,$$
$$A_{mn} = |m\rangle \langle n| . \qquad (2.1.2)$$

The unperturbed Hamiltonian of the quantized radiation field is given by

$$H_R = \sum_{ks} \omega_{ks} a^+_{ks} a_{ks} , \hbar = 1 \qquad (2.1.3)$$

where the following mode expansion is used for the quantized electric field,

$$\vec{E}_R(r) = i \sum_{ks} \left(\frac{2\pi ck}{L^3} \right)^{1/2} a_{ks} \hat{\epsilon}_{ks} e^{i\vec{k}.\vec{r}} + H.c. \qquad (2.1.4)$$

Here L^3 is the volume in which the field is quantized and $\hat{\epsilon}_{ks}$ is the polarization vector and a^+_{ks} and a_{ks} are the

creation and annihilation operators respectively. The interaction Hamiltonian in the electric dipole approximation is given by

$$H_{AR}[H_{ext}(t)] = - \vec{d}.\vec{E}_R(\vec{E}(t)) \text{ and } H_c(t) = - \vec{d}.\vec{E}_c(t) \quad (2.1.5)$$

Here $\vec{d}$ is the dipole moment operator of the atom having only off-diagonal elements

$$\vec{d} = \sum_{i,j} \vec{d}_{ij} A_{ij} + H.c. \qquad \vec{d}_{ij} = 0 \text{ if } i = j \quad (2.1.6)$$

and $\vec{E}$ is the plane-polarized pump field at the point r where the atom is located and $\vec{E}_c(t)$ is the circularly polarized off-resonant electric field. The classical expression for the plane polarized electric (pump) field $\vec{E}(t)$ may be written as

$$\vec{E}(t) = \frac{1}{2} \sum_j \vec{\mathcal{E}}_{oj}(t) \exp [-i(\Omega_j t + \Phi_j(t))] + c.c. \quad (2.1.7)$$

where $\vec{\mathcal{E}}_{oj}(t)$ is the amplitude of the j^{th} component oscillating at the mean frequency Ω_j and $\Phi_j(t)$ is the phase of the j^{th} component. $\vec{\mathcal{E}}_{oj}(t)$ and $\Phi_j(t)$ are assumed to be slowly varying functions of time. For a strictly monochromatic field $\vec{\mathcal{E}}_{oj}(t)$ and $\Phi_j(t)$ are independent of time t and are not random variables whereas for a fluctuating electric field, $\vec{\mathcal{E}}_{oj}(t)$ and $\Phi_j(t)$ are stochastic functions.

The circularly polarized electric field $\vec{E}_c(t)$ is written in the form

$$\vec{E}_c(t) = \vec{\mathcal{E}}_c e^{-i\omega_c t} + \vec{\mathcal{E}}_c^* e^{i\omega_c t} . \qquad (2.1.8)$$

This circularly polarized off-resonant electric field lifts the degeneracy of the excited states and also shifts the ground state. This plays the role of magnetic field used in usual magnetic field Hanle type of experiments with the difference that the magnetic field does not shift the non-degenerate ground state. It is well known that when a two level atom is subjected to an off-resonant light field, its ground and excited states will be shifted by equal amounts in opposite directions[26], the magnitude of this light shift being equal to β^2/Δ_c where β is the Rabi frequency of the transition and Δ_c is the frequency detuning between the atom and the off-resonant electric field. Depending upon the polarization characteristics of the circularly polarized electric field, only particular sublevels of the atomic system will be shifted. As an example, consider a J=0 to J=1 transition. The level $|+\rangle$ (corresponding to the magnetic quantum number + 1) and the ground state $|g\rangle$ will be shifted by equal amounts in opposite directions were the light to be left circularly polarized and the levels $|-\rangle$ (corresponding to the magnetic quantum number - 1) and $|g\rangle$ will be shifted in opposite directions if the polarization is right handed.

2.2 The equations of motion for the atomic system

Here our interest is focussed on the study of the properties of the atomic system in which case, the degrees of freedom corresponding to spontaneous emission and other relaxation processes have to be suppressed. As a first step, consider the case when no external fields are present i.e., $H_{ext}(t)$ $(H_c(t)) = 0$. Let $\sigma_{A+R}(t)$ be the density operator describing the combined statistical state of the atom and the radiation field or in other words a general reservoir which takes into account all other relaxation mechanisms. It satisfies the Schrödinger equation of motion

$$\dot{\sigma}_{A+R}(t) = -i[H, \sigma_{A+R}(t)] = \mathcal{L}\, \sigma_{A+R}(t) \qquad (2.2.1)$$

where $\mathcal{L}$ is the Liouville operator defined by

$$\mathcal{L} \ldots = -i[H, \ldots] \quad . \qquad (2.2.2)$$

Let $\sigma_A(t)$ be the reduced density operator describing the atomic system alone. The density operators $\sigma_A(t)$ and $\sigma_{A+R}(t)$ are related by

$$\sigma_A(t) = Tr_R\, \sigma_{A+R}(t) \quad . \qquad (2.2.3)$$

Tr_R denotes the trace over the radiation field variables and all the relaxation processes. The master equation for

the reduced density operator $\sigma_A(t)$ in the Born-Markov and rotating wave approximations[32-34] is given by

$$\frac{\partial}{\partial t}\,\sigma_{ij} = -i\,\omega_{ij}\,\sigma_{ij} + \delta_{ij} \sum_{k\neq i} 2\gamma_{ik}\,\sigma_{kk} - \Big(\sum_{k\neq i}\gamma_{ki} + \sum_{k\neq j}\gamma_{kj}\Big)\,\sigma_{ij} \qquad (2.2.4)$$

where ω_{ij} is the renormalized transition frequency between the atomic levels $|i\rangle$ and $|j\rangle$ and $2\gamma_{ik}$ is the transition probability per unit time that the atom will make a transition from $|k\rangle$ to $|i\rangle$ in the absence of any external field, due to spontaneous, collisional and all other relaxation processes. For the case when the relaxation mechanism is due to spontaneous emission only, then $2\gamma_{ik}$ is equal to the Einstein A coefficient of the system and is given by

$$\gamma_{ik} = 2/3\,|d_{lk}|^2\,\frac{\omega_{ki}^3}{c^3} \quad \text{if } E_k > E_i$$

$$= 0 \quad \text{if } E_k < E_i\ . \qquad (2.2.5)$$

Equation (2.2.4) may be rewritten as

$$\frac{\partial\sigma}{\partial t} = -i[H_A,\sigma] + \mathcal{L}_{inc}\,\sigma \qquad (2.2.6)$$

where $\mathcal{L}_{inc}$ represents the contribution from all the incoherent terms arising due to spontaneous emission, collisions etc. For a more general case, in the presence of external fields, this equation is modified as

$$\frac{\partial \sigma}{\partial t} = -i[H_A + H_c(t) + H_{ext}(t) , \sigma] + \mathcal{L}_{inc}\, \sigma \qquad (2.2.7)$$

which means that the effect of incoherent interactions and external fields can be superimposed. Now, the fast time dependence from $\sigma(t)$ is removed and the slowly varying quantities $\tilde{\sigma}(t)$ are obtained (where tilde denotes a quantity in rotating frame rotating with the frequency of the pump field) and the terms oscillating at twice the optical frequency are neglected. The equation of motion for $\tilde{\sigma}(t)$ is

$$\frac{\partial \tilde{\sigma}}{\partial t} = \mathcal{L}_{inc}\, \tilde{\sigma} - i[H', \tilde{\sigma}] \qquad (2.2.8)$$

where H' is the sum of the unperturbed part of the atomic Hamiltonian and the interaction Hamiltonian describing the interaction of the atom with the pump field and the circularly polarized laser field.

It could be seen from the following chapters that the equation for the evolution of the density matrix elements as obtained from equation (2.2.8) for an atomic system with discrete number of energy levels interacting with external radiation fields will form a set of coupled linear differential equations with constant coefficients. In matrix notation they can be represented as

$$\frac{\partial \psi(t)}{\partial t} = M\, \psi\, (t) + I \qquad (2.2.9)$$

where $\psi(t)$ is a column matrix with elements $\tilde{\sigma}_{ij}(t)$ $i,j = 1,--,N$. N is the number of relevant energy levels of the atomic system under consideration and I also is a column matrix. The order of $\psi(t)$ and I is (N^2-1) since we use the normalization condition that $\sum_i \sigma_{ii} = 1$ to eliminate the ground state energy density matrix element. This is performed to avoid the difficulty that would arise in computing the solutions by the Laplace transformation techniques were the matrix M to possess a zero eigenvalue. M is a square matrix of the same rank as ψ and is time independent due to RWA. The structure of the matrix M depends on the nature of atomic/molecular transitions ; hence the eigenvalues of M will give information about the complex transition frequencies of the system.

2.3 Solution of the master equation

Consider equation (2.2.9)

$$\frac{\partial}{\partial t}\psi(t) = M\psi + I \qquad (2.3.1)$$

On taking the Laplace transform of this equation, one obtains

$$\hat{\psi}(z) = (z-M)^{-1}\psi(o) + z^{-1}(z-M)^{-1} I \qquad (2.3.2)$$

where $\hat{\psi}(z)$ represents the Laplace transform of $\psi(t)$ given by

$$\hat{\psi}(z) = \int_0^\infty e^{-zt}\, \psi(t)\, dt, \quad \text{Re}\ \ z > 0 \ . \qquad (2.3.3)$$

The steady state solution of (2.3.2) is obtained as

$$\psi(\infty) = \lim_{z \to 0} z\, \hat{\psi}(z) = (-M)^{-1}\, I \qquad (2.3.4)$$

i.e. by evaluating the matrix elements of M^{-1}, one can obtain the density matrix elements.

2.4 Intensities of the Fluorescence Signals and the Fluorescence Spectra

In this section, expressions for the intensities of the fluorescence signals and the fluorescence spectra emitted in different directions with different polarizations are obtained in terms of the atomic density matrix elements. Let $\vec{E}^{+}(r,t)$ be the positive frequency part of the radiation field emitted by the atom. In the radiation zone, the field can be expressed as[76]

$$\vec{E}^{+}(r,t) = \vec{E}_o^{+}(r,t) - \sum_{kl}{}' (\omega_{kl}^2/rc^2)\ (\hat{r}x(\hat{r}x\vec{d}_{kl}))$$

$$A_{lk}(t-r/c)\ e^{-i\omega_{lk}(t-r/c)} \qquad (2.4.1)$$

where $\vec{E}_o^{+}(r,t)$ is the free field part and the remaining terms relate the far-field zone behaviour of the radiation emitted with the properties of the atomic system under study. The prime on the summation sign indicates that the summation on the energy levels is only for those terms for

which $\omega_{kl} > 0$ and the transition $|k\rangle \longrightarrow |l\rangle$ is a radiative decay. The expression for the total intensity of the scattered radiation I is equal to the normally ordered correlation function $\langle \vec{E}^{-}(r,t) \cdot \vec{E}^{+}(r,t) \rangle$ and is given by

$$I = \sum_{klm} \frac{\omega_{kl}^2 \, \omega_{ml}^2}{r^2 \, c^4} (\hat{r}x(\hat{r}x\vec{d}_{ml}^{*})) \cdot (\hat{r}x(\hat{r}x\vec{d}_{kl})) \langle A_{mk}(t) \rangle \quad (2.4.2)$$

where the orthogonalisation condition that $\langle A_{mn}(t) A_{lk}(t) \rangle = \langle A_{mk}(t) \rangle \delta_{n,l}$ has been used. $\langle A_{mk}(t) \rangle$'s can be obtained from the solution of the master equation as $\langle A_{mk}(t) \rangle = \sigma_{km}(t)$. Since the intensity of the fluorescence signal is detected at times much larger than the natural lifetimes or the decay constants in the problem, the relevant density matrix elements σ_{km}'s have to be evaluated in the steady state limit.

Expression for the fluorescence spectrum :

The spectrum of the fluorescence radiation is defined in terms of the first-order normally ordered two-time correlation function $\langle \vec{E}_{\alpha}^{-}(r,t_2) \cdot \vec{E}_{\beta}^{+}(r,t_1) \rangle$ which we denote as $G_{\alpha\beta}^{(1)}(r,t_2;r,t_1)$. This is given by

$$G_{\alpha\beta}^{(1)}(r,t_2;r,t_1) = \sum_{klmn}' \frac{\omega_{kl}^2 \, \omega_{mn}^2}{r^2 \, c^4} [\hat{r}x(\hat{r}x\vec{d}_{mn}^{*})]_{\alpha} \cdot$$

$$[\hat{r}x(\hat{r}x\vec{d}_{kl})]_{\beta} \langle A_{mn}(t_2) \, A_{lk}(t_1) \rangle \quad (2.4.3)$$

neglecting the retardation effects, the time r/c is omitted in comparison with the other times which are much larger. The free field term does not contribute in (2.4.3) because the radiation field is initially in the vacuum state. The two-time correlation functions $\langle A_{mn}(t_2)\, A_{lk}(t_1)\rangle$ can be evaluated in terms of the single-time expectation values using quantum regression theorem[35]. The regression theorem states that if $\langle A_{ij}(t_2)\rangle$ is a member (or a linear combination) of a complete set of system Markovian operators, then the time evolution of such an operator can be written in the form

$$\langle A_{ij}(t_2)\rangle = \sum_{\alpha\beta} f_{ij\alpha\beta}(t_2, t_1)\, \langle A_{\alpha\beta}(t_1)\rangle, \quad t_2 > t_1 \qquad (2.4.4)$$

where $f_{ij\alpha\beta}(t_2,t_1)$ are numerical coefficients and $A_{\alpha\beta}(t_1)$ form a complete set of operators. For the two-time stationary correlation functions

$$\langle A_{ij}(t_2)\, A_{kl}(t_1)\rangle = \sum_{\alpha\beta} f_{ij\alpha\beta}(t_2-t_1)\, \langle A_{\alpha\beta}(t_1)\, A_{kl}(t_1)\rangle \qquad (2.4.5)$$

where the one-time mean values appearing in (2.4.5) can be obtained from the solution of the master equation.

We will be interested in cases when the atomic system is in equilibrium with the driving field, i.e., the atomic system is in steady state, so that the atomic correlation

function $G^{(1)}_{\alpha\beta}$ depends only on (t_2-t_1). Therefore, the spectrum in steady state[47], i.e., in the limit as $t \longrightarrow \infty$, is given by

$$S(\omega) = \sum_{\alpha} \int_{-\infty}^{\infty} d\omega \; e^{-i\omega(t_2-t_1)} \; G^{(1)}_{\alpha\alpha}(t_2-t_1)$$

$$= 2 \,\text{Real} \int_{0}^{\infty} d\omega \; e^{-i\omega(t_2-t_1)} \left(\sum_{\alpha} G^{(1)}_{\alpha\alpha}(t_2-t_1)\right) \qquad (2.4.6)$$

which is nothing but the Laplace transform of the function $G^{(1)}_{\alpha\alpha}$ namely

$$S(\omega) = \sum_{\alpha} 2 \,\text{Real} \; G^{(1)}_{\alpha\alpha}(z) \Big|_{z = i\omega} \qquad (2.4.7)$$

The expressions for spectra in special cases depending on the geometry of the transitions can then be obtained from the above.

CHAPTER III

OPTICAL HANLE EFFECT - TOTAL INTENSITY OF FLUORESCENT LIGHT

In this chapter, a general theory to study the fluorescence intensities for the case of optical Hanle effect is developed which is valid for arbitrary values of the strength and bandwidth of the pump field. For simplicity, we consider the case when the levels involved in the Hanle transitions correspond to the levels with a

total angular momentum J=0 and J=1 respectively. In section 3.1 the bandwidth effects[38] of the pump field are taken into account in the equations of motion of the density matrix and it is also shown how the off-resonant laser field leads to light shift terms[26] in the equations of motion. These equations are solved and expressions for the fluorescence signals are obtained in section 3.2. A numerical study of the fluorescence signals is carried out in section 3.3. The variations in the signals with change in the strength and bandwidth of the exciting laser are studied. For the sake of completeness the effect of laser bandwidth on the magnetic field Hanle effect is also discussed. In section 3.3 a rigorous treatment of the optical Hanle effect in intense broadband fields is carried out.

3.1 Density matrix formulation of optical Hanle effect

In this section, we obtain the most general equations valid for arbitrary values of the field strengths and bandwidths. For simplicity and in view of the recent experimental work[25,29,30] on optical Hanle effect, we restrict our considerations to the case when the two levels involved in the transition possess angular momenta 0 and 1 respectively. A schematic diagram of the energy levels is shown in Figure 1a.

The geometry used for studying the fluorescence signals for optical Hanle effect is shown in Fig. 2. The physical situation here, corresponds to a circularly polarized light propagating along the z axis intersecting the atomic beam directed along the x axis. A second linearly polarized laser beam (pump field) propagating along the z axis with its electric vector making an angle θ with the x direction, interacts with the atomic beam. The linearly polarized (pump) light creates the atomic coherences, i.e., it prepares the atomic system in a coherent superposition of the excited states. These atomic coherences are monitored by observing the fluorescence signals in different directions. Two common situations used for observing the fluorescence correspond to the detection of radiation in the directions (i) x with polarization along the y axis, (ii) y with its polarization along the x axis. The circularly polarized off-resonant radiation lifts the degeneracy of the excited states and also shifts the ground state[26]. As was already mentioned in chapter II, the magnitude of the light shift is β^2/Δ_c, where β is the Rabi frequency of the transition and Δ_c is the frequency detuning of the atom and the light field. For our system, using a left-circularly polarized electric field, we expect the levels $|+\rangle$ (corresponding to the magnetic quantum number +1) and $|g\rangle$ to be shifted. The positions of the shifted levels are shown in Fig.1a.

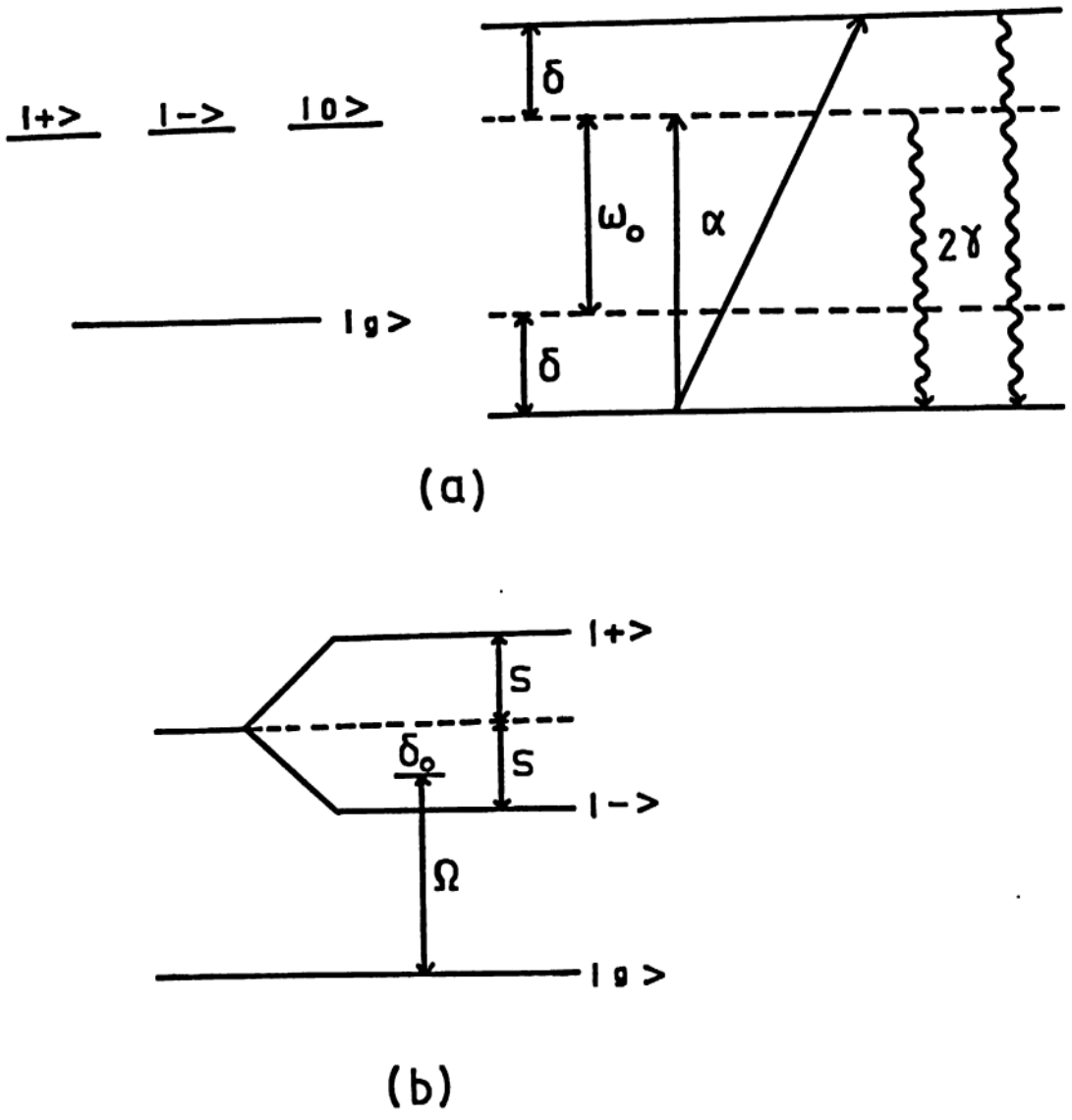

Fig.1 Schematic representation of the energy levels involved in (a) Optical Hanle effect, (b) Magnetic field Hanle effect

The total Hamiltonian for the system interacting with the pump field $\vec{E}(t)$ and the circularly polarized field $\vec{E}_c(t)$ can be written as [cf. Sec.2.1]

$$H = \hbar\omega_o(A_{++} + A_{--}) - [\vec{d}_{+g}.\vec{E}(t)A_{+g}+\vec{d}_{-g}.\vec{E}(t)A_{-g}+H.c.]$$

$$- [\vec{d}_{+g}.\ \vec{E}_c(t)\ A_{+g} + H.c.]\ , \qquad (3.1.1)$$

where the atomic operators A_{ij}'s and the dipole moment matrix elements $\vec{d}_{ij}$'s are defined earlier in Section 2.1, and $\omega_o = (E_+ - E_g)/\hbar$. The pump field is written in the form

$$\vec{E}(t) = \mathcal{E}_o(t)\ (\hat{x}\cos\theta + \hat{y}\sin\theta)\ e^{-i\Omega t - i\phi(t)} + c.c.$$

$$= \vec{\mathcal{E}}(t)\ e^{-i\Omega t} + c.c. \qquad (3.1.2)$$

where, as shown in Fig. 2, the angle θ gives the direction of polarization of the pump. The functions $\mathcal{E}_o(t)$ and $\phi(t)$ are taken to be slowly varying functions of time. The frequency of the pump is either at resonance or close to resonance with the frequency of the J=0 to J=1 transition. The terms in the last brackets in (3.1.1) represent the interaction of the system with the circularly polarized radiation given by (2.1.8).

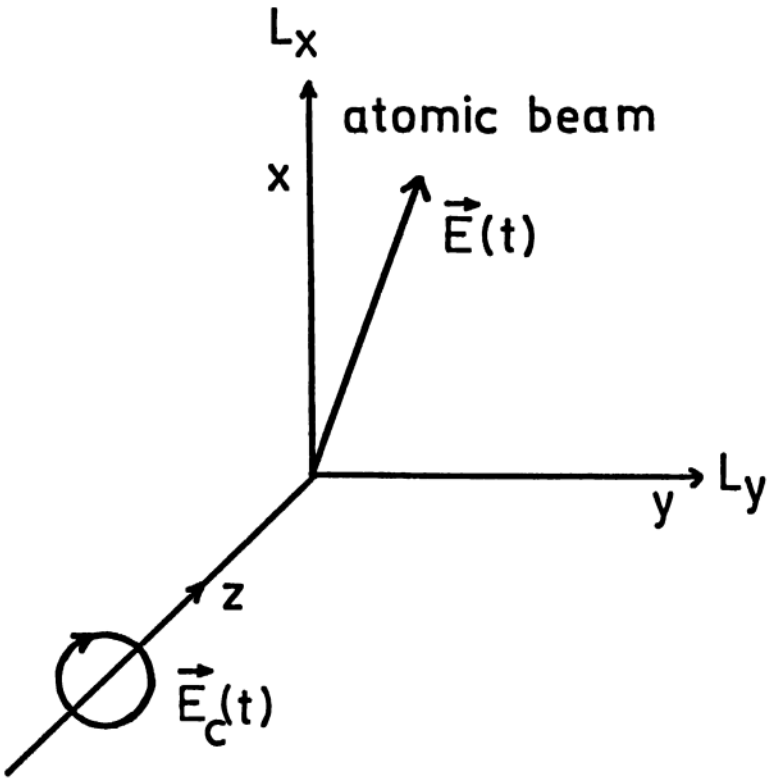

FIG. 2

Schematic diagram showing the directions and polarizations of the various beams for the optical Hanle geometry

The density matrix σ of the system satisfies the equation (2.2.7). On transforming this to a frame rotating with the angular frequency of the pump field Ω and on making rotating wave approximation, (2.2.7) reduces to the following

$$\frac{\partial\tilde{\sigma}}{\partial t} = \frac{-i}{\hbar} [\tilde{H}(t), \tilde{\sigma}] + \mathcal{L}_{inc}\tilde{\sigma} - i [G A_{+g} e^{i(\Omega-\omega_c)t} + G^* A_{g+} e^{-i(\Omega-\omega_c)t}, \tilde{\sigma}] \quad (3.1.3)$$

where all the slow time dependence is contained in $\tilde{H}(t)$ and the fast time dependence in the $\tilde{\sigma}$ equation is explicitly displayed. $\tilde{H}(t)$ and G are given by

$$\tilde{H}(t) = [-\vec{d}_{+g} \cdot \vec{\mathcal{E}}(t) A_{+g} - \vec{d}_{-g} \cdot \vec{\mathcal{E}}(t) A_{-g} + H.c.] + \hbar(\omega_o - \Omega)(A_{++} + A_{--}) , \quad (3.1.4)$$

$$G = (\vec{d}_{+g} \cdot \vec{\mathcal{E}}_c)/\hbar . \quad (3.1.5)$$

The matrix elements of $\tilde{\sigma}$ are related to σ by

$$\tilde{\sigma}_{ij}(t) = \delta_{ij}\, \sigma_{ij}(t) + (1-\delta_{ij})\, \sigma_{ij}(t)\, e^{i\omega_{ij}t} ,$$

$$\omega_{+g} = \omega_{-g} = \Omega , \quad \omega_{+-} = 0 . \quad (3.1.6)$$

As a first step in calculation, it will be shown how the rapidly oscillating terms in (3.1.3) lead to light shifts. For this purpose, we use Bogoliubov - Mitropolsky's method of time averaging. This method when applied to the density matrix equation[36,37]

$$\frac{\partial \sigma}{\partial t} = \mathcal{L}_o \sigma + \mathcal{L}_1(t)\ \sigma \qquad (3.1.7)$$

shows that the effect of rapidly oscillating terms in $\mathcal{L}_1(t)$ in leading order could be taken into account by replacing (3.1.7) by

$$\frac{\partial \sigma}{\partial t} = \mathcal{L}_o \sigma + \mathcal{L}_1(t) \int^t \mathcal{L}_1(\tau)\ \sigma(t)\ d\tau \ . \qquad (3.1.8)$$

On using (3.1.8), we find that (3.1.3) reduces to

$$\frac{\partial \tilde{\sigma}}{\partial t} = \frac{-i}{\hbar} [H'(t), \tilde{\sigma}] + \mathcal{L}_{inc}\ \tilde{\sigma}$$

where

$$H'(t) = -[\vec{d}_{+g} \cdot \vec{\mathcal{E}}(t) A_{+g} + \vec{d}_{-g} \cdot \vec{\mathcal{E}}(t) A_{-g} + H.c.]$$

$$+\hbar(\omega_o - \Omega + \delta) A_{++} + \hbar(\omega_o - \Omega) A_{--} - \hbar\delta\, A_{gg} \ , \qquad (3.1.9)$$

where

$$\delta = |G|^2 / (\Omega - \omega_c) \ . \qquad (3.1.10)$$

The effective Hamiltonian (3.1.9) now explicitly has light shift terms $(A_{++} - A_{gg})$.

We next eliminate the explicit Θ dependence and the phase dependence from the Hamiltonian by making use of the relations among the dipole moment matrix elements

$$\vec{d}_{+g} = R(-\hat{x} + i\hat{y}) , \quad \vec{d}_{-g} = R(\hat{x} + i\hat{y}) \qquad (3.1.11)$$

and by making the transformations

$$\bar{\sigma}_{ii} = \tilde{\sigma}_{ii} , \ \bar{\sigma}_{+-} = -\tilde{\sigma}_{+-} e^{2i\Theta}$$

$$\bar{\sigma}_{+g} = -\tilde{\sigma}_{+g} \exp i[\Theta + \Phi(t) + \Omega t] ,$$

$$\bar{\sigma}_{-g} = \tilde{\sigma}_{-g} \exp i[\Phi(t) - \Theta + \Omega t] . \qquad (3.1.12)$$

We further assume that the relaxation is only due to the radiative decay from the level $|\pm\rangle$ to the ground level $|g\rangle$ at the rate 2γ and include no other relaxations. In such a case, the density matrix elements $\bar{\sigma}_{ij}$ satisfy the following set of coupled differential equations.

$$\dot{\bar{\sigma}}_{++} = i\alpha \bar{\sigma}_{g+} - i\alpha^* \bar{\sigma}_{+g} - 2\gamma \bar{\sigma}_{++} ,$$

$$\dot{\bar{\sigma}}_{--} = i\alpha \bar{\sigma}_{g-} - i\alpha^* \bar{\sigma}_{-g} - 2\gamma \bar{\sigma}_{--} ,$$

$$\dot{\bar{\sigma}}_{gg} = -i\alpha(\bar{\sigma}_{g+}+\bar{\sigma}_{g-}) + i\alpha^*(\bar{\sigma}_{+g}+\bar{\sigma}_{-g})+2\gamma(\bar{\sigma}_{++}+\bar{\sigma}_{--}) ,$$

$$\dot{\bar{\sigma}}_{+-} = -(2\gamma+i\delta) \bar{\sigma}_{+-}+i\alpha \bar{\sigma}_{g-} - i\alpha^* \bar{\sigma}_{+g} ,$$

$$\dot{\bar{\sigma}}_{+g} = -[2i\delta+\gamma+i\mu(t)] \bar{\sigma}_{+g}+i\alpha(\bar{\sigma}_{gg}-\bar{\sigma}_{++}-\bar{\sigma}_{+-})$$

$$\dot{\bar{\sigma}}_{-g} = -[i\delta+\gamma+i\mu(t)] \bar{\sigma}_{-g}+i\alpha(\bar{\sigma}_{gg}-\bar{\sigma}_{--}-\bar{\sigma}_{-+}) , \qquad (3.1.13)$$

where

$$\dot{\phi}(t) = \mu(t) \text{ and } \alpha = R\, \mathcal{E}_o(t) \,. \qquad (3.1.14)$$

The above set of equations could be solved if $\mu(t)$ and $\mathcal{E}_o(t)$ were constants, as in the case of a monochromatic pump. For a fluctuating pump, the nature of the pump requires to be specified, i.e., we have to specify the stochastic processes $\mu(t)$ and $\mathcal{E}_o(t)$. The model, for which exact solutions could be obtained, corresponds to (i) $\mathcal{E}_o(t)$ being a time-independent constant, and (ii) $\mu(t)$ being a Gaussian delta correlated process, i.e.,

$$\langle \mu(t)\, \mu(t') \rangle = 2\gamma_c\, \delta(t-t') \,, \langle \mu(t) \rangle = 0 \,. \qquad (3.1.15)$$

This is the well known phase-diffusion model of the laser light in which the amplitude remains constant. In this model, the amplitude correlations are given by

$$\langle \mathcal{E}^*(t)\, \mathcal{E}(t') \rangle = \exp\{-\gamma_c |t-t'|\} \,, \langle \mathcal{E}(t)\, \mathcal{E}(t') \rangle = 0 \qquad (3.1.16)$$

i.e. the spectrum is Lorentzian. Higher order correlations of the field have more complicated structure though these can be evaluated in a closed form[39]. The above equation (3.1.15) has the form of the standard equation of the multiplicative stochastic processes discussed in detail by Agarwal[38]. The equations of motion for the

ensemble-averaged values of $\bar{\sigma}_{ij}$ over the distribution of $\mu(t)$, which we will be denoting as $\psi_{ij} = \langle\bar{\sigma}_{ij}\rangle$, are obtained as

$$\begin{aligned}
\dot{\psi}_{++} &= i\alpha\,(\psi_{g+} - \psi_{+g}) - 2\gamma\,\psi_{++}\,, \\
\dot{\psi}_{--} &= i\alpha\,(\psi_{g-} - \psi_{-g}) - 2\gamma\,\psi_{--}\,, \\
\dot{\psi}_{gg} &= i\alpha\,(\psi_{+g} + \psi_{-g} - \psi_{g+} - \psi_{g-}) + 2\gamma\,(\psi_{++} + \psi_{--})\,, \\
\dot{\psi}_{+-} &= i\alpha\,(\psi_{g-} - \psi_{+g}) - (2\gamma + i\delta)\,\psi_{+-}\,, \qquad (3.1.17) \\
\dot{\psi}_{+g} &= i\alpha\,(\psi_{gg} - \psi_{++} - \psi_{+-}) - (2i\delta + \gamma + \gamma_c)\,\psi_{+g}\,, \\
\dot{\psi}_{-g} &= i\alpha(\psi_{gg} - \psi_{--} - \psi_{-+}) - (i\delta + \gamma + \gamma_c)\,\psi_{-g}\,.
\end{aligned}$$

The above equations no longer involve any explicit time dependence and could be solved in a straight forward manner. The solutions of these equations can then be used to obtain the fluorescence signals detected in different directions. The fluorescence signals detected along y and x directions, denoted respectively by L_y and L_x, with polarizations along x and y, respectively, can be obtained [cf. ref.16] from eq. (2.4.2) as will be shown below. The nonvanishing terms under the summation sign in eq. (2.4.2) are obtained as

$$I = \frac{\omega_{+g}^4}{r^2 c^4} [\hat{r}x(\hat{r}x\vec{d}^*_{+g})].[\hat{r}x(\hat{r}x\vec{d}_{+g})] \; < A_{++}(t) >$$

$$+ \frac{\omega_{-g}^4}{r^2 c^4} [\hat{r}x(\hat{r}x\vec{d}^*_{-g})].[\hat{r}x(\hat{r}x\vec{d}_{-g})] \; <A_{--}(t)>$$

$$+ \frac{\omega_{+g}^2 \omega_{-g}^2}{r^2 c^4} [\hat{r}x(\hat{r}x\vec{d}^*_{+g})].[\hat{r}x(\hat{r}x\vec{d}_{-g})] <A_{+-}(t)>$$

$$+ [\hat{r}x(\hat{r}x\vec{d}^*_{-g})].[\hat{r}x(\hat{r}x\vec{d}_{+g})] \; <A_{-+}(t)> \qquad (3.1.18)$$

where the dipole matrix elements are given by eq.(3.1.11). For the direction of detection along the x axis, we have

$$\hat{r}x(\hat{r}x\vec{d}_{+g}) = -i\hat{y}R = \hat{r}x(\hat{r}x\vec{d}_{-g}) \; . \qquad (3.1.19)$$

On using (3.1.19) in (3.1.18), we can obtain an expression for L_x. From Fig. 1a, one can see that

$$\omega_{-g} = \omega_{+g} \left(1 - \frac{\delta}{\omega_{+g}}\right) . \qquad (3.1.20)$$

In our study, the maximum value assigned to the Stark splitting is of the order of 10γ, where γ is typically of the order of a few tens of MHz. Hence, $\frac{\delta}{\omega_{+g}} \sim 10^{-6}$ which is a negligibly small quantity, so that $\omega_{+g} \sim \omega_{-g}$. In view of this simplification, we can write L_x as

$$L_x \propto \sigma_{++} + \sigma_{--} + 2 \, \mathrm{Re} \, \sigma_{+-} \; . \qquad (3.1.21)$$

Similarly for the detection along y direction, we obtain

$$L_y \propto \sigma_{++} + \sigma_{--} - 2\,\mathrm{Re}\,\sigma_{+-} \,. \qquad (3.1.22)$$

ituting for the density matrix elements σ_{ij}'s in
of $\bar{\sigma}_{ij}$'s we obtain

$$\bar{\sigma}_{++} + \bar{\sigma}_{--} - 2(\mathrm{Re}\,\bar{\sigma}_{+-}\cos 2\theta + \mathrm{Im}\,\bar{\sigma}_{+-}\sin 2\theta),$$

$$\bar{\sigma}_{++} + \bar{\sigma}_{--} + 2(\mathrm{Re}\,\bar{\sigma}_{+-}\cos 2\theta + \mathrm{Im}\,\bar{\sigma}_{+-}\sin 2\theta) \qquad (3.1.23)$$

ience the ensemble averaged signals will be

$$\propto \psi_{++} + \psi_{--} - 2(\mathrm{Re}\,\psi_{+-}\cos 2\theta + \mathrm{Im}\,\psi_{+-}\sin 2\theta)$$

$$\propto \psi_{++} + \psi_{--} + 2(\mathrm{Re}\,\psi_{+-}\cos 2\theta + \mathrm{Im}\,\psi_{+-}\sin 2\theta). \qquad (3.1.24)$$

In the following section, the set of equations
.17) is solved analytically under steady state condi-
s and the analytical expressions for the fluorescence
als are obtained. The signals are studied as a func-
of the Stark shift δ for various values of the para-
rs such as field strengths and bandwidths. Hereafter,
ensemble averaged signals will be denoted by L_x and L_y,
the angular brackets omitted for simplicity.

For comparison, we discuss the effect of laser band-
h on the magnetic field Hanle signals for a nonresonant
. For the magnetic field Hanle situation when the
laser is detuned from the atomic frequency by an

$$L_y \propto \sigma_{++} + \sigma_{--} - 2\,\mathrm{Re}\,\sigma_{+-} \,. \qquad (3.1.22)$$

Substituting for the density matrix elements σ_{ij}'s in terms of $\bar{\sigma}_{ij}$'s we obtain

$$L_x \propto \bar{\sigma}_{++} + \bar{\sigma}_{--} - 2(\mathrm{Re}\,\bar{\sigma}_{+-}\cos 2\theta + \mathrm{Im}\,\bar{\sigma}_{+-}\sin 2\theta),$$

$$L_y \propto \bar{\sigma}_{++} + \bar{\sigma}_{--} + 2(\mathrm{Re}\,\bar{\sigma}_{+-}\cos 2\theta + \mathrm{Im}\,\bar{\sigma}_{+-}\sin 2\theta) \qquad (3.1.23)$$

and hence the ensemble averaged signals will be

$$\langle L_x \rangle \propto \psi_{++} + \psi_{--} - 2(\mathrm{Re}\,\psi_{+-}\cos 2\theta + \mathrm{Im}\,\psi_{+-}\sin 2\theta)$$

$$\langle L_y \rangle \propto \psi_{++} + \psi_{--} + 2(\mathrm{Re}\,\psi_{+-}\cos 2\theta + \mathrm{Im}\,\psi_{+-}\sin 2\theta). \qquad (3.1.24)$$

In the following section, the set of equations (3.1.17) is solved analytically under steady state conditions and the analytical expressions for the fluorescence signals are obtained. The signals are studied as a function of the Stark shift δ for various values of the parameters such as field strengths and bandwidths. Hereafter, the ensemble averaged signals will be denoted by L_x and L_y, with the angular brackets omitted for simplicity.

For comparison, we discuss the effect of laser bandwidth on the magnetic field Hanle signals for a nonresonant case. For the magnetic field Hanle situation when the pump laser is detuned from the atomic frequency by an

amount δ_o and the Zeeman splitting denoted by s (see Fig. 1b), one has instead of (3.1.17) the following set of equations

$$\dot{\psi}_{++} = i\alpha\,(\psi_{g+} - \psi_{+g}) - 2\gamma\,\psi_{++}\ ,$$

$$\dot{\psi}_{--} = i\alpha\,(\psi_{g-} - \psi_{-g}) - 2\gamma\,\psi_{--}\ ,$$

$$\dot{\psi}_{gg} = i\alpha\,(\psi_{+g} + \psi_{-g} - \psi_{g+} - \psi_{g-}) + 2\gamma(\psi_{++}+\psi_{--}),$$

$$\dot{\psi}_{+-} = i\alpha\,(\psi_{g-} - \psi_{+g}) - (2\gamma + 2is)\,\psi_{+-}\ , \qquad (3.1.25)$$

$$\dot{\psi}_{+g} = i\alpha\,(\psi_{gg} - \psi_{++} - \psi_{+-}) - [\gamma+\gamma_c+i(\delta_o+s)]\psi_{+g}$$

and

$$\dot{\psi}_{-g} = i\alpha\,(\psi_{gg} - \psi_{--} - \psi_{-+}) - [\gamma+\gamma_c+i(\delta_o-s)]\psi_{-g}\ .$$

The signals L_x and L_y for this case are given by

$$L_x \alpha\, \psi_{++} + \psi_{--} + 2\ \mathrm{Re}\ \psi_{+-}$$

$$L_y \alpha\, \psi_{++} + \psi_{--} - 2\ \mathrm{Re}\ \psi_{+-} \qquad (3.1.26)$$

Solving the set of equations (3.1.25) in steady state and substituting in (3.1.26), we can obtain expressions for the signals in the magnetic Hanle case. Avan and Cohen Tannoudji[16,87] have calculated such signals for the cases when (a) pump laser bandwidth $\gamma_c=0$ and for a nonzero laser detuning δ_o and (b) $\gamma_c\neq 0$ and $\delta_o=0$, separately. In our calculation we have considered a more general case when both γ_c as well as δ_o are nonzero. In the next section we present numerical results of our analytical expressions obtained from the solution of (3.1.25).

3.2 Analytical and Numerical results for the Fluorescence Signals

The fluorescence signals L_x and L_y defined in the previous section are determined by the steady-state solutions of the density matrix elements ψ_{++}, ψ_{--}, and ψ_{+-}. Under steady-state conditions, the left-hand side of the set of eq. (3.1.17) becomes zero. Therefore, these nine algebraic equations can be solved analytically. A long but straightforward calculation yields the results

$$\psi_{++}+\psi_{--}=2\alpha^2\mu[(4\gamma^2\mu^2+4\alpha^2\mu+\delta^2)(\delta^2\mu+4\gamma^2\mu+4\alpha^2)+9\delta^2(\delta^2+4\gamma^2)\mu]D^{-1} \tag{3.2.1}$$

which for $\delta \to 0$ goes over to $2\alpha^2/(4\alpha^2+\gamma^2\mu)$, which in the limit of strong and weak fields further reduces to

$$\psi_{++} + \psi_{--} = \begin{cases} \frac{1}{2} \text{ for } \alpha^2 >> \gamma^2\mu \ , \quad \delta = 0 \\ 2\alpha^2/\gamma^2\mu \text{ for } \alpha^2 << \gamma^2\mu \ , \ \delta = 0. \end{cases} \tag{3.2.2}$$

In Eq. (3.2.1), μ and D are given by

$$\mu = 1 + (\gamma_c/\gamma) \ ,$$

$$D = (\gamma^2\mu^2+4\alpha^2\mu+2\delta^2 + \frac{\delta^2\alpha^2(1-\mu)}{(4\gamma^2+\delta^2)}) \ [(4\gamma^2\mu^2+4\alpha^2\mu+\delta^2) \ x$$

$$(4\gamma^2\mu+\delta^2\mu+4\alpha^2) + 9\delta^2(\delta^2+4\gamma^2)\mu]$$

$$+ (\delta^2/2)(9\delta^2+(4\gamma^2\mu^2+4\alpha^2\mu+\delta^2) \ \frac{(4\alpha^2-4\gamma^2-\delta^2)}{(4\gamma^2+\delta^2)}) \ x$$

$$[\ 2\alpha^2(\mu-1) - \mu(4\gamma^2+\delta^2)] \ . \tag{3.2.3}$$

The atomic coherences are given by

$$\text{Re}\,\psi_{+-} = \alpha^2\mu[(\delta^2+4\gamma^2\mu^2+4\alpha^2\mu)(4\gamma^2\mu+4\alpha^2-\delta^2)+9\delta^2(\delta^2+4\gamma^2)\mu]D^{-1}, \tag{3.2.4}$$

which for $\delta \to 0$ goes over to $\alpha^2/(4\alpha^2+\gamma^2\mu)$, which in the limiting cases further reduces to

$$\text{Re}\,\psi_{+-} = \begin{cases} \frac{1}{4} \text{ for } \alpha^2 \gg \gamma^2\mu , \\ \alpha^2/\gamma^2\mu \text{ for } \alpha^2 \ll \gamma^2\mu , \end{cases} \qquad \delta = 0 . \tag{3.2.5}$$

Similarly we have the results

$$\text{Im}\,\psi_{+-} = 2\alpha^2\,\mu\delta\gamma[9\delta^2(1-\mu) - (4\gamma^2\mu^2+4\alpha^2\mu+\delta^2)(1+\mu)]D^{-1} , \tag{3.2.6}$$

$$\text{Im}\,\psi_{+-} \to 0 \text{ as } \delta \to 0 . \tag{3.2.7}$$

Now, let us examine the symmetry properties of the above expressions when we change δ to $-\delta$. We see that $(\psi_{++}+\psi_{--})$ and Re ψ_{+-} are even functions of δ, and Im ψ_{+-} is an odd function of δ. The symmetry properties of the fluorescence signals depend on the direction of polarization of the incident pump field. We note that

$$L_x(-\delta) = L_x(\delta) ,$$
$$L_y(-\delta) = L_y(\delta) , \tag{3.2.8}$$

for $\theta = 0, \pi/2$ etc., i.e., $L_x(\delta)$ and $L_y(\delta)$ are symmetric about $\delta = 0$ for these values of θ. Moreover, for $\theta = \pi/4, \frac{3}{4}\pi$ etc. we have the relations

$$L_x(\delta) = L_y(-\delta) ,$$

$$L_y(\delta) = L_x(-\delta) . \qquad (3.2.9)$$

Let us now consider some special cases under which the expressions for signals have a simplified form.

a) Monochromatic pump

Let us first examine the results for the case of narrow-band excitation, i.e., in the limit $\gamma_c \to 0$, for an arbitrary strength of the linearly polarized pump laser. In this limit, the results are given by

$$(\psi_{++} + \psi_{--}) = 2\alpha^2[9\delta^2(\delta^2+4\gamma^2) + (4\gamma^2+\delta^2+4\alpha^2)^2]D_1^{-1} , \qquad (3.2.10)$$

$$\text{Re } \psi_{+-} = \alpha^2[(\delta^2+4\gamma^2+4\alpha^2)(4\gamma^2+4\alpha^2-\delta^2)+9\delta^2(\delta^2+4\gamma^2)]D_1^{-1} \qquad (3.2.11)$$

and

$$\text{Im } \psi_{+-} = -4\gamma\delta\alpha^2 (4\gamma^2+4\alpha^2+\delta^2)D_1^{-1} , \qquad (3.2.12)$$

where

$$D_1 = (\gamma^2+4\alpha^2+\tfrac{3}{2}\delta^2)[9\delta^2(\delta^2+4\gamma^2)+(\delta^2+4\gamma^2+4\alpha^2)^2] + \delta^2[(4\gamma^2+4\alpha^2+\delta^2)(\delta^2+ 4\gamma^2)] . \qquad (3.2.13)$$

The positions and widths of peaks in $(\psi_{++} + \psi_{--})$, etc., could be ascertained from the roots of D_1, which are rather complicated as D_1 is cubic in δ^2.

Now, if we assume, as usual, that the pump is weak, i.e., $\alpha << \gamma$, then in this limit the results of (3.2.10) to (3.2.13) simplify considerably to

$$(\psi_{++} + \psi_{--}) = \alpha^2 \left(\frac{1}{\delta^2+\gamma^2} + \frac{1}{4\delta^2+\gamma^2}\right) , \qquad (3.2.14)$$

$$\text{Re } \psi_{+-} = \frac{\alpha^2}{3} \left(\frac{1}{\delta^2+\gamma^2} + \frac{2}{4\delta^2+\gamma^2}\right) , \qquad (3.2.15)$$

and

$$\text{Im } \psi_{+-} = \frac{2}{3} \alpha^2 \frac{\delta}{\gamma} \left(\frac{1}{\delta^2+\gamma^2} - \frac{4}{4\delta^2+\gamma^2}\right) . \qquad (3.2.16)$$

In this limit, it can be seen that each of the functions $(\psi_{++} + \psi_{--})$ and Re ψ_{+-} can be expressed as the sum of two Lorentzians, one with a width γ and the other with a width $\gamma/2$. Im ψ_{+-} is dispersive in nature, which results from its dependence on δ. Therefore, the signal for the case $\theta = 0, \pi/2$ etc. could be written as the sum of two Lorentzians (the weight factor associated with one of them may be negative) of widths γ and $\gamma/2$, respectively, and for the case when $\theta = \pi/4, 3\pi/4$ there are two dispersion terms in the signal which come from the term Im ψ_{+-}, in addition to the absorption type of terms.

b) Broadband pump

As Hanle experiments have been performed with both monochromatic and broadband sources, it is worthwhile to examine the effect of the source bandwidth on the nature of the spectra. We first consider the weak field spectra $\alpha << \gamma, \gamma_c$. In this case, expressions (3.2.1) to (3.2.6) simplify to

$$(\psi_{++} + \psi_{--}) = \alpha^2 \mu \left(\frac{1}{(4\delta^2+\gamma^2\mu^2)} + \frac{1}{(\delta^2+\gamma^2\mu^2)}\right), \qquad (3.2.17)$$

$$\text{Re } \psi_{+-} = \frac{2\alpha^2}{(\delta^2+4\gamma^2)} \left(\frac{(\mu+2)}{(\mu^2-16)} + \frac{(\mu-1)}{(\mu^2-4)}\right)$$

$$- \frac{2\mu\alpha^2(\mu^2-16)^{-1}(\mu+4)}{(4\delta^2+\gamma^2\mu^2)} + \frac{\mu(\mu^2-4)^{-1}\alpha^2(\mu-2)}{(\delta^2+\gamma^2\mu^2)}, \qquad (3.2.18)$$

$$\text{Im } \psi_{+-} = \frac{\delta}{\gamma}\alpha^2 \left(\frac{[(2-\mu)(\mu^2-4)^{-1} - (\mu+1)(\mu^2-16)^{-1}]}{(\delta^2 + 4\gamma^2)}\right.$$

$$\left. + \frac{4(1+\mu)(\mu^2-16)^{-1}}{(4\delta^2 + \gamma^2\mu^2)} - \frac{(2-\mu)(\mu^2-4)^{-1}}{(\delta^2 + \gamma^2\mu^2)}\right). \qquad (3.2.19)$$

We can see from the above that the fluorescence signal for $\theta = 0, \pi/2$ etc. is a sum of three Lorentzians, with the possibility of the weight factors associated with some of them being negative, of widths 2γ, $\gamma\mu$, and $\gamma\mu/2$,

respectively. For the case $\Theta = \pi/4$, the signal has, in addition to the above, a dispersive contribution which comes from the term Im ψ_{+-}. Although the signal has a dispersive contribution, it always remains positive. For arbitrary values of the strength of the broadband field, the signals are examined in the next section.

From the analytical expressions given above, it is difficult to get an insight into the actual behavior of the fluorescence signals $L_x(\delta)$ and $L_y(\delta)$. Therefore, we now proceed to present some of the numerical results for the line shapes of the fluorescence signals $L_x(\delta)$ and $L_y(\delta)$, for various values of the field strengths and the fluctuation parameter γ_c, as functions of δ.

The normalized plot of the signal $L_x(\delta)$, i.e., of $L_x(\delta)/L_x(0)$, which is detected along the x direction with its polarization vector directed along the y direction, as a function of δ, for $\Theta = \pi/2$, for the weak-field case is shown in Fig. 3. This signal is a symmetric function of δ. It can be seen that with increase in γ_c, the line broadens. It is to be noted that the value $\delta = 0$ corresponds to the zero value of the intensity of the circularly polarized light. Figure 4 shows the normalized plot (normalized so that the maximum value is unity) of the signal $L_y(\delta)$, detected along the y direction with its polarization parallel to the x direction, for $\Theta = \pi/2$, for the weak-field case.

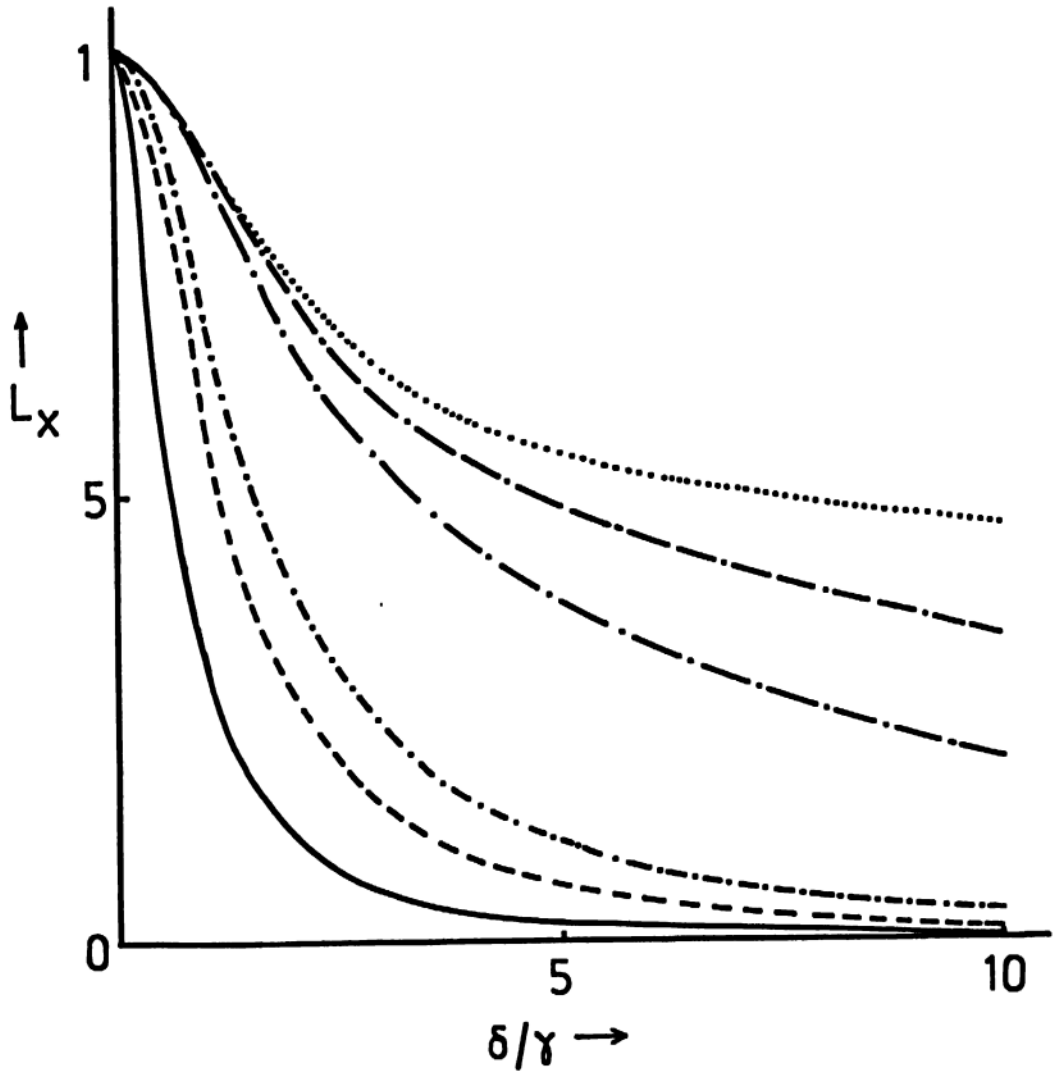

Fig.3 The normalized fluorescence signal L_x as a function of δ for $\theta = \pi/2$, $\alpha = .01$, $\gamma = 1$ and for the following values of the bandwidth parameter γ_c:

(a) ——— $\gamma_c = 0$ (b) – – – $\gamma_c = 1$ (c) —·—·— $\gamma_c = 2$

(d) ——·——·—— $\gamma_c = 10$ (e) – –·– –·– – $\gamma_c = 20$

(f) ..... $\gamma_c = 50$

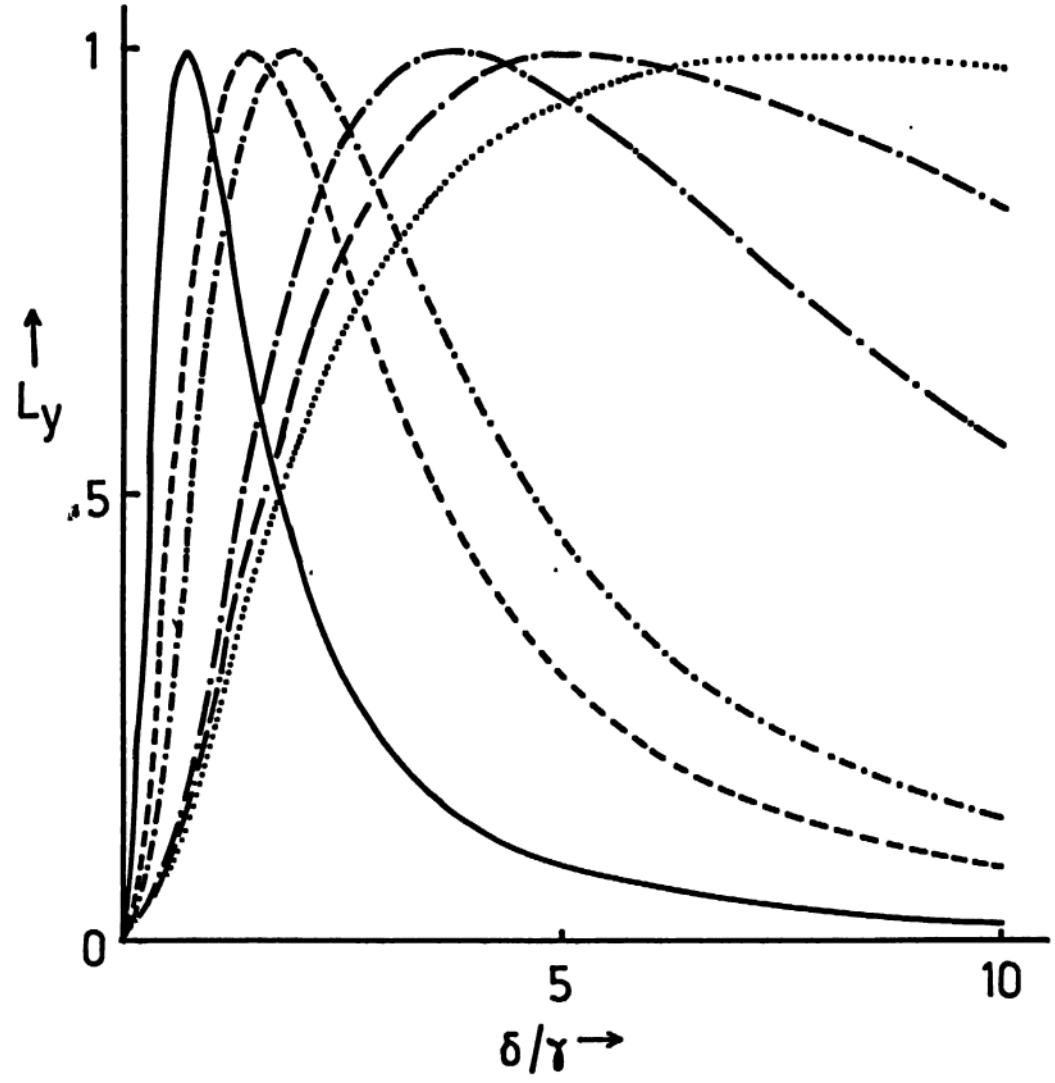

Fig.4 The normalized fluorescence signal L_y as a function of δ for the same values of parameters as in Fig.3.

The signal $L_y(\delta)$, which is symmetric with respect to δ, has a double-humped structure. Here, again, a similar effect, as in the case of Fig. 3 viz. broadening of the line with increase in γ_c, is observed. In both the above cases (Figs. 3 and 4) it is seen that the lines are much narrower with monochromatic excitation (γ_c=0) than with broadband excitation. A similar result was found by Rasmussen et al.[11] for the case of usual magnetic-field Hanle effect.

Figure 5 is a plot of the fluorescence signal $L_x(\delta)$ for the weak-field case for $\theta = \pi/4$. It is to be noted that the signal for $\theta = \pi/4$ has the property $L_x(\delta)=L_y(-\delta)$, and vice versa. The signal has a single-peaked structure with slight asymmetry about $\delta = 0$. As the fluctuations become larger, the asymmetry increases and the line attains a dispersive shape for large enough γ_c. However, the signal always remains positive. Here, the signal for the case when $\gamma_c = 10$ has been magnified by a factor of 10.

Figure 6 shows the normalized fluorescence signal $L_x(\delta)$, for $\theta = \pi/2$, for the strong-field case. The signal has a similar shape to that of the weak-field case, but with a much larger magnitude than that of the weak-field case, which is due to saturation effects [cf. eq.(3.2.2)].

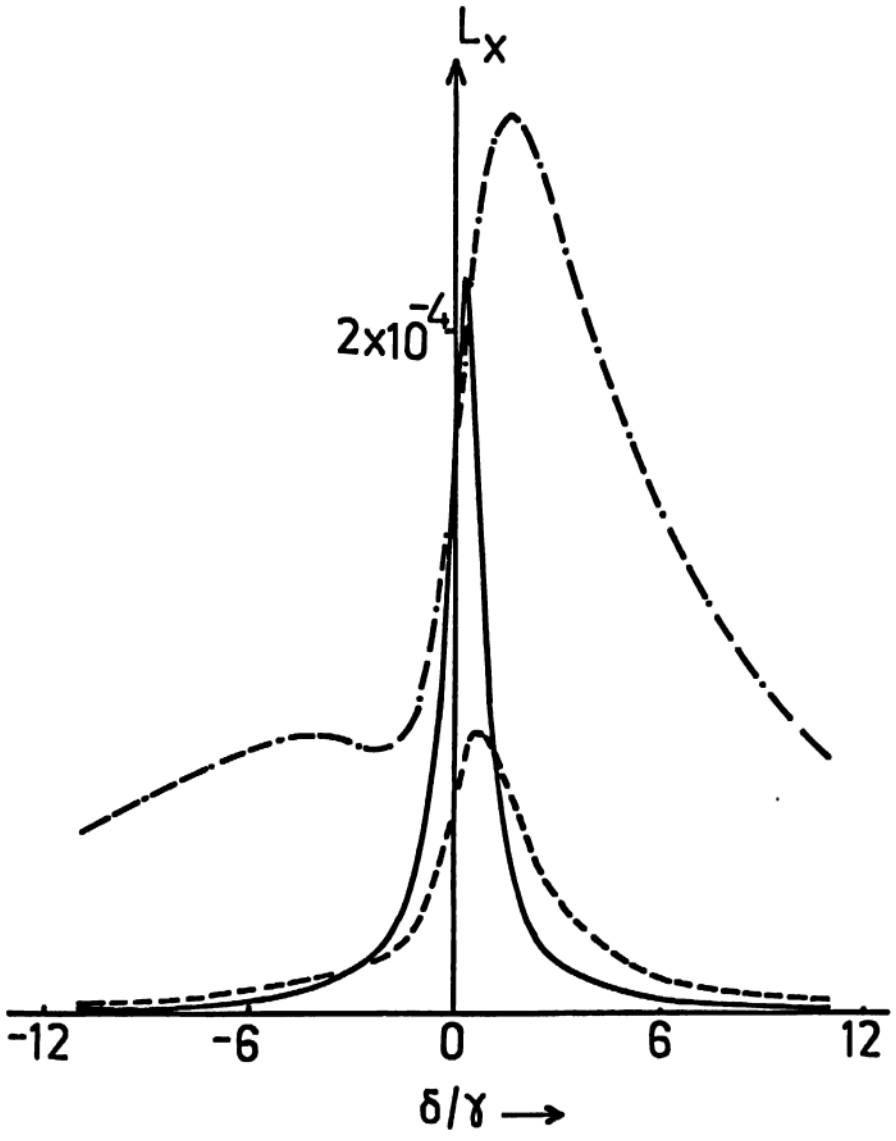

Fig.5 The fluorescence signal L_x as a function of δ for $\Theta = \pi/4$, $\alpha = .01$, $\gamma = 1$ and for the following values of γ_c:

(a) ——— $\gamma_c = 0$ (b) – – – $\gamma_c = 2$

(c) — — · — — · — $\gamma_c = 10$

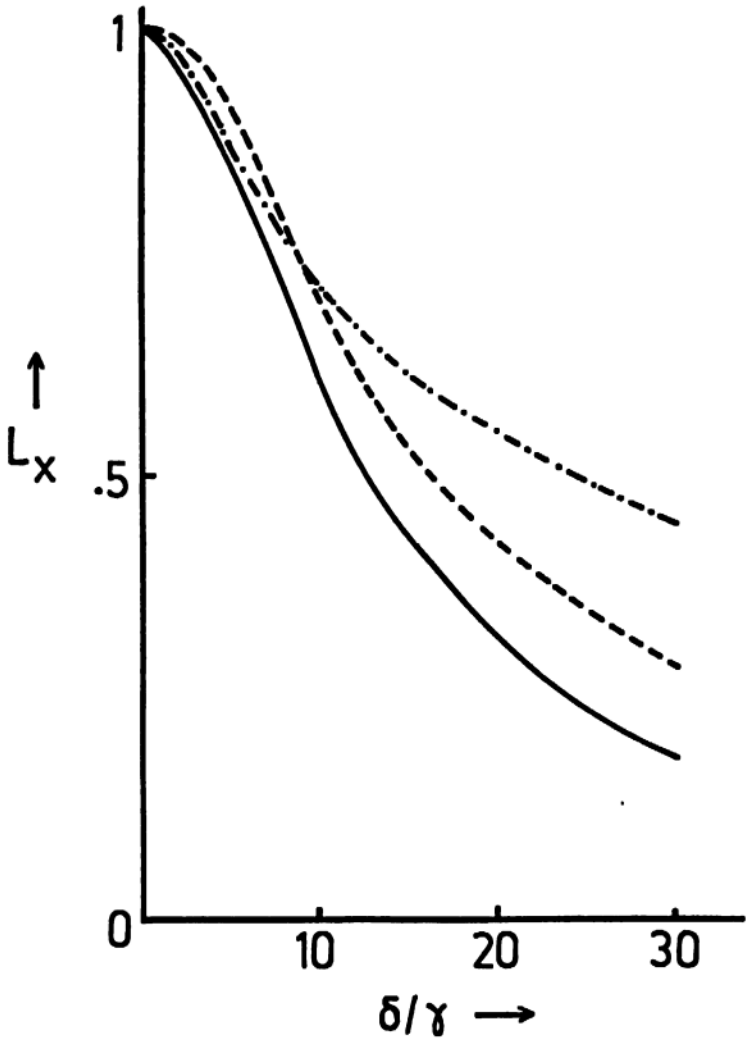

Fig.6 The normalized fluorescence signal L_x as a function of δ for $\Theta = \pi/2$, $\alpha = 10$, $\gamma = 1$ and for the following values of γ_c:

(a) ——— $\gamma_c = 0$ (b) – – – $\gamma_c = 2$

(c) — · — · — · — · $\gamma_c = 10$

In Fig. 7, the normalized fluorescence signal $L_y(\delta)$ for the case when $\Theta = \pi/2$ is plotted for the strong-field case. Here, again, the signal has a double-humped structure like that of the weak-field case. The width of the signal (i.e., dip at the origin) does not depend critically on the width of the pump laser, in contrast to the weak-field case. The width first increases slightly with increase in γ_c and then decreases with further increase in γ_c. One may compare the results of Figs. 6 and 7 with those of Avan and Cohen Tannoudji[16] for the case of the usual magnetic-field Hanle effect. We see that the qualitative effect of bandwidth on the optical Hanle signals is similar to that in the case of magnetic-field Hanle effect. We also note that the optical Hanle signals do not show very pronounced narrowing due to laser linewidth, as is typical of the magnetic-field Hanle effect. The differences may be due to the fact that the pumping laser is always asymmetrically off the two atomic transitions, due to Stark shifts induced by the nonresonant laser[87]. In Fig. 8, a plot of the fluorescence signal $L_x(\delta$ for $\Theta = \pi/4$, for the strong-field case is shown. For the narrow-band excitation, the line has a single peaked structure with slight asymmetry about $\delta = 0$. As the fluctuation are increased, the asymmetry becomes more pronounced and the line attains a dispersive shape. However, it is to be noted that the signal always remains positive.

We have also solved the set of equations (3.1.25) in steady state and obtained expressions looking similar to

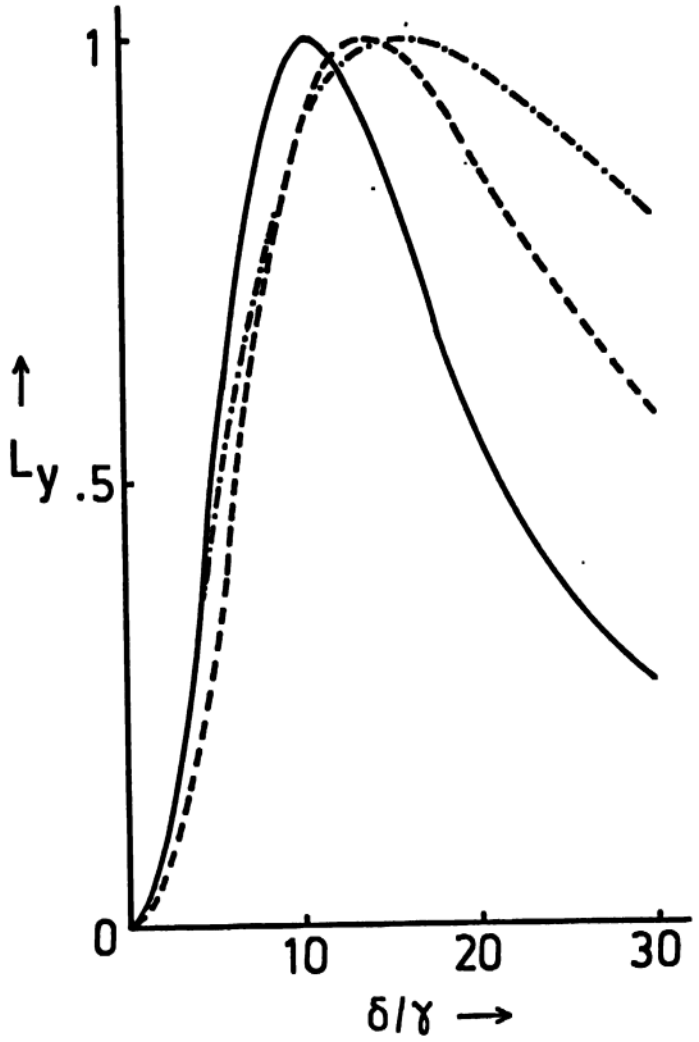

Fig. 7 The normalized fluorescence signal L_y as a function of δ for the same values of parameters as in Fig.6

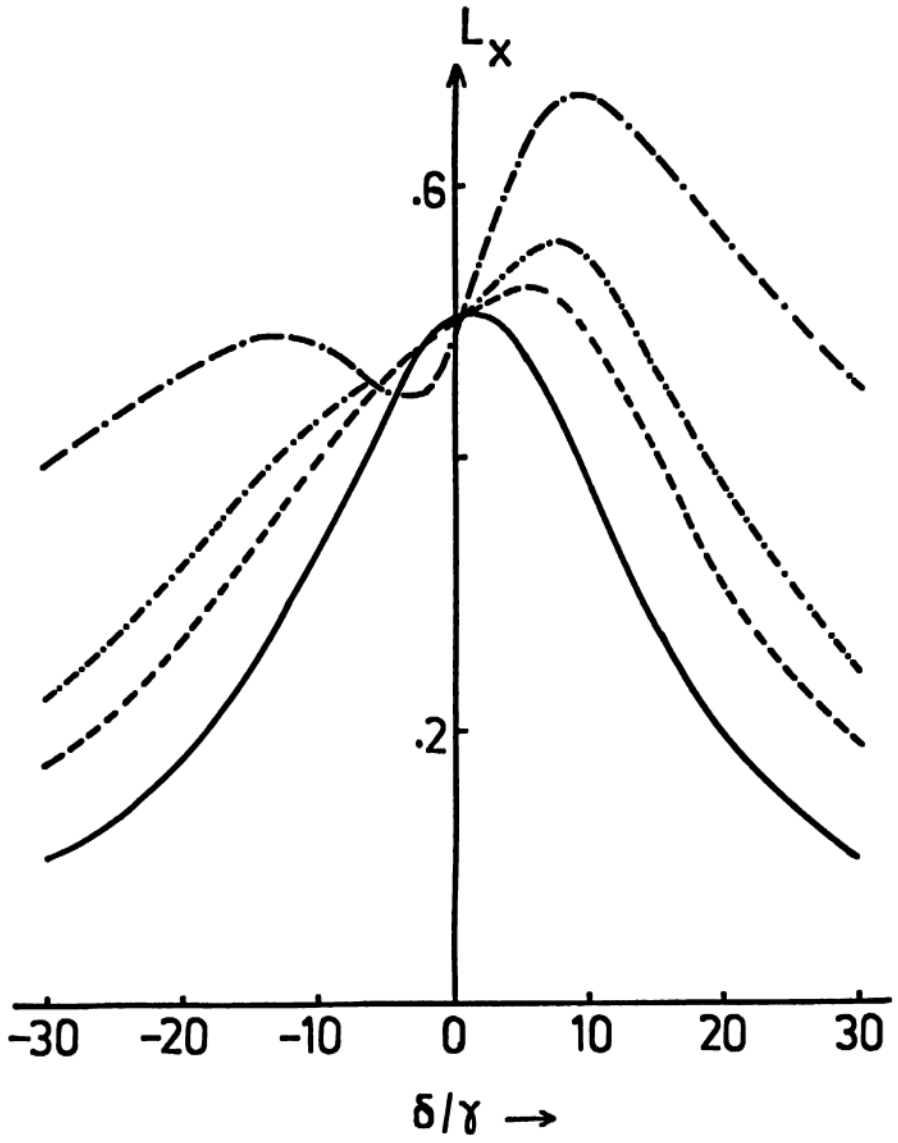

Fig.8 The fluorescence signal L_x as a function of δ for $\theta = \pi/4$, $\alpha = 10$, $\gamma = 1$ and for the values of the bandwidth parameter γ_c given by

(a) ——— $\gamma_c = 10$ (b) – – – $\gamma_c = 1$

(c) —·—·—· $\gamma_c = 2$ (d) ——·——·—— $\gamma_c = 10$

the set of solutions (3.2.17) to (3.2.19). We now present some of our numerical results in Figs. 9-11. Figure 9 shows the behaviour of the excited state population ψ_{++} as a function of the Zeeman splitting s for the detuning parameter $\delta_o = 100\gamma$ and for different values of the pump laser bandwidth γ_c. We find that when $\gamma_c=0$ (monochromatic pump) the function ψ_{++} has a well defined two-peaked structure and as the bandwidth parameter γ_c is increased, the resolution decreases. There is an asymmetry in the lineshape due to the presence of laser detuning. In Figs. 10 and 11, the behaviour of the signals L_x and L_y is shown respectively. A general feature of all these signals is that there is broadening of the signal sufficiently away from s=0 with an increase in the bandwidth parameter γ_c. Another important feature of these magnetic field Hanle signals is a pronounced narrowing of the line with increase in γ_c arround the point s=0. Avan and Cohen Tannoudji[16,87] have also found a similar behaviour in their magnetic field Hanle signals for the cases when either $\delta_o=0$ or $\gamma_c=0$ [cf. Sec.3.1]. Thus we conclude that the fluorescence signals in the magnetic field Hanle case depend strongly on the laser bandwidth γ_c.

3.3 Optical Hanle effect under strong broadband excitation

In this section, we outline an alternate approach to the Hanle effect in strong broadband fields, although in the literature several treatments[17,88] of the broadband fields already exist. We will use some general results from the theory of multiplicative stochastic processes.

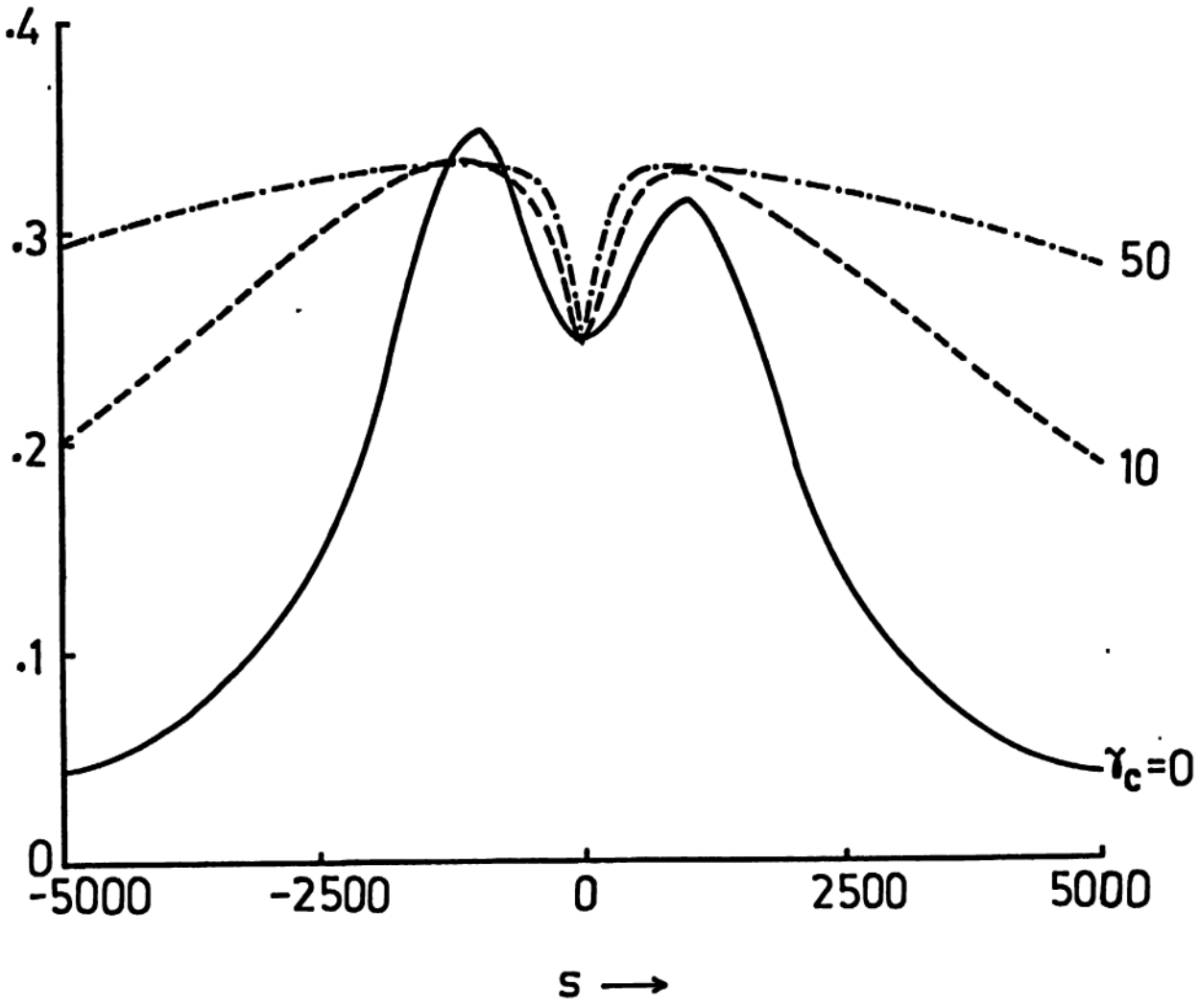

Fig.9 Excited state population Ψ_{++} as a function of the Zeeman splitting s in the magnetic field Hanle case for different values of the laser bandwidth γ_c (values as indicated in the figure) for the values of the parameters $\delta_o = 100$, $\gamma = 1$.

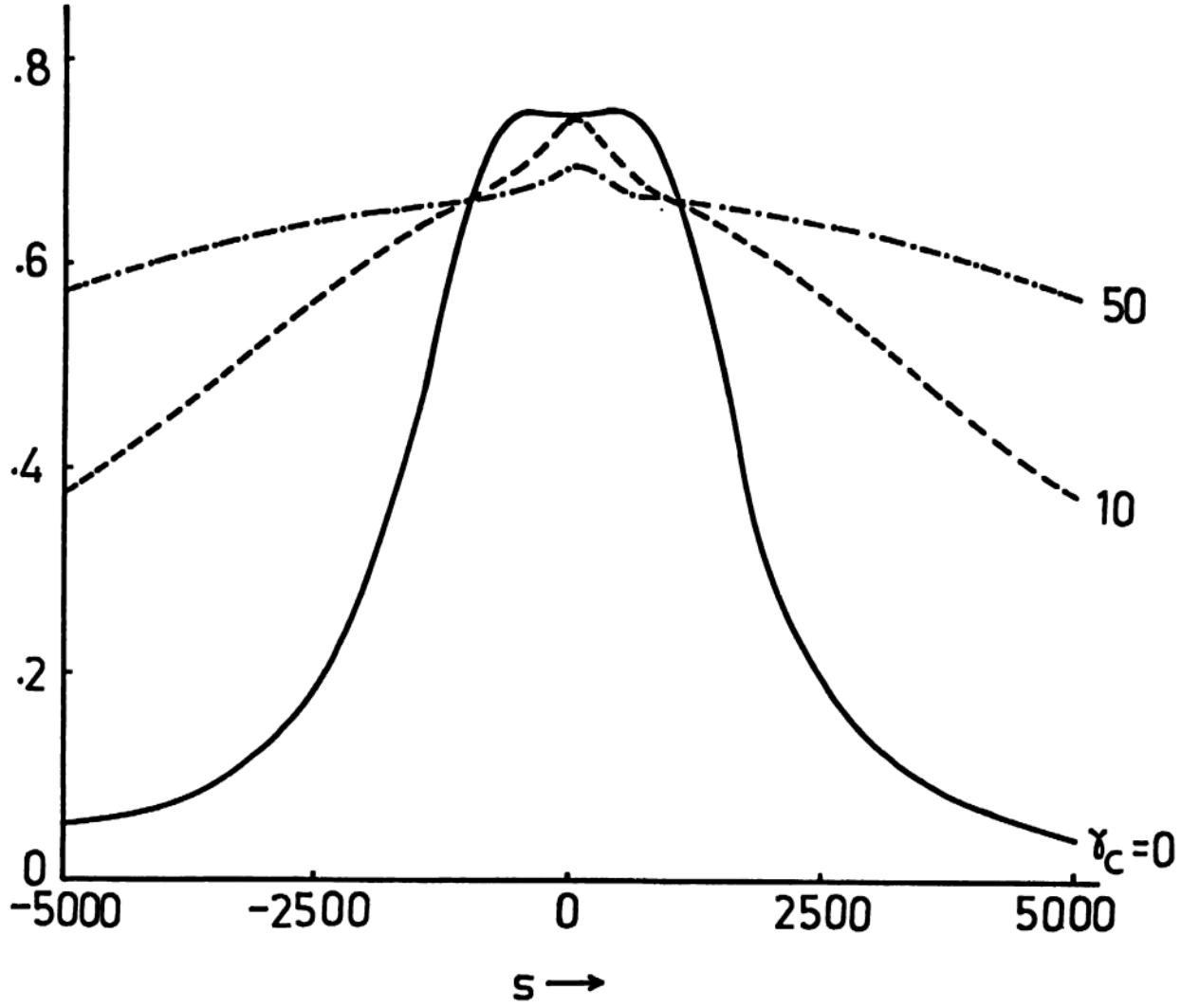

Fig.10 Fluorescence signal L_x vs s for the magnetic field Hanle case for the same values of the parameters as in Fig.9

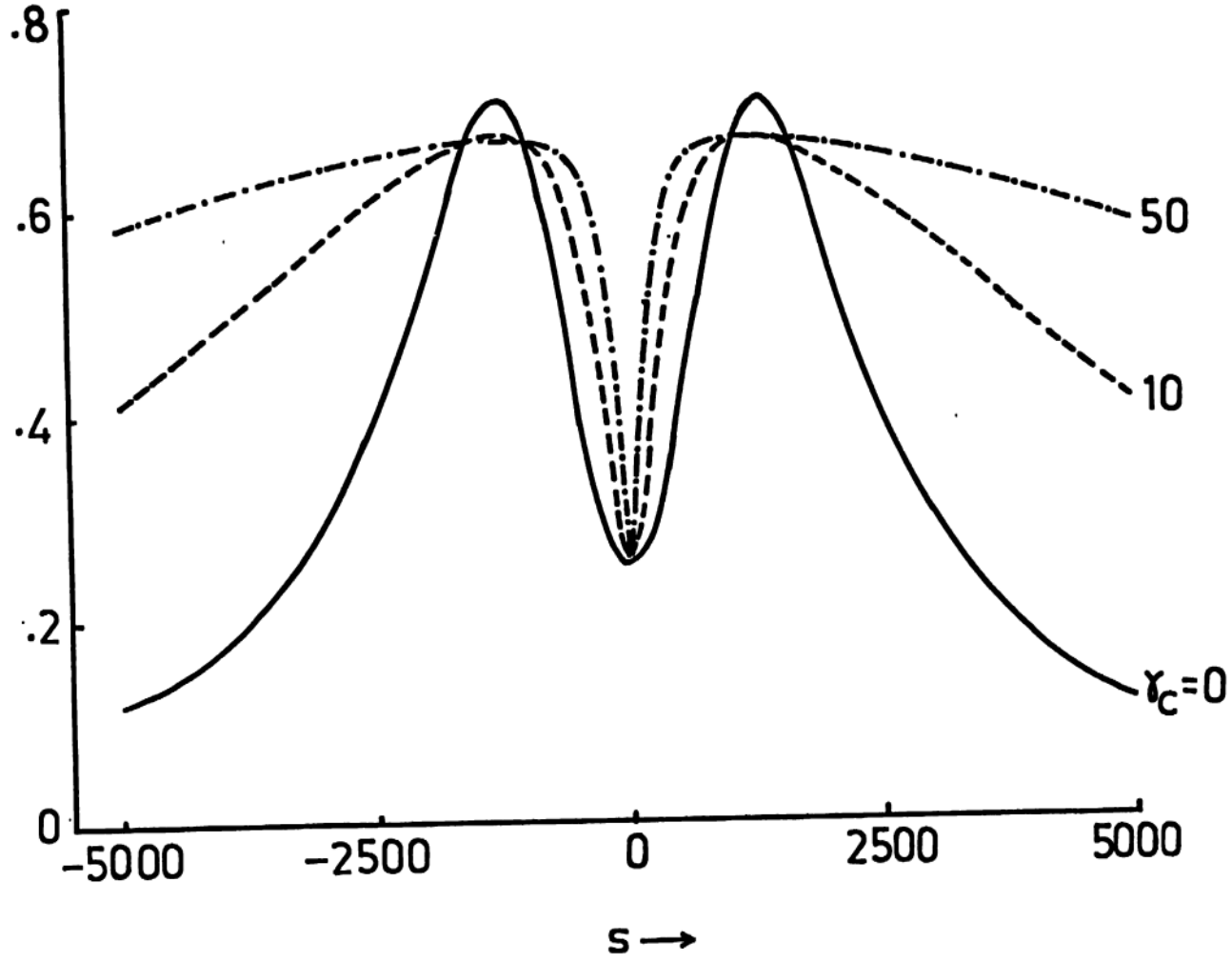

Fig.11 Fluorescence signal L_y for the magnetic field Hanle situation for the same set of parameters as in Fig.9

by a delta correlated Gaussian random process. Both these assumptions are justified in view of the central-limit theorem, since a broadband field, in principle, can be represented by a superposition of an infinitely large number of modes. Therefore, the electric field $\vec{\mathcal{E}}(t)$ in (3.1.9) is now regarded as a Gaussian stochastic process with correlation function

$$\langle \mathcal{E}'(t)\, \mathcal{E}'^{*}(t')\rangle = 2D\delta(t-t'),\ \langle \mathcal{E}'(t)\, \mathcal{E}'(t')\rangle = 0 \qquad (3.3.1)$$

where

$$\vec{\mathcal{E}}(t) = \mathcal{E}'(t)\,(\hat{x}\cos\theta + \hat{y}\sin\theta)\ . \qquad (3.3.2)$$

On using (3.1.11) and (3.3.2), the Hamiltonian $H'(t)$ simplifies to

$$H'(t) = \hbar(\omega_o - \Omega + \delta)A_{++} + \hbar(\omega_o - \Omega - \delta)A_{gg} + [A_{+g}R\ \mathcal{E}'(t)e^{-i\theta} - A_{-g}R\ \mathcal{E}'(t)e^{i\theta} + \text{H.c.}]\ . \qquad (3.3.3)$$

On using the theory of multiplicative stochastic processes , the ensemble average of $\tilde{\sigma}$ can be written as

$$\frac{\partial}{\partial t}\langle\sigma\rangle = L_{inc}\langle\tilde{\sigma}\rangle - i[(\omega_o - \Omega + \delta)A_{++} + (\omega_o - \Omega - \delta)A_{gg},\ \langle\tilde{\sigma}\rangle]$$
$$-(R^2/\hbar^2)D[A_{+g}e^{-i\theta} - A_{-g}e^{i\theta}, [A_{g+}e^{+i\theta} - A_{g-}e^{-i\theta}, \langle\tilde{\sigma}\rangle]]$$
$$-(R^2/\hbar^2)D[A_{g+}e^{+i\theta} - A_{g-}e^{-i\theta}, [A_{+g}e^{-i\theta} - A_{-g}e^{i\theta}, \langle\tilde{\sigma}\rangle]]. \qquad (3.3.4)$$

On making use of the transformation of type (3.2.12) (with ϕ replaced by zero), the equations of motion for the ensemble-averaged elements of the density matrix are given by

$$\dot{\psi}_{++}=-2(\gamma_1+\gamma)\psi_{++} - D_o(2\psi_{++} + \psi_{+-} + \psi_{-+} - 2\psi_{gg}) ,$$

$$\dot{\psi}_{--}=-2(\gamma_1+\gamma)\psi_{--} - D_o(2\psi_{--} + \psi_{+-} - \psi_{-+} - 2\psi_{gg}),$$

$$\dot{\psi}_{gg}= p-2\gamma_o\psi_{gg}+2\gamma(\psi_{++}+\psi_{--}) + 2D_o(\psi_{++}+\psi_{--}+\psi_{+-}+\psi_{-+}-2\psi_{gg}),$$

$$\dot{\psi}_{+-}=-(2\gamma+2\gamma_1+i\delta)\psi_{+-}-D_o(2\psi_{+-}+\psi_{++}+\psi_{--}-2\psi_{gg}),$$

$$\dot{\psi}_{+g}=-(\gamma_o+\gamma_1+\gamma+2i\delta)\psi_{+g}-D_o(\psi_{-g}+3\psi_{+g}) ,$$

$$\dot{\psi}_{-g}=-(\gamma_o+\gamma_1+\gamma+i\delta)\psi_{-g}-D_o(\psi_{+g}+3\psi_{-g}) , \qquad (3.3.5)$$

where $R^2D/\hbar^2=D_o$ and where we have also included the incoherent decay of the levels J=0 and J=1 at the rates $2\gamma_o$ and $2\gamma_1$, respectively, as well as the pumping of the level J=0 at the rate p [cf. fig. 18]. This kind of situation was considered by Carrington and Corney and Ducloy[17], who also assumed that $\gamma<<\gamma_o$ and γ_1, in the context of the usual Hanle effect. The steady-state solutions of eq. (3.3.5) are given by

$$(\psi_{++} + \psi_{--}) = \frac{D_o p}{\Lambda}\left(1 - \frac{4D_o\gamma_o(\gamma_1+\gamma)(\gamma_1+\gamma+D_o)}{(\delta^2+\Gamma^2)\Lambda}\right), \qquad (3.3.6)$$

$$\text{Re}\,\psi_{+-} = \frac{2D_o p(\gamma+\gamma_1)^2[1+D_o/(\gamma+\gamma_1)]}{(\delta^2+\Gamma^2)\Lambda}\ , \qquad (3.3.7)$$

$$\text{Im}\,\psi_{+-} = \frac{-\delta D_o p(\gamma_1+\gamma)}{(\delta^2+\Gamma^2)\Lambda}\ , \qquad (3.3.8)$$

where

$$\Gamma^2 = \frac{4[(\gamma+\gamma_1+2D_o)\gamma_o+2D_o\gamma_1](\gamma+\gamma_1+D_o)(\gamma+\gamma_1)}{\Lambda} \qquad (3.3.9a)$$

and

$$\Lambda = [(\gamma_1+\gamma+D_o)\ \gamma_o+2D_o\gamma_1]\ . \qquad (3.3.9b)$$

The fluorescence signals L_x and L_y for the case when $\theta=\pi/2$ are given by

$$L_x(\theta=\pi/2) = \frac{D_o p}{\Lambda}\left(1 + \frac{4(\gamma+\gamma_1)^2[1+D_o/(\gamma+\gamma_1)][(\gamma+\gamma_1)\gamma_o+2D_o\gamma_1]}{(\delta^2+\Gamma^2)\Lambda}\right), \qquad (3.3.10)$$

$$L_y(\theta=\pi/2) = \frac{D_o p}{\Lambda}\left(1 - \frac{4(\gamma+\gamma_1)^2[1+D_o/(\gamma+\gamma_1)][(\gamma+\gamma_1)\gamma_o+2D_o(\gamma_o+\gamma}{(\delta^2+\Gamma^2)\Lambda}\right. \qquad (3.3.11)$$

The above results, which are valid to all powers in D_o and for arbitrary values of decay parameters γ_o, γ_1 and γ, have been derived rigorously under the assumption of a delta

correlated Gaussian pump field. Ducloy, in an extensive study[88] of the magnetic-field Hanle effect, has examined the nature of the Hanle signals in the presence of a broadband field. He considered the broadband field to be a superposition of a large number of laser modes, with the spacing between the laser modes taken to be much smaller than say the width of the excited state. His model of the broadband laser is very much like our model (3.3.1). It is interesting to note that our results for optical Hanle signals in broadband fields are rather similar to those for the magnetic-field Hanle signals - the most important property being the Lorentzian characteristic of the signals, with intensity-dependent detunings.

The degree of polarization produced by the pump radiation for the case when $\Theta = \pi/2$ is given by

$$P\left(\Theta = \frac{\pi}{2}\right) = \left| \frac{L_x - L_y}{L_x + L_y} \right| = \frac{2\mathrm{Re}\psi_{+-}}{\psi_{++} + \psi_{--}} = \frac{\Gamma_o^2}{\Gamma_o^2 + \delta^2} , \quad (3.3.12)$$

where the full width at half-maximum of the degree of polarization signal is given by

$$\Gamma_o = 2(\gamma+\gamma_1)[1+D_o/(\gamma+\gamma_1)]^{1/2} . \quad (3.3.13)$$

It is important to note that the width of the polarization as a function of δ, for the case when $\Theta = \pi/2$, does not

depend on the decay rate γ_o of the ground state, although the width of the signals L_x and L_y does depend on the parameter γ_o.

A series expansion of (3.3.6), (3.3.7) and (3.3.8) in powers of the intensity parameter D_o leads to

$$(\psi_{++}+\psi_{--}) = \frac{pD_o}{\gamma_o(\gamma_1+\gamma)} - \frac{D_o^2 p}{\gamma_o^2}\left(\frac{\gamma_o}{X} + \frac{(\gamma_o+2\gamma_1)}{(\gamma+\gamma_1)^2}\right)+\ldots \quad (3.3.14)$$

$$\text{Re}\,\psi_{+-} = \frac{2p(\gamma+\gamma_1)D_o}{\gamma_o X} - \frac{4p[\gamma_1 X+4\gamma_o(\gamma+\gamma_1)^2]D_o^2}{\gamma_o^2 X^2} +\ldots \quad (3.3.15)$$

$$\text{Im}\,\psi_{+-} = \frac{-\delta p D_o}{\gamma_o X} + \left(\frac{(2\gamma_1+\gamma_o)}{\gamma_o^2(\gamma+\gamma_1)} + \frac{8(\gamma+\gamma_1)}{\gamma_o X}\right)\frac{\delta p D_o^2}{X} +\ldots, \quad (3.3.16)$$

where

$$X = [\delta^2 + 4(\gamma+\gamma_1)^2] \,. \quad (3.3.17)$$

The results of (3.3.14)to (3.3.16) in the limit when $\gamma \ll \gamma_o$ and γ_1 are in agreement with the general observations and remarks made by Ducloy[17] in the context of the usual magnetic-field Hanle effect studies.

In the next section, we draw a comparison of our theoretical results with the recently reported experiments[29], on optical Hanle system both for monochromatic and broadband pump cases.

3.4 Comparison with recent experiments

Recently Delsart, Keller and Kaftandjian[29,30] have investigated the optical Hanle effect experimentally. They performed the experiment with the barium resonance transition at 553.5 nm($6s^2\ ^1S_0 - 6s6p\ ^1P_1$) using a highly collimated beam. In their experiment, the Barium atomic beam is resonantly excited by a weak linearly polarized laser beam and the Stark shift is induced with another strong off-resonant laser beam. These two laser beams are counter propagating and crossed at right angles with the Barium atomic beam. The weak beam is frequency locked to the ^{138}Ba line and the strong beam is detuned in the range $-750 - 6000$ MHz from the same line. They have recorded the in phase and in-quadrature signals, which are respectively proportional to Re ψ_{+-} and Im ψ_{+-}, as a function of the strong beam power for various values of its detuning. They have performed the experiment both for monochromatic as well as broadband excitations. However they have used a weak pump field and therefore saturation effects are not important in their analysis. They have observed that the signal in the case of broadband excitation has twice the width of that in the case of monochromatic excitation. The experimental results of Delsart, Keller and Kaftandjian[29,3] can be theoretically explained as a special case of our analysis in sections 3.2 and 3.3.

For example, consider the equations (3.2.14) to (3.2.16) for a weak monochromatic excitation. The signals for $\theta = \pi/2$ can be written from these expressions as

$$L_x(\theta=\pi/2) = \frac{\alpha^2}{3}\left(\frac{5}{\delta^2+\gamma^2} + \frac{7}{4\delta^2+\gamma^2}\right) \qquad (3.4.1)$$

$$L_y(\theta=\pi/2) = \frac{\alpha^2}{3}\left(\frac{1}{\delta^2+\gamma^2} - \frac{1}{4\delta^2+\gamma^2}\right) . \qquad (3.4.2)$$

Now, consider our results for broadband excitation. The first terms in the series expansions (3.3.14) to (3.3.16) in the limiting case when $p \to 0$ and $\gamma_o \to 0$ such that $p/\gamma_o \to 1$ and $\gamma_1 \to 0$ and in units of D_o. From these equations, the expressions for the signals for the case when $\theta = \pi/2$ can be written as

$$L_x\ (\theta=\pi/2) = \frac{1}{\gamma} + \frac{4\gamma}{\delta^2+4\gamma^2} \qquad (3.4.3)$$

$$L_y\ (\theta=\pi/2) = \frac{1}{\gamma} - \frac{4\gamma}{\delta^2+4\gamma^2} . \qquad (3.4.4)$$

Comparing (3.4.1) and (3.4.2) with (3.4.3) and (3.4.4) respectively, one can see that the width of the signals in broadband case is roughly twice that of the signals in monochromatic excitation which is in agreement with the experimental observation of Delsart et al.[29,30].

CHAPTER IV

SPECTRAL CHARACTERISTICS OF OPTICAL HANLE SIGNALS

The purpose of this chapter is to study the power spectrum of the optical Hanle signals with regard to the various directions of observation and polarizations of the emitted and exciting radiations.

As is well known, the scattered radiation in general possesses in addition to a monochromatic elastic component, inelastic (incoherent) contribution[47] that results from the interaction of the time dependent driving(pump) field. In the

limit of weak pump intensities and when the collisions and bandwidth of the pump field are ignored, the scattering is predominantly elastic and the inelastic contribution increases and becomes appreciable when the Rabi frequency α of the transition becomes comparable to the atomic relaxation rate γ. In the limit of strong pump field ($\alpha >> \gamma$), inelastic scattering predominates over elastic scattering.

From the earlier chapters, one can see that in the case of optical Hanle effect, there is a considerable selectivity of Zeeman sublevels depending on the polarization of the strong off-resonant laser field used to lift the degeneracy of the excited states. Therefore, it is important to carry out a detailed experimental and theoretical study of the fluorescence signals produced by such a system. It would also be of interest to see how the fluorescence spectra emitted by the optical Hanle system depend upon the direction of observation, strength of the two laser fields (the pump field and the off-resonant circularly polarized electric field), the polarization of the exciting radiation. One more aspect of interest in this problem would be to look for differences, if any, between the spectra emitted by the optical Hanle system and the spectra for the usual magnetic Hanle case.

In this chapter, we present such a study. It must be mentioned here that the spectra of radiation emitted by multi-level atomic systems have been studied by a number of workers[43-52]. The most relevant study involving Hanle transitions has been made by Kornblith and Eberly[46] who studied the dependence of spectra in the magnetic field Hanle problem, on the direction of observation. But, since in the optical Hanle effect the lifting of degeneracy of the excited and ground states is caused by an altogether different mechanism[23,24] from that in the magnetic Hanle situation, and since this process introduces important asymmetries in the problem, it is worthwhile to examine the spectrum of the scattered radiation with parameters appropriate to the optical Hanle case. We also present the analytical perturbation calculation of the spectra for the optical Hanle effect in the presence of phase interrupting collisions.

4.1 Equations of motion for the density matrix

The model of the system that is chosen to illustrate the results is same as that in chapter III, with an additional incoherent relaxation rate γ_u from the ground to the excited states. The two levels involved in the

transition possess angular momenta J=0 and 1 respectively. A circularly polarized electric field propagating along the z axis interacts with the atomic beam which is directed along the x axis. A second linearly polarized pump field propagating along z direction, with its electric vector making an angle θ with the direction of the atomic beam, couples the levels $|J=0, m=0\rangle$ to $|J=1, m=\pm 1\rangle$. We also include relaxation rates Γ_{ij}'s arising due to phase interrupting collisions. Following the mathematical formulation of chapter III, the final equations for the atomic density matrix elements are obtained from eq. (3.1.17) as

$$\dot{\psi}_{++} = i\alpha\,(\psi_{g+}-\psi_{+g}) - 2\gamma\,\psi_{++} + 2\gamma_u\,\psi_{gg}\,,$$

$$\dot{\psi}_{--} = i\alpha\,(\psi_{g-}-\psi_{-g}) - 2\gamma\,\psi_{--} + 2\gamma_u\,\psi_{gg}\,,$$

$$\dot{\psi}_{gg} = i\alpha\,(\psi_{+g}+\psi_{-g}-\psi_{g+}-\psi_{g-}) + 2\gamma(\psi_{++}+\psi_{--}) - 4\gamma_u\,\psi_{gg}\,,$$

$$\dot{\psi}_{+-} = i\alpha\,(\psi_{g-}-\psi_{+g}) - (2\gamma + \Gamma_{+-}+i\delta)\,\psi_{+-}\,,$$

$$\dot{\psi}_{+g} = i\alpha\,(\psi_{gg}-\psi_{++}-\psi_{+-}) - (\gamma+2\gamma_u+\Gamma_{+g}+2i\delta)\,\psi_{+g}\,, \qquad (4.1.1)$$

$$\dot{\psi}_{-g} = i\alpha\,(\psi_{gg}-\psi_{--}-\psi_{-+}) - (\gamma+2\gamma_u+\Gamma_{-g}+i\delta)\,\psi_{-g}\,,$$

where ψ_{ij}'s are the ensemble averages of the density matrix elements defined as $\psi_{ij} = \langle\bar{\sigma}_{ij}\rangle$ where $\bar{\sigma}_{ij}$ are defined by

(3.1.12) (which will be given below for the sake of completeness). In the set of equations(4.1.1) the bandwidth of the pump field has been chosen to be zero. γ is the total relaxation rate for the downward transitions and γ_u is that for the upward transitions arising due to the incoherent relaxation. Γ_{ij}'s are the relaxation terms arising due to phase interrupting collisions. δ is the Stark shift parameter and α denotes the Rabi frequency of the atomic transition.

The set of eqs. (4.1.1) can be cast into the form of a matrix [cf. eq.(2.2.9)] as

$$\dot{\psi}(t) = M\,\psi(t) + I \tag{4.1.2}$$

where

$$\psi_1 = \langle\sigma_{++}\rangle,\ \psi_2 = -\langle\sigma_{+-}\rangle e^{2i\theta},\ \psi_3 = -\langle\sigma_{+g}\rangle e^{-i(\theta+\Omega t)},$$

$$\psi_4 = \psi_2^*,\ \psi_5 = \langle\sigma_{--}\rangle,\ \psi_6 = \langle\sigma_{-g}\rangle\ e^{-i(\theta-\Omega t)},\ \psi_7 = \psi_3^*, \psi_8 = \psi_6^*, \tag{4.1.3}$$

$$I_1 = I_5 = 2\gamma_u,\ I_3 = I_6 = I_7^* = I_8^* = i\alpha,\ I_2 = I_4 = 0 \tag{4.1.4}$$

and

$$
\begin{bmatrix}
2(\gamma+\gamma_u) & 0 & -i\alpha^* & 0 & -2\gamma_u & 0 & i\alpha & 0 \\
0 & -(2\gamma+i\delta+\Gamma_{+-}) & -i\alpha^* & 0 & 0 & 0 & 0 & i\alpha \\
2i\alpha & -i\alpha & -(2i\delta+\gamma+2\gamma_u+\Gamma_{+g}) & 0 & -i\alpha & 0 & 0 & 0 \\
0 & 0 & 0 & (i\delta-2\gamma+\Gamma_{+-}) & 0 & -i\alpha^* & i\alpha & 0 \\
0 & 0 & 0 & 0 & -2(\gamma+\gamma_u) & -i\alpha^* & 0 & i\alpha \\
-i\alpha & 0 & 0 & -i\alpha & -2i\alpha & -(i\delta+\gamma+2\gamma_u+\Gamma_{-g}) & 0 & 0 \\
2i\alpha^* & 0 & 0 & i\alpha^* & i\alpha^* & 0 & (2i\delta-\gamma-2\gamma_u-\Gamma_{+g}) & 0 \\
i\alpha^* & i\alpha^* & 0 & 0 & 2i\alpha^* & 0 & 0 & (i\delta-\gamma-2\gamma_u-\Gamma_{-g})
\end{bmatrix}
$$

(4.1.5)

One can note the characteristic feature of the optical Hanle signals in the matrix M, in the sense that the states $|+\rangle$ and $|-\rangle$ have different δ values rather than equal and opposite values as in the case of magnetic field Hanle effect.

The Laplace transforms and the steady state values of the matrix elements are obtained from (2.3.2) and (2.3.4) respectively. For completeness sake, we write them below. The Laplace transform of (4.1.2) is given by

$$\hat{\psi}(z) = (z-M)^{-1}\,\psi(o) + z^{-1}\,(z-M)^{-1}\,I \qquad (4.1.6)$$

where $\hat{\psi}(z)$ is the Laplace transform of $\psi(t)$ and the steady state solution of (4.2.6) is obtained as

$$\psi(\infty) = \psi_{st} = \lim_{z\to o} z\,\hat{\psi}(z) = (-M)^{-1}\,I. \qquad (4.1.7)$$

4.2 The Fluorescence signals

Following the formalism in section (2.4), the scattered electric field in the radiation zone[76] can be written, from (2.4.1), as

$$\vec{E}^{+}(r,t) = \vec{E}_o^{+}(r,t) - \frac{(\omega_{+g})^2}{rc^2}\,(\hat{r}x(\hat{r}x\vec{d}_{+g}))\,A_{g+}(t-r/c)\,e^{i\omega_{+g}(t-r/c)}$$
$$- \frac{(\omega_{-g})^2}{rc^2}\,(\hat{r}x(\hat{r}x\vec{d}_{-g}))\,A_{g-}(t-r/c)\,e^{i\omega_{-g}(t-r/c)} \qquad (4.2.1)$$

where $\hat{r}$ denotes the unit vector along the direction of detection. The two-time correlation function $\langle\vec{E}^{-}(r,t_2)\cdot\vec{E}^{+}(r,t_1)\rangle$ whose Fourier transform is directly proportional to the emission spectrum therefore is given by

$$\langle E^{-}(r,t_2)\cdot E^{+}(r,t_1)\rangle = \frac{\omega^4}{r^2c^4}\,(\hat{r}x(\hat{r}x\vec{d}_{+g}))\,.(\hat{r}x(\hat{r}x\vec{d}^{*}_{+g}))$$
$$\langle A_{+g}(t_2)A_{g+}(t_1)\rangle + (\hat{r}x(\hat{r}x\vec{d}_{-g}))\,.(\hat{r}x(\hat{r}x\vec{d}^{*}_{-g})\langle A_{-g}(t_2)A_{g-}(t_1)\rangle$$
$$+ (\hat{r}x(\hat{r}x\vec{d}_{+g}))\,.(\hat{r}x(\hat{r}x\vec{d}^{*}_{-g}))\,\langle A_{-g}(t_2)A_{g+}(t_1)\rangle$$
$$+ (\hat{r}x(\hat{r}x\vec{d}_{-g}))\,.(\hat{r}x(\hat{r}x\vec{d}^{*}_{+g}))\,\langle A_{+g}(t_2)A_{g-}(t_1)\rangle\,. \qquad (4.2.2)$$

Since we deal with the correlation function in the steady state, i.e., when the system is in equilibrium with the driving fields, we will be making the observations at times much larger than r/c and therefore this time r/c, in comparison with the other times that occur in the problem, is neglected. As mentioned earlier in section (2.4), the free-field term does not contribute in (4.2.2) as the radiation field is initially in the vacuum state. In the above

$$\omega_{-g} = \omega_{+g} \left(1 - \delta/_{\omega+g}\right) . \qquad (4.2.3)$$

In our study, the maximum value one may assign to the Stark splitting is about 10γ where γ is typically of the order of a few tens of MHz. Hence $\frac{\delta}{\omega_{+g}} \sim 10^{-7}$ which is a negligibly small quantity so that $\omega_{-g} \sim \omega_{+g} = \omega$. In view of this the correlation function is written in the form (4.2.2). Let the spectrum of fluorescence signals detected along x and y directions with their respective polarizations along y and x directions be denoted by S_x and S_y respectively. These can be calculated as will be shown below.

The dipole matrix elements occuring in (4.2.2) are given by [cf. eq. (3.1.11)]

$$\vec{d}_{+g} = R\,(-\hat{x}+i\hat{y}) \;,\quad \vec{d}_{-g} = R\,(\hat{x}+i\hat{y}) \qquad (4.2.4)$$

where R is the radial part of the matrix element.
For the direction of detection along the x axis, we have

$$\hat{r}x(\hat{r}x\vec{d}_{+g}) = -i\hat{y}R = \hat{r}x(\hat{r}x\vec{d}_{-g}) \qquad (4.2.5)$$

and for detection along the y axis

$$\hat{r}x(\hat{r}x\vec{d}_{+g}) = \hat{x}\,R = -\,[\hat{r}x(\hat{r}x\vec{d}_{-g})]\;. \qquad (4.2.6)$$

By making use of the transformations (4.1.3) and the relations (4.2.5) to (4.2.6) in (4.2.1), we obtain the correlation function of the scattered electric field in the time domain for detection along x and y directions as

$$\langle \bar{E}(r,t_2)\cdot E^{+}(r,t_1)\rangle_{\substack{x\\y}} = \frac{\omega^4 R^2}{r^2 c^4}\,\{\langle A_{+g}(t_2)A_{g+}(t_1)\rangle$$

$$+ \langle A_{-g}(t_2)A_{g-}(t_1)\rangle \mp (e^{2i\theta}\langle A_{+g}(t_2)A_{g-}(t_1)\rangle$$

$$+ e^{-2i\theta}\,\langle A_{-g}(t_2)\,A_{+g}(t_1)\rangle)\,\} \qquad (4.2.7)$$

where the '−' and '+' signs correspond to detection along x and y directions respectively and the two time correlation functions occuring in (4.2.7) are in the initial frame of reference before any transformation is made. Since we are interested in the steady state behaviour of these two-

time correlation functions which then are functions of the difference of time $t_2-t_1 = \tau$, we evaluate these in steady state and take the Laplace transform of each of these to obtain the expressions for the spectra in different directions of detection. Let the Laplace transform of the correlation function $\langle A_{\alpha\beta}(\tau)\, A_{\gamma\delta}(o)\rangle$ be denoted by $\hat{\Gamma}_{\alpha\beta\gamma\delta}(z)$ where $z = i(\omega-\Omega)$. The spectrum of fluorescence signals detected along x and y directions which are denoted respectively by S_x and S_y (which are related to the Laplace transform of the atomic correlation functions [cf. eq.(2.4.7)] can therefore be expressed as

$$S_{\substack{x\\y}}(\omega) = \frac{\omega^4 R^2}{c^4 r^2}\ \text{Real}\ [\ \hat{\Gamma}_{+gg+}(z) + \hat{\Gamma}_{-gg-}(z) \mp$$

$$(\ e^{2i\theta}\ \hat{\Gamma}_{+gg-}(z) + e^{-2i\theta}\ \hat{\Gamma}_{-gg+}(z)\ )\ ] \qquad (4.2.8)$$

Expression (4.2.8) shows that the spectral features could depend in an important way on the exciting radiation as well as direction of observation.

Each of the correlation functions occuring in (4.2.8) can be evaluated by making use of quantum regression theorem[35] [cf. Sec.(2.4)].

From (4.1.6) and (2.4.3-4), one can see that each of these correlation functions can be written in the form

$$\hat{\Gamma}(z) = A(z) + \frac{B(z)}{z} \quad . \tag{4.2.9}$$

The function $\frac{B(z)}{z}$ is singular at $z=0$. To eliminate this problem in numerical computation, we write it as a sum of coherent and incoherent parts and subtract the coherent part i.e.,

$$\hat{\Gamma}(z)_{incoh} = \hat{\Gamma}(z) - \hat{\Gamma}_{coh}(z) \tag{4.2.10}$$

where the coherent part of $\hat{\Gamma}(z)$ is given by

$$\hat{\Gamma}(z)_{coh} = \frac{1}{z} \lim_{z \to o^+} z\,\hat{\Gamma}(z) = \frac{B(o)}{z} \tag{4.2.11}$$

Therefore $\hat{\Gamma}(z)_{incoh}$ can be written as

$$\hat{\Gamma}(z)_{incoh} = A(z) + \frac{B(z) - B(o)}{z} \quad . \tag{4.2.12}$$

Now consider

$$[\tfrac{1}{z}\,(z-M)^{-1} - \tfrac{(-M)^{-1}}{z}]\,I = \tfrac{1}{z}\,[\tfrac{1}{(z-M)} + \tfrac{1}{M}]\,I = \tfrac{1}{z}\,[M^{-1}(z-M)^{-1}]\,z\,I$$

$$= M^{-1}\,(z-M)^{-1}\,I \tag{4.2.13}$$

Therefore using (4.2.13) in (4.1.6) we obtain for the incoherent part of each of the correlation functions the following.

$$\hat{\Gamma}_{+gg+}(z) = (z-M)^{-1}_{77}\,\psi_1(st)+(z-M)^{-1}_{78}\,\psi_2(st)+i\alpha\,[(M^{-1}(z-M)^{-1})_{73}$$

$$+(M^{-1}(z-M)^{-1})_{76} - (M^{-1}(z-M)^{-1})_{77} - (M^{-1}(z-M)^{-1})_{78}]\psi_3(st)$$

$$\hat{\Gamma}_{-gg-}(z) = (z-M)^{-1}_{87}\,\psi_4(st)+(z-M)^{-1}_{88}\,\psi_5(st)+i\alpha\,[(M^{-1}(z-M)^{-1})_{83}$$

$$+ (M^{-1}(z-M)^{-1})_{86}-(M^{-1}(z-M)^{-1})_{87}-(M^{-1}(z-M)^{-1})_{88}]\psi_6(st)$$

$$\hat{\Gamma}_{+gg-}(z) = (z-M)^{-1}_{77}\,\psi_4(st)+(z-M)^{-1}_{78}\,\psi_5(st)+i\alpha[(M^{-1}(z-M)^{-1})_{73}$$

$$+ (M^{-1}(z-M)^{-1})_{76}-(M^{-1}(z-M)^{-1})_{77} - (M^{-1}(z-M)^{-1})_{78}]\psi_6(st)$$

$$\hat{\Gamma}_{-gg+}(z) = (z-M)^{-1}_{87}\,\psi_1(st)+(z-M)^{-1}_{88}\,\psi_2(st)+i\alpha[(M^{-1}(z-M)^{-1})_{83}$$

$$+ (M^{-1}(z-M)^{-1})_{86}-(M^{-1}(z-M)^{-1})_{87}-(M^{-1}(z-M)^{-1})_{88}]\psi_3(st)$$

(4.2.14)

where 'st' indicates that the matrix elements are computed in steady state. Note that the expressions in (4.2.14) give only the incoherent part of the correlation functions and the subscript incoh. is not explicitly written on the left hand side for simplicity of notation. Since the coherent part is, in the weak field limit and for $\gamma_u=0$, just related to the total intensity, and in the strong field limit is rather small, we will present plots of the incoherent part of the spectrum, for some typical values of $\delta,\theta,\alpha,\gamma_u$.

In this numerical calculation, we have chosen the relaxation parameters Γ_{ij}'s arising due to phase changing collisions to be zero.

4.3 Numerical results for the spectra in intense fields

In this section we present plots of the numerical spectra in moderately strong fields and strong fields. Figures 12 and 13 show the behaviour of the spectra S_x and S_y respectively in moderate fields ($\alpha/\gamma=1$, $\delta/\gamma=10$, $\gamma_u=0$ and for (a) $\theta = \pi/4$; (b) $\theta = \pi/2$, the solid curve represents S_x and the dashed curve S_y) showing thus the marked dependence on the direction of polarization of the incident beam and the direction of observation. It is to be noted that the matrix elements $\langle + | \vec{d}.\vec{E} | g \rangle$ and $\langle - | \vec{d}.\vec{E} | g \rangle$ are in phase for $\theta = \pi/2$ whereas they are out of phase for $\theta = \pi/4$. The five peaks in the spectra can be understood by examining the behaviour of the eigenvalues of the coherent part of the interactions. The Hamiltonian H can be written in the form of a matrix as

$$H = \begin{bmatrix} 2\delta & 0 & \alpha \\ 0 & \delta & \alpha \\ \alpha & \alpha & 0 \end{bmatrix} . \qquad (4.3.1)$$

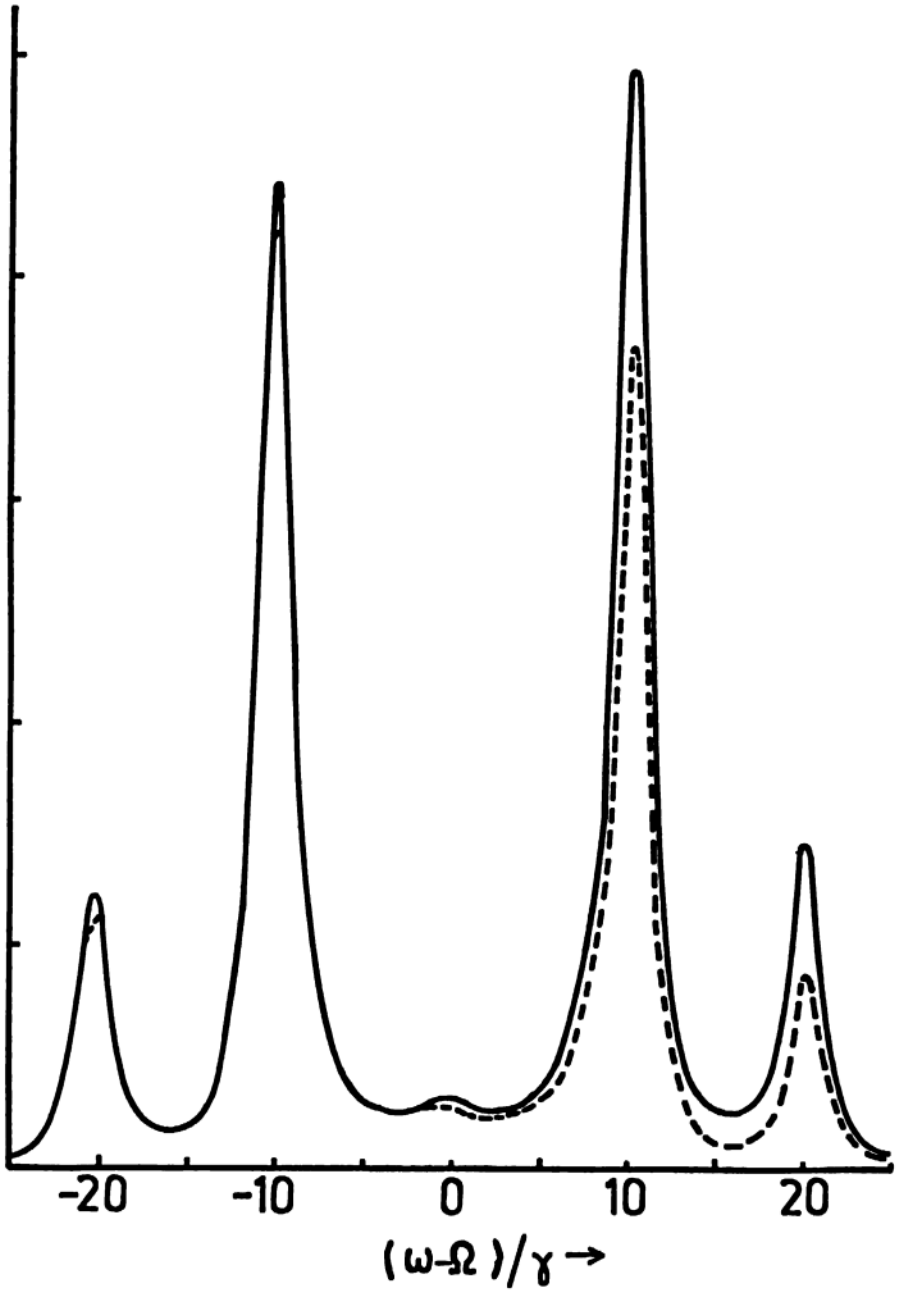

Fig.12 Spectrum of the radiation in the optical Hanle effect for moderate field $\alpha/\gamma = 1$, $\delta/\gamma = 10$, $\gamma_u = 0$ and $\Theta = \pi/4$ (the solid curve represents S_x and the dashed curve S_y)

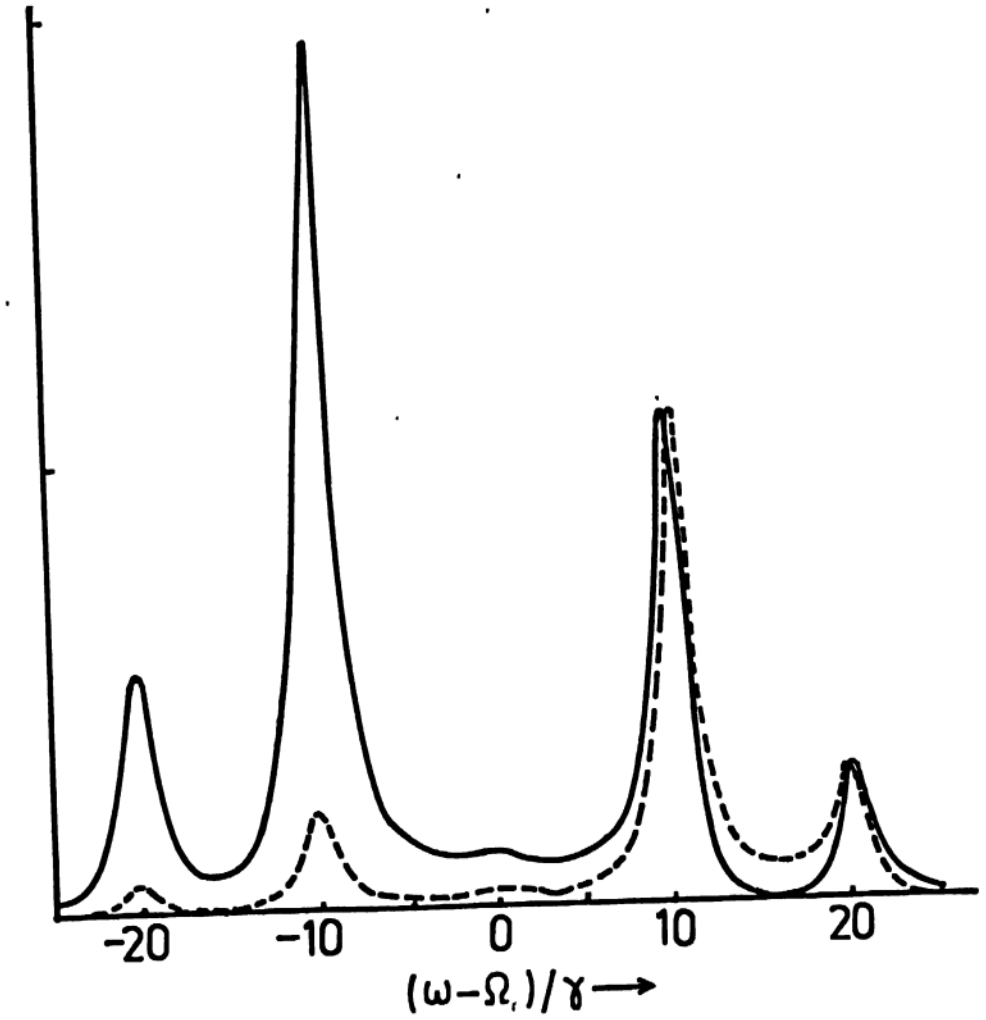

Fig.13 Spectrum of the radiation in the optical Hanle effect for moderate field $\alpha/\gamma = 1$, $\delta/\gamma = 10$, $\gamma_u = 0$ and $\Theta = \pi/2$

Since α has been taken to be much smaller than δ, the approximate eigenvalues of (4.3.1) are $2\delta+\alpha^2/2\delta$, $\delta+\alpha^2/\delta$, $\frac{-3\alpha^2}{2\delta}$ and the approximate eigenfunctions are

$$|\phi_1\rangle = |+\rangle - \frac{\alpha}{2\delta}|g\rangle \ , \ |\phi_2\rangle = |-\rangle - \frac{\alpha}{\delta}|g\rangle$$

$$|\phi_3\rangle = |g\rangle + \frac{\alpha}{2\delta}|+\rangle + \frac{\alpha}{\delta}|-\rangle \quad . \qquad (4.3.2)$$

The seven peaks that appear in the spectrum arise due to transitions between these new states, the two of which cannot be resolved as $\alpha^2/\delta \ll \gamma$. Figure 14 gives the spectra S_x and S_y respectively when the Stark shift is of the same order as the Rabi frequency associated with the transition (parameters same as in Fig.13 except the field $\alpha/\gamma = 10$). In this case, all the seven peaks are clearly resolved as predicted by the eigenvalues of (4.3.1). A much smaller value of S_y as compared to S_x is connected with the fact that the total intensity of the signal S_x is much greater than that for S_y as is easily verified from eqs. (3.2.10-12). Finally Fig. 15 gives the dependence of the spectra on the incoherent relaxation rate γ_u, which is present in certain types of experimental situations. The asymmetry of the spectra has again a strong dependence on γ_u. The behaviour of the various peaks in Fig.15 (which shows a plot of S_x for $\alpha/\gamma = 10$, $\delta/\gamma = 10$ and for $\gamma_u/\gamma = 0$ (solid curve), 0.5 (dashed curve) and 1.0 (dot-dashed curve), as

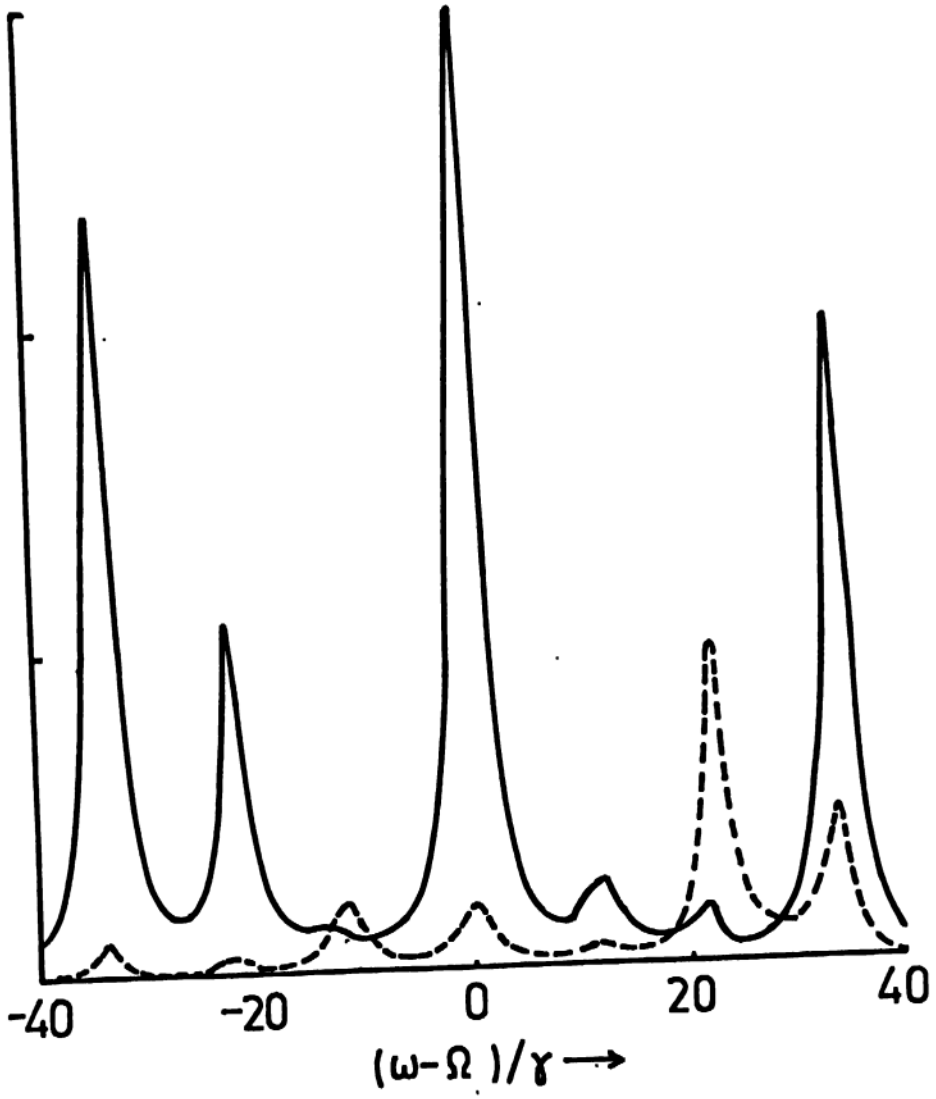

Fig.14 Spectrum of scattered radiation in optical Hanle effect for strong field $\alpha/\gamma = 10$, $\delta/\gamma = 10$, $\gamma_u = 0$ and $\theta = \pi/2$

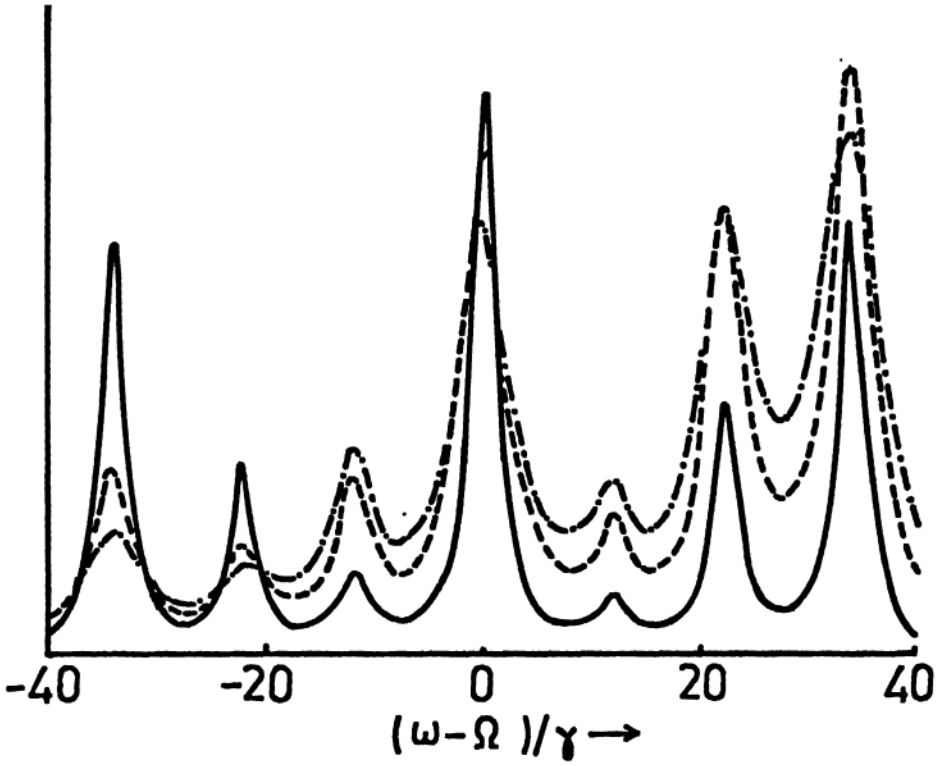

Fig.15 Effect of the relaxation rate γ_u on the spectra S_x for $\alpha/\gamma = 10$, $\delta/\gamma = 10$ and for $\gamma_u/\gamma = 0$ (solid curve), 0.5 (dashed curve), and 1.0 (dot-dashed curve)

γ_u is changed, can be understood by doing a calculation on the density matrix equation in the basis in which the matrix (4.3.1) is diagonal[43,44]. Thus, we have illustrated how sensitively the spectral features of the signals in optical Hanle effect depend on the direction of polarization of the incident radiation, its strength, the direction of observation and the incoherent relaxation rates.

4.4 Analytical results for fluorescence spectra in weak fields

For weak fields ($\alpha/\gamma << 1$), we may expand the expectation values of the density matrix elements in α and obtain the perturbation results to various orders. We are interested in calculating the spectra to first order in the laser intensity i.e., to second order in the Rabi frequency α of the exciting laser. In calculating the different two time correlation functions in steady state to second order in the Rabi frequency α, we will be requiring the steady state values of the density matrix elements $\langle A_{ij} \rangle$'s to the same order. Therefore, as a first step, we proceed with the calculation of the density matrix elements to second order in α. We indicate the order of perturbation with respect to the laser field with a superscript within parentheses and it has to be noted here that all the calculations are

carried out in steady state only. Consider the set of equations(4.1.1) in steady state (i.e. LHS = 0). The density matrix elements in steady state to various orders in α are evaluated and found to be

$$\langle A_{++}\rangle^{(o)} = \langle A_{--}\rangle^{(o)} = \frac{\gamma_u}{2\gamma_u+\gamma} \quad \text{and} \quad \langle A_{gg}\rangle^{(o)} = \frac{\gamma}{(2\gamma_u+\gamma)} \tag{4.4.1}$$

and all the other $\langle A_{ij}\rangle^{(o)}$'s are zero.

The density matrix elements in the first order are given by

$$\langle A_{+g}\rangle^{(1)} = \frac{i\alpha(\gamma-\gamma_u)}{(2\gamma_u+\gamma)[2i\delta-2\gamma_u-\gamma-\Gamma_{+g}]},$$

$$\langle A_{-g}\rangle^{(1)} = \frac{i\alpha(\gamma-\gamma_u)}{(2\gamma_u+\gamma)[i\delta-2\gamma_u-\gamma-\Gamma_{-g}]} \tag{4.4.2}$$

and the remaining $\langle A_{ij}\rangle^{(1)}$'s are all zero. The second order solutions are given by

$$\langle A_{+-}\rangle^{(2)} = \langle A_{-+}\rangle^{*(2)} = \frac{i\alpha}{(i\delta-2\gamma-\Gamma_{+-})} (\langle A_{g-}\rangle^{(1)} - \langle A_{+g}\rangle^{(1)}) =$$

$$\frac{\alpha^2(\gamma-\gamma_u)\ (4\gamma_u+2\gamma+\Gamma_{+g}+\Gamma_{-g}-i\delta)}{(2\gamma_u+\gamma)[2\gamma+\Gamma_{+-}-i\delta][i\delta+2\gamma_u+\gamma+\Gamma_{-g}][2\gamma_u+\gamma+\Gamma_{+g}-2i\delta]}, \tag{4.4.3}$$

$$\langle A_{++}\rangle^{(2)} = \frac{\alpha\gamma_u}{\gamma(2\gamma_u+\gamma)}\ \mathrm{Im}\ \langle A_{-g}\rangle^{(1)} - \frac{\alpha(\gamma_u+\gamma)}{\gamma(2\gamma_u+\gamma)}\ \mathrm{Im}\ \langle A_{+g}\rangle^{(1)} =$$

$$\frac{\alpha^2\ (\gamma-\gamma_u)}{(2\gamma_u+\gamma)^2\gamma}\ \frac{(\gamma+\gamma_u)(2\gamma_u+\gamma+\Gamma_{+g})}{[(2\gamma_u+\gamma+\Gamma_{+g})^2+4\delta^2\ ]} - \frac{\gamma_u(2\gamma_u+\gamma+\ \Gamma_{-g})}{[(2\gamma_u+\gamma+\Gamma_{-g})^2+\ \delta^2]} \tag{4.4.4}$$

$$\langle A_{--}\rangle^{(2)} = \frac{\alpha\gamma_u}{\gamma(2\gamma_u+\gamma)}\ \mathrm{Im}\langle A_{+g}\rangle^{(1)} - \frac{\alpha(\gamma_u+\gamma)}{\gamma(2\gamma_u+\gamma)}\ \mathrm{Im}\langle A_{-g}\rangle^{(1)} =$$

$$\frac{\alpha^2(\gamma-\gamma_u)}{(2\gamma_u+\gamma)^2\gamma}\ \frac{(\gamma+\gamma_u)(2\gamma_u+\gamma+\Gamma_{-g})}{[(2\gamma_u+\gamma+\Gamma_{-g})^2\ +\ \delta^2]} - \frac{\gamma_u(2\gamma_u+\gamma+\Gamma_{+g})}{[(2\gamma_u+\gamma+\Gamma_{+g})^2+4\delta^2]}\ , \tag{4.4.5}$$

$$\langle A_{gg}\rangle^{(2)} = -\ (\langle A_{++}\rangle^{(2)} + \langle A_{--}\rangle^{(2)}) \tag{4.4.6}$$

and the rest of the $\langle A_{ij}\rangle^{(2)}$'s are all zero.

Now, we proceed with a calculation of the Laplace transforms of the two-time correlation functions in the steady state limit to second order in the Rabi frequency α.

We have the following equations from (4.1.1).

$$\frac{d}{d\tau}\ \langle A_{+g}(\tau)\ A_{g+}(o)\rangle^{(2)} = (2i\delta-2\gamma_u-\gamma-\Gamma_{+g})\langle A_{+g}(\tau)A_{g+}(o)\rangle^{(2)}$$

$$- i\alpha\langle A_{gg}(\tau)A_{g+}(o)\rangle^{(1)} + i\alpha\langle A_{++}(\tau)A_{g+}(o)\rangle^{(1)}$$

$$+ i\alpha\ \langle A_{+-}(\tau)\ A_{g+}(o)\rangle^{(1)}\ , \tag{4.4.7}$$

$$\frac{d}{d\tau}\langle A_{+g}(\tau)A_{g-}(o)\rangle^{(2)} = (2i\delta-2\gamma_u-\gamma-\Gamma_{+g})\langle A_{+g}(\tau)A_{g-}(o)\rangle^{(2)}$$

$$- i\alpha\langle A_{gg}(\tau)A_{g-}(o)\rangle^{(1)} + i\alpha\langle A_{++}(\tau)A_{g-}(o)\rangle^{(1)}$$

$$+ i\alpha\langle A_{+-}(\tau)A_{g-}(o)\rangle^{(1)}, \qquad (4.4.8)$$

$$\frac{d}{d\tau}\langle A_{-g}(\tau)A_{g-}(o)\rangle^{(2)} = (i\delta-2\gamma_u-\gamma-\Gamma_{-g})\langle A_{-g}(\tau)A_{g-}(o)\rangle^{(2)}$$

$$- i\alpha\langle A_{gg}(\tau)A_{g-}(o)\rangle^{(1)} + i\alpha\langle A_{--}(\tau)A_{g-}(o)\rangle^{(1)}$$

$$+ i\alpha\langle A_{-+}(\tau)A_{g-}(o)\rangle^{(1)} \qquad (4.4.9)$$

and

$$\frac{d}{d\tau}\langle A_{-g}(\tau)A_{g+}(o)\rangle^{(2)} = (i\delta-2\gamma_u-\gamma-\Gamma_{-g})\langle A_{-g}(\tau)A_{g+}(o)\rangle^{(2)}$$

$$- i\alpha\langle A_{gg}(\tau)A_{g+}(o)\rangle^{(1)} + i\alpha\langle A_{--}(\tau)A_{g+}(o)\rangle^{(1)}$$

$$+ i\alpha\langle A_{-+}(\tau)A_{g+}(o)\rangle^{(1)}. \qquad (4.4.10)$$

Let us first consider eq. (4.4.7). We will be required to calculate the first order correlations whose equations can again be obtained with the help of the set of equations (4.1.1). We therefore obtain

$$\frac{d}{d\tau}\langle A_{gg}(\tau)A_{g+}(o)\rangle^{(1)} = 2\gamma\langle A_{g+}\rangle^{(1)} - 2(2\gamma_u+\gamma)\times$$

$$\langle A_{gg}(\tau)A_{g+}(o)\rangle^{(1)} - i\alpha\langle A_{+g}(\tau)A_{g+}(o)\rangle^{(o)}. \qquad (4.4.11)$$

$\langle A_{+g}(\tau)A_{g+}(o)\rangle^{(o)}$ is obtained from the equation

$$\frac{d}{d\tau}\langle A_{+g}(\tau)A_{g+}(o)\rangle^{(o)} = (2i\delta-2\gamma_u-\gamma-\Gamma_{+g})\langle A_{+g}(\tau)A_{g+}(o)\rangle^{(o)} ,$$

which on integration will yield

$$\langle A_{+g}(\tau)A_{g+}(o)\rangle^{(o)} = e^{(2i\delta-2\gamma_u-\gamma-\Gamma_{+g})\tau}\langle A_{+g}(\tau)A_{g+}(o)\rangle^{(o)} =$$

$$= e^{(2i\delta-2\gamma_u-\gamma-\Gamma_{+g})\tau}\langle A_{++}\rangle^{(o)} = e^{(2i\delta-2\gamma_u-\gamma-\Gamma_{+g})\tau}\frac{\gamma_u}{(2\gamma_u+\gamma)} \qquad (4.4.12)$$

Substituting (4.4.12) in (4.4.11), we have

$$\frac{d}{d\tau}\langle A_{gg}(\tau)\, A_{g+}(o)\rangle^{(1)} = 2\gamma\langle A_{g+}\rangle^{(1)} - 2(2\gamma_u+\gamma)\ x$$

$$\langle A_{gg}(\tau)A_{g+}(o)\rangle^{(1)} - \frac{i\alpha\gamma_u}{(2\gamma_u+\gamma)}\ e^{(2i\delta-2\gamma_u-\gamma-\Gamma_{+g})\tau} \qquad (4.4.13)$$

Taking the Laplace transform of (4.4.13), we obtain

$$z\,\langle A_{gg}(z)\hat{A}_{g+}(o)\rangle^{(1)} - \langle A_{g+}\rangle^{(1)} = \frac{2\gamma}{z}\langle A_{g+}\rangle^{(1)} - 2(2\gamma_u+\gamma)\ x$$

$$\langle A_{gg}(z)\hat{A}_{g+}(o)\rangle^{(1)} - \frac{i\alpha\gamma_u}{(2\gamma_u+\gamma)(z+2\gamma_u+\gamma+\Gamma_{+g}-2i\delta)} \qquad (4.4.14)$$

On simplifying this equation, we obtain for the Laplace transform of the first order correlation function $\langle A_{gg}(\tau)A_{g+}(o)\rangle^{(1)}$ the following :

$$\langle A_{gg}(z)\hat{A}_{g+}(o)\rangle^{(1)} = \frac{\langle A_{g+}(o)\rangle^{(1)}(z+2\gamma)}{z(z+2\gamma+4\gamma_u)} -$$

$$\frac{i\alpha\gamma_u/(2\gamma_u+\gamma)}{(z+2\gamma_u+\gamma+\Gamma_{+g}-2i\delta)(z+2\gamma+4\gamma_u)} \quad . \qquad (4.4.15)$$

The equation for $\langle A_{++}(\tau)A_{g+}(o)\rangle^{(1)}$ is written from (4.1.1) as

$$\frac{d}{d\tau}\langle A_{++}(\tau)A_{g+}(o)\rangle^{(1)} = i\alpha\langle A_{+g}(\tau)A_{g+}(o)\rangle^{(o)} +$$

$$2\gamma_u \langle A_{gg}(\tau)A_{g+}(o)\rangle^{(1)} - 2\gamma\langle A_{++}(\tau)A_{g+}(o)\rangle^{(1)} \qquad (4.4.16)$$

The Laplace transform of which is given by

$$(z+2\gamma)\langle A_{++}(z)\hat{A}_{g+}(o)\rangle^{(1)} = \frac{i\alpha\gamma_u}{(2\gamma_u+\gamma)(z+2\gamma_u+\gamma+\Gamma_{+g}-2i\delta)} +$$

$$2\gamma_u \langle A_{gg}(z)\hat{A}_{g+}(o)\rangle^{(1)} \qquad (4.4.17)$$

where $\langle A_{gg}(z)\hat{A}_{g+}(o)\rangle^{(1)}$ is given by (4.4.15).

Finally, the equation for the last of the first order correlations occuring in (4.4.7) is given by

$$\frac{d}{d\tau}\langle A_{+-}(\tau)A_{g+}(o)\rangle^{(1)} = (i\delta-2\gamma-\Gamma_{+-})\langle A_{+-}(\tau)A_{g+}(o)\rangle^{(1)} - i\alpha \times$$

$$\langle A_{g-}(\tau)A_{g+}(o)\rangle^{(o)} + i\alpha\langle A_{+g}(\tau)A_{g+}(o)\rangle^{(o)} . \qquad (4.4.18)$$

The Laplace transform equation of this is obtained as

$$\langle A_{+-}(z)\hat{A}_{g+}(o)\rangle^{(1)} = \frac{i\alpha\gamma_u}{(2\gamma_u+\gamma)(z+2\gamma_u+\gamma+\Gamma_{+g}-2i\delta)(z+2\gamma+\Gamma_{+-}-i\delta)} \cdot \tag{4.4.19}$$

Taking the Laplace transform on either side of (4.4.7) and substituting for all the first order correlation functions, we obtain

$$(z+2\gamma_u+\gamma+\Gamma_{+g}-2i\delta)\ \langle A_{+g}(z)\hat{A}_{g+}(o)\rangle^{(2)} = \langle A_{++}\rangle^{(2)} - \frac{\alpha^2\gamma_u}{(2\gamma_u+\gamma)} \times$$

$$\left[\frac{1}{(z+2\gamma_u+\gamma+\Gamma_{+g}-2i\delta)}\left(\frac{1}{(z+2\gamma+\Gamma_{+-}-i\delta)} + \frac{1}{(z+2\gamma)}\right)\right]$$

$$+ i\alpha\ \langle A_{gg}(z)\hat{A}_{g+}(o)\rangle^{(1)}\left(\frac{2\gamma_u}{(z+2\gamma)} - 1\right) \cdot \tag{4.4.20}$$

On simplifying (4.4.20), we have

$$\langle A_{+g}(z)\hat{A}_{g+}(o)\rangle^{(2)} = \hat{\Gamma}_{+gg+}(z) = \frac{\langle A_{++}\rangle^{(2)}}{(z+2\gamma_u+\gamma+\Gamma_{+g}-2i\delta)} -$$

$$\frac{\alpha^2\gamma_u/(2\gamma_u+\gamma)}{(z+2\gamma_u+\gamma+\Gamma_{+g}-2i\delta)^2}\left[\frac{1}{(z+2\gamma+\Gamma_{+-}-i\delta)} + \frac{1}{z+2\gamma}\right]$$

$$+ i\alpha\left(\frac{2\gamma_u}{z+2\gamma} - 1\right)\frac{\langle A_{g+}\rangle^{(1)}\ (z+2\gamma)}{z(z+2\gamma+4\gamma_u)(z+2\gamma_u+\gamma+\Gamma_{+g}-2i\delta)} -$$

$$\frac{i\alpha\gamma_u/(2\gamma_u+\gamma)}{(z+2\gamma_u+\gamma+\Gamma_{+g}-2i\delta)^2(z+2\gamma+4\gamma_u)} \tag{4.4.21}$$

We now proceed with the calculation of (4.4.8) in which we require to calculate the following first order correlations

$$\frac{d}{d\tau}\langle A_{gg}(\tau)A_{g-}(o)\rangle^{(1)} = 2\gamma\langle A_{g-}\rangle^{(1)} - 2(2\gamma_u+\gamma)\langle A_{gg}(\tau)A_{g-}(o)\rangle^{(1)}$$

$$- i\alpha\langle A_{+g}(\tau)A_{g-}(o)\rangle^{(o)} - i\alpha\langle A_{-g}(\tau)A_{g-}(o)\rangle^{(o)}. \quad (4.4.22)$$

From the equation for $\langle A_{-g}(\tau)A_{g-}(o)\rangle^{(o)}$, we find that

$$\langle A_{-g}(\tau)A_{g-}(o)\rangle^{(o)} = e^{(i\delta-2\gamma_u-\gamma-\Gamma_{-g})\tau}\frac{\gamma_u}{(2\gamma_u+\gamma)}. \quad (4.4.23)$$

It can easily be seen that

$$\langle A_{+g}(\tau)\, A_{g-}(o)\rangle^{(o)} = 0 .$$

Substituting (4.4.23) in (4.4.22) and taking the Laplace transform we obtain

$$\langle A_{gg}(z)\,\hat{A}_{g-}(o)\rangle^{(1)} = \frac{(z+2\gamma)\langle A_{g-}\rangle^{(1)}}{z\,(z+2\gamma+4\gamma_u)} -$$

$$\frac{i\alpha\gamma_u/(2\gamma_u+\gamma)}{(z+2\gamma+4\gamma_u)(z+2\gamma_u+\gamma+\Gamma_{-g}-i\delta)}, \quad (4.4.24)$$

and the equation for $\langle A_{++}(\tau)A_{g-}(o)\rangle^{(1)}$ is given as

$$\frac{d}{d\tau}\langle A_{++}(\tau)A_{g-}(o)\rangle^{(1)} = i\alpha\langle A_{+g}(\tau)A_{g-}(o)\rangle^{(o)} + 2\gamma_u \times$$

$$\langle A_{gg}(\tau)A_{g-}(o)\rangle^{(1)} - 2\gamma \langle A_{++}(\tau)A_{g-}(o)\rangle^{(1)}. \quad (4.4.25)$$

The Laplace transform of equation (4.4.25) is given by

$$\hat{\langle A_{++}(z)A_{g-}(o)\rangle}^{(1)} = \frac{2\gamma_u \langle A_{g-}\rangle^{(1)}}{z(z+2\gamma+4\gamma_u)} -$$

$$\frac{2i\alpha\, \gamma_u^2 / (2\gamma_u+\gamma)}{(z+2\gamma+4\gamma_u)(z+2\gamma)(z+2\gamma_u+\gamma+\Gamma_{-g}-i\delta)} . \quad (4.4.26)$$

We further find that

$$\langle A_{+-}(\tau)\, A_{g-}(o)\rangle^{(1)} = 0 .$$

Taking the Laplace transform of (4.4.8) and substituting for the first order Laplace transforms, we obtain

$$\hat{\Gamma}_{+gg-}(z) = \hat{\langle A_{+g}(z)A_{g-}(o)\rangle}^{(2)} = \frac{\langle A_{+-}\rangle^{(2)}}{(z+2\gamma_u+\gamma+\Gamma_{+g}-2i\delta)} +$$

$$\frac{(2\gamma_u - 2\gamma - z)}{(z+2\gamma+4\gamma_u)(z+2\gamma_u+\gamma+\Gamma_{+g}-2i\delta)} \left\{ \frac{i\alpha \langle A_{g-}\rangle^{(1)}}{z} \right.$$

$$\left. + \frac{\alpha^2 \gamma_u/(2\gamma_u+\gamma)}{(z+2\gamma)(z+2\gamma_u+\gamma+\Gamma_{-g} - i\delta)} \right\} . \quad (4.4.27)$$

We require to find the following first order correlation functions to evaluate (4.4.9)

$$\frac{d}{d\tau}\langle A_{--}(\tau)A_{g-}(o)\rangle^{(1)} = i\alpha\,\langle A_{-g}(\tau)A_{g-}(o)\rangle^{(o)}$$

$$+ 2\gamma_u\langle A_{gg}(\tau)A_{g-}(o)\rangle^{(1)} - 2\gamma\langle A_{--}(\tau)A_{g-}(o)\rangle^{(1)} \qquad (4.4.28)$$

Taking the Laplace transform of this, we obtain

$$\langle A_{--}(z)\hat{A}_{g-}(o)\rangle^{(1)} = \frac{i\alpha\gamma_u/(2\gamma_u+\gamma)}{(z+2\gamma)(z+2\gamma_u+\gamma+\Gamma_{-g}-i\delta)}$$

$$+ \frac{2\gamma_u\,(z+2\gamma)\langle A_{g-}\rangle^{(1)}}{z\,(z+2\gamma+4\gamma_u)} - \frac{2i\alpha\gamma_u^2\,/\,(2\gamma_u+\gamma)}{(z+2\gamma+4\gamma_u)(z+2\gamma_u+\gamma+\Gamma_{-g}-i\delta)}$$

(4.4.29)

and

$$\frac{d}{d\tau}\langle A_{-+}(\tau)A_{g-}(o)\rangle^{(1)} = -(2\gamma+\Gamma_{+-}+i\delta)\,\langle A_{-+}(\tau)A_{g-}(o)\rangle^{(1)}$$

$$+ i\alpha\,\langle A_{-g}(\tau)A_{g-}(o)\rangle^{(o)}\,. \qquad (4.4.30)$$

Substituting for $\langle A_{-g}(\tau)A_{g-}(o)\rangle^{(o)}$ and taking the Laplace transform, we have

$$\langle A_{-+}(z)\hat{A}_{g-}(o)\rangle^{(1)} = \frac{i\alpha\gamma_u/(2\gamma_u+\gamma)}{(z+2\gamma_u+\gamma+\Gamma_{-g}-i\delta)(z+2\gamma+\Gamma_{+-}+i\delta)}\,.$$

(4.4.31)

Substituting these in the Laplace transform equation of (4.4.9) and simplifying will yield for $\hat{\Gamma}_{-gg-}(z)$, the following :

$$\hat{\Gamma}_{-gg-}(z) = \langle A_{-g}(z)\hat{A}_{g-}(o)\rangle^{(2)} = \frac{\langle A_{--}\rangle^{(2)}}{(z+2\gamma_u+\gamma+\Gamma_{-g}-i\delta)}$$

$$- \frac{\alpha^2\gamma_u/(2\gamma_u+\gamma)}{(z+2\gamma_u+\gamma+\Gamma_{-g}-i\delta)^2}\left[\frac{1}{(z+2\gamma)} + \frac{1}{(z+2\gamma+\Gamma_{+-}+i\delta)}\right]$$

$$+ \frac{\alpha^2\gamma_u(2\gamma_u-2\gamma-z)(2\gamma_u+\gamma)}{(z+2\gamma)(z+2\gamma+4\gamma_u)(z+2\gamma_u+\gamma+\Gamma_{-g}-i\delta)^2}$$

$$+ \frac{i\alpha(2\gamma_u-z-2\gamma)\ \langle A_{g-}\rangle^{(1)}}{(z+2\gamma+4\gamma_u)(z+2\gamma_u+\gamma+\Gamma_{-g}-i\delta)z} \qquad (4.4.32)$$

Lastly we calculate the correlation function $\langle A_{-g}(\tau)\ A_{g+}(o)\rangle^{(2)}$ and evaluate its Laplace transform. The first order correlation functions required in this are calculated in the following.

$$\frac{d}{d\tau}\langle A_{--}(\tau)A_{g+}(o)\rangle^{(1)} = 2\gamma_u\langle A_{gg}(\tau)A_{g+}(o)\rangle^{(1)}$$

$$- 2\gamma\langle A_{--}(\tau)A_{g+}(o)\rangle^{(1)} \ . \qquad (4.4.33)$$

The Laplace transform of this is given by

$$\langle A_{--}(z)\hat{A}_{g+}(o)\rangle^{(1)} = \frac{2\gamma_u}{(2\gamma_u+\gamma)} \langle A_{gg}(z)\hat{A}_{g+}(o)\rangle^{(1)} \quad (4.4.34)$$

where $\langle A_{gg}(z)\hat{A}_{g+}(o)\rangle^{(1)}$ is given by (4.4.15) and it can further be seen that

$$\langle A_{-+}(\tau)\, A_{g+}(o)\rangle^{(1)} = 0 \ .$$

Therefore, the Laplace transform of the second order correlation function $\langle A_{-g}(\tau)A_{g+}(o)\rangle^{(2)}$ is given by

$$\hat{\Gamma}_{-gg+}(z) = \langle A_{-g}(z)\hat{A}_{g+}(o)\rangle^{(2)} = \frac{\langle A_{-+}\rangle^{(2)}}{(z+2\gamma_u+\gamma+\Gamma_{-g}-i\delta)}$$

$$+ \frac{\langle A_{g+}\rangle^{(1)}\ i\alpha\ (2\gamma_u-z-2\gamma)}{z(z+2\gamma+4\gamma_u)\ (z+2\gamma_u+\gamma+\Gamma_{-g}-i\delta)}$$

$$+ \frac{\alpha^2\gamma_u\ (2\gamma_u-z-2\gamma)\ /\ (2\gamma_u+\gamma)}{(z+2\gamma)(z+2\gamma+2\gamma_u)(z+2\gamma_u+\gamma+\Gamma_{+g}-2i\delta)(z+2\gamma_u+\gamma+\Gamma_{-g}-i\delta)}$$

(4.4.35)

The incoherent part of each of these correlation functions is obtained by substracting the $\frac{1}{z}$ portion of each quantity from the quantity itself. It has to be noted that there is a zeroth order contribution to the spectrum which arises due to the terms $\langle A_{+g}(z)\hat{A}_{g+}(o)\rangle^{(o)}$ and $\langle A_{-g}(z)\hat{A}_{g-}(o)\rangle^{(o)}$.

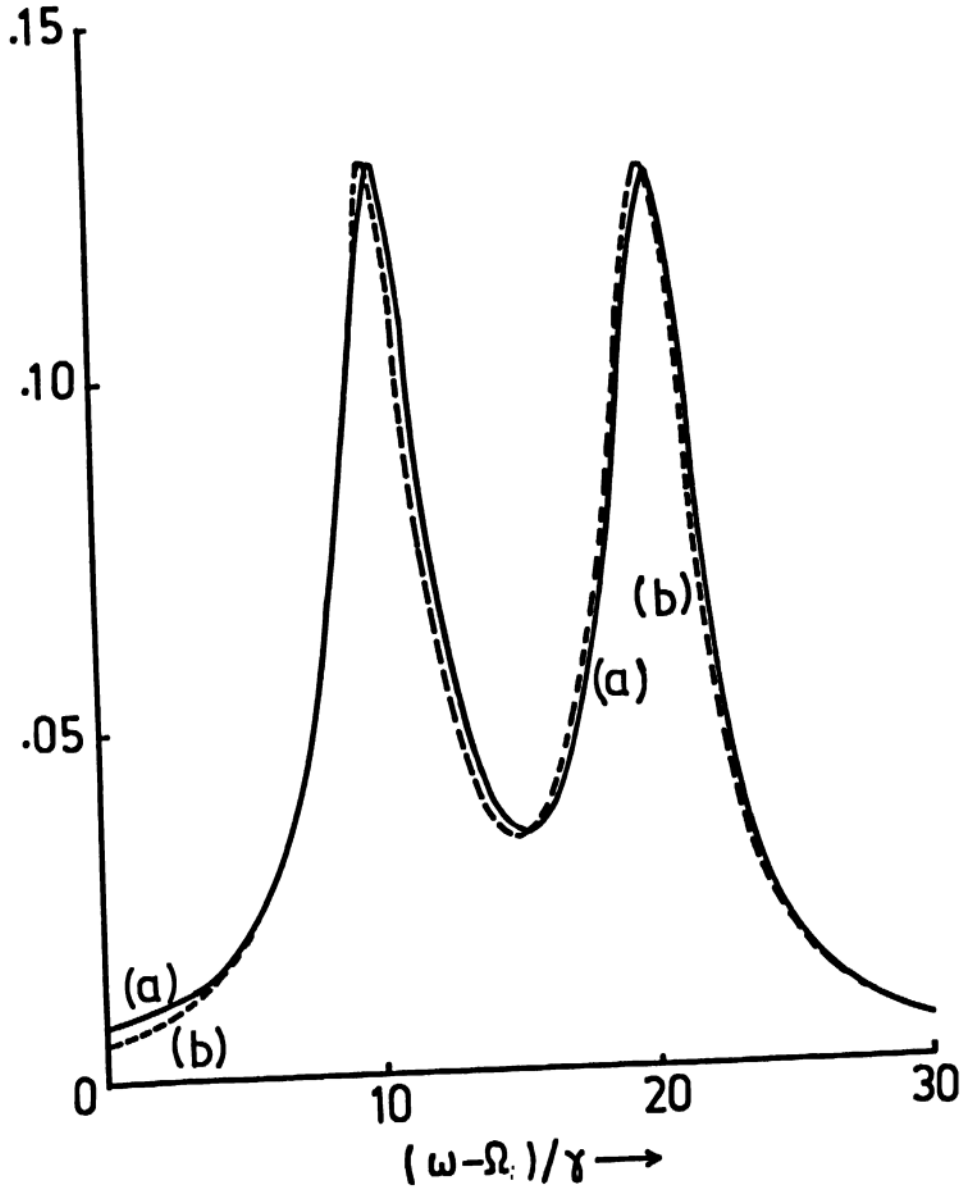

Fig.16 Weak field spectra S_x in optical Hanle case to second order in Rabi frequency for the values of parameters $\gamma_u = .5\gamma$, $\Gamma_{ij} = 0$, $\delta = 10\gamma$, $\theta = \pi/4$ and

(a) $\alpha = \gamma$ (b) $\alpha = .1\gamma$

From the analytical expressions, it is clear that the incoherent part of the spectrum of scattered radiation upto second order in the Rabi frequency of the driving field has resonances at $\omega = \Omega \pm i\delta$ and $\Omega + 2i\delta$. We now present the numerical results of our analytical formulae. Figure 16 shows the behaviour of the incoherent part of the fluorescence signal S_x for weak fields upto second order in α for the values of the parameters $\theta = \pi/4$, $\gamma = 1$, $\gamma_u = .5$, $\Gamma_{ij} = 0$, $\delta = 10$ (a) $\alpha = 1$ and (b) $\alpha = .1$. The spectra exhibit two peaks at $\omega = \Omega + \delta$ and $\Omega + 2\delta$. The peak at $\omega = \Omega - \delta$ is not visible because the weight factor corresponding to this peak is negligibly small when compared to that for the other two peaks. The signal S_x and S_y for the case when $\theta = \pi/2$ exhibit a very similar behaviour as shown in Fig. 16. Since the curves corresponding to this case are not very much different from those of Fig. 16 such curves are not shown here. The contribution to the spectrum arising due to the zeroth order term is much larger compared to that of the second order term. Therefore the spectra for different values of the field strength α do not show any marked difference.

In the limit when $\gamma_u \rightarrow 0$, the two-time correlation functions to second order in field strength simplify considerably and further there is no zeroth order contribution to the spectrum in this case unlike the situation

when $\gamma_u \neq 0$. The spectra S_x and S_y for the case when $\theta = \pi/4$ and for $\gamma_u = 0$ have the form

$$S_{\substack{x \\ y}}(\omega) = \alpha^2 \left[\frac{\Gamma_{+g}/\gamma}{[(\gamma+\Gamma_{+g})^2+4\delta^2]} \pm \frac{A(\Gamma_{+g}+\Gamma_{-g}-\Gamma_{+-})}{D}\right] \times$$

$$\frac{(\gamma+\Gamma_{+g})}{[(\gamma+\Gamma_{+g})^2+(\omega-\Omega-2\delta)^2]} + \left[\frac{\Gamma_{-g}/\gamma}{[(\gamma+\Gamma_{-g})^2+\delta^2]} \pm \frac{A(\Gamma_{+g}+\Gamma_{-g}-\Gamma_{+-})}{D}\right] \times$$

$$\frac{(\gamma+\Gamma_{-g})}{[(\gamma+\Gamma_{-g})^2+(\omega-\Omega-\delta)^2]} \pm \frac{(\Gamma_{+g}+\Gamma_{-g}-\Gamma_{+-})B}{D} \times$$

$$\left[\frac{(\omega-\Omega-\delta)}{[(\gamma+\Gamma_{-g})^2+(\omega-\Omega-\delta)^2]} - \frac{(\omega-\Omega-2\delta)}{[(\gamma+\Gamma_{+g})^2+(\omega-\Omega-2\delta)^2]}\right] \qquad (4.4.36)$$

where A, B and D are given by

$$A = \delta[(\gamma+\Gamma_{+g})(\gamma+\Gamma_{-g})+2\delta^2+(\gamma+2\Gamma_{-g}-\Gamma_{+g})(2\gamma+\Gamma_{+-})]$$

$$B = [(\gamma+\Gamma_{+g})(\gamma+\Gamma_{-g})+2\delta^2](2\gamma+\Gamma_{+-})-\delta^2(\gamma+2\Gamma_{-g}-\Gamma_{+-}) \qquad (4.4.37)$$

$$D = [(\gamma+\Gamma_{+g})^2+4\delta^2][(\gamma+\Gamma_{-g})^2][(2\gamma+\Gamma_{+-})^2+\delta^2] .$$

Here the '+' and '−' signs correspond to detection along x and y directions respectively and further only the incoherent part of the spectra S_x and S_y is presented in the above

From the expression (4.4.36), one can see that the width of the fluorescence signals depends on the relaxation parameters Γ_{+g} and Γ_{-g} which are pressure - dependent. Thus, in an experiment, by observing the spectra, an estimate of these pressure-dependent relaxation parameters can be made.

CHAPTER V

COHERENT OPTICAL HANLE EFFECT

So far, in our analysis, we have focussed our attention on single atom effects neglecting the atom-atom interactions. We have assumed that each atom emits independently of the other atoms in the sample. But in reality, one finds that, under certain conditions it is not true and that the atom-atom interaction plays a crucial role giving rise to new effects

such as N^2-dependent intensities etc. In fact, one might imagine the existence of optical bistability[53-64] which has drawn considerable interest from the aspect of practical application as optical devices and also from the fundamental standpoint as a model for studying the interaction between an ensemble of atoms and a radiation field. Optical bistability is a remarkable manifestation of the cooperative behaviour of atoms[53-56]. Experimentally, Gibbs, McCall and Venkatesan[54] showed that a Fabry-Perot cavity filled with sodium vapour as a nonlinear medium exhibits optical bistability. Recently experiments on absorptive optical bistability using multiple atomic beams have been reported[59,60].

In this chapter, we consider a mechanism for optical bistability utilizing the atomic coherence effects which occur in three level atomic systems[63-68]. The cooperative behaviour in the optical Hanle case, where the atomic sample is placed in a cavity with two modes of excitation[64] with different polarizations and under pumping by a linearly polarized electric field is investigated. The transmission characteristics for such a system in the special case when the intensities of both the cavity modes are identical, show that the system exhibits bistable behaviour. We also study the transmission characteristics of a cavity containing

atoms with a degenerate excited state and driven by external driving fields in the optical Hanle geometry. Here also the system exhibits bistable behaviour.

5.1 Description of the model and mathematical formulation

We consider a system of N atoms contained in a cell placed in a cavity with two modes of excitation[64] with different polarizations, under pumping by a linearly polarized electric field propagating along the z-direction. In addition to this, the system is interacting with a circularly polarized off-resonant laser field which lifts the degeneracy of the excited states and shifts and ground state also.

The cavity field is defined by

$$E_{cavity}(t) = g_1 a_1 \hat{\epsilon}_1 e^{-i\Omega t} + g_2 a_2 \hat{\epsilon}_2 e^{-i\Omega t} + H.c. \qquad (5.1.1)$$

where a_i and $\hat{\epsilon}_i$ $(i=1,2)$ are the annihilation operator and the polarization of the two modes of the cavity field respectively and a_i obeys the equation

$$\dot{a}_i = -i[H,a_i] - \kappa a_i \qquad (5.1.2)$$

where κ is the decay constant for the cavity field and the polarizations of the cavity field are taken to be

$$\hat{\epsilon}_1 = \frac{1}{\sqrt{2}} (\hat{x} + i\ \hat{y}) \text{ and } \hat{\epsilon}_2 = \frac{1}{\sqrt{2}} (\hat{x} - i\ \hat{y}) . \quad (5.1.3)$$

The pump field $\vec{E}(t)$ is defined by

$$\vec{E}(t) = (\hat{x} \cos\Theta + \hat{y} \sin\Theta)\ \mathcal{E}_o\ e^{-i\Omega t} + c.c.$$

$$= \vec{\mathcal{E}}(t)\ e^{-i\Omega t} + c.c. \quad (5.1.4)$$

where Θ is the angle which the electric vector of the pump field makes with the x-direction. Let us designate the total electric field which is a sum of the pump field and the cavity field by $\vec{E}_T$, i.e.,

$$\vec{E}_T = \vec{E}_{cavity}(t) + \vec{E}(t) . \quad (5.1.5),$$

Therefore, the Hamiltonian for the system in interaction with the total electric field and the circularly polarized off-resonant laser field in the electric dipole approximation is given by

$$H = \hbar\omega_o(A_{++}+A_{--}) - (\vec{d}_{+g}.\vec{E}_T A_{+g}+\vec{d}_{-g}.\vec{E}_T A_{-g}+H.c)$$

$$- (\vec{d}_{+g}.\vec{E}_c(t)A_{+g}+H.c.) \quad (5.1.6)$$

where $\vec{E}_c$ stands for the circularly polarized off-resonant laser field of frequency ω_c defined by

$$\vec{E}_c(t) = \vec{\mathcal{E}}_c \, e^{-i\omega_c t} + \text{c.c.} \qquad (5.1.7)$$

After applying the Bogoliubov-Mitropolsky's method of time averaging for treating the interaction of E_c with the atomic system, which results in the light shift terms[36,37] [cf. Sec. (3.1)], we obtain

$$H'(t) = -[\vec{d}_{+g}A_{+g}+\vec{d}_{-g}A_{-g}+\vec{d}^{*}_{+g}A_{g+}+\vec{d}^{*}_{-g}A_{g-}].[\vec{\mathcal{E}}(t)+g_1a_1\hat{\epsilon}_1+ g_2a_2\hat{\epsilon}_2) \, e^{-i\Omega t} + \text{H.c.}]+\hbar(\omega_o-\Omega+\delta) \, A_{++}+\hbar(\omega_o-\Omega) \, A_{--} - \hbar\delta \, A_{gg} \, . \qquad (5.1.8)$$

As a next step in our calculation, we obtain the equations of motion for the atomic density matrix elements using the master equation (2.2.7) (where $\mathcal{L}_{inc}$ represents a general relaxation mechanism which comprises of spontaneous, collisional and other incoherent relaxations) as follows :

$$\dot{\sigma}_{++} = i \, \vec{d}_{+g}.\vec{E}_T \, \sigma_{g+} - i \, \vec{d}^{*}_{+g}.\vec{E}_T\sigma_{+g} - 2\gamma\sigma_{++}+2\gamma_u\sigma_{gg} \, ,$$

$$\dot{\sigma}_{--} = i \, \vec{d}_{-g}.\vec{E}_T\sigma_{g-} - i \, \vec{d}^{*}_{-g}.\vec{E}_T \, \sigma_{-g} - 2\gamma\sigma_{--}+2\gamma_u\sigma_{gg} \, ,$$

$$\dot{\sigma}_{gg} = -(\sigma_{++} + \sigma_{--}) ,$$

$$\dot{\sigma}_{+-} = i\,\vec{d}_{+g}.\vec{E}_T\sigma_{g-} - i\vec{d}^{*}_{-g}.\vec{E}_T\sigma_{+g} - (2\gamma+i\delta)\sigma_{+g} ,$$

$$\dot{\sigma}_{+g} = i\,\vec{d}_{+g}.\vec{E}_T(\sigma_{gg}-\sigma_{++}) - i\vec{d}_{-g}.\vec{E}_T\sigma_{+-} - [i(\omega_o+2\delta)+\gamma+2\gamma_u]\sigma_{+g} ,$$

$$\dot{\sigma}_{-g} = i\,\vec{d}_{-g}.\vec{E}_T(\sigma_{gg}-\sigma_{--}) - i\vec{d}_{+g}.\vec{E}_T\sigma_{-+} - [i(\omega_o+\delta)+\gamma+2\gamma_u]\sigma_{-g} ,$$

(5.1.9)

where γ_u represents a general relaxation mechanism which is a sum of the collisional and other incoherent relaxations. The equations of motion for the cavity field operators are given by

$$\dot{a}_1 = i[\vec{d}_{+g}.\hat{\epsilon}_1 A_{+g} + \vec{d}_{-g}.\hat{\epsilon}_1 A_{-g} + H.c.]N\,g_1\,e^{i\Omega t} - \kappa\,a_1 ,$$

$$\dot{a}_2 = i[\vec{d}_{+g}.\hat{\epsilon}_2 A_{+g} + \vec{d}_{-g}.\hat{\epsilon}_2 A_{-g} + H.c.]N\,g_2\,e^{i\Omega t} - \kappa\,a_2 ,$$

(5.1.10)

where N is the number of atoms interacting with the cavity field. The matrix elements of the dipole moment operator for J=0 to J=1 transition from the previous analysis are given by [cf. eq. (3.1.11)]

$$\vec{d}_{+g} = R(-\hat{x} + i\hat{y}) \text{ and } \vec{d}_{-g} = R(\hat{x} + i\hat{y}) \qquad (5.1.11)$$

where R represents the radial part of the dipole matrix element. After making the rotating wave approximation and

substituting for the matrix elements of the dipole moment, the equations for the cavity operators simplify to

$$\langle \dot{a}_1 \rangle = -iR\sqrt{2}Ng_1 \langle A_{g+} \rangle - \kappa \langle a_1 \rangle$$

$$\langle \dot{a}_2 \rangle = iR\sqrt{2}Ng_2 \langle A_{g-} \rangle - \kappa \langle a_2 \rangle \ . \qquad (5.1.12)$$

Substituting for the different polarizations in (5.1.5), the total electric field $\vec{E}_T(t)$ can be rewritten as

$$\vec{E}_T(t) = [(\hat{x}\cos\theta + \hat{y}\sin\theta)\,\mathcal{E}_o + \frac{(\hat{x}+i\hat{y})g_1a_1}{\sqrt{2}} + \frac{(\hat{x}-i\hat{y})g_2a_2}{\sqrt{2}}]\, e^{-i\Omega t} + H.c.$$

$$= \vec{\mathcal{E}}_T\, e^{-i\Omega t} + \vec{\mathcal{E}}_T^{*}\, e^{i\Omega t} \qquad (5.1.13)$$

and therefore

$$\vec{d}_{+g}\cdot\vec{\mathcal{E}}_T = -R\mathcal{E}_o\, e^{-i\theta}\, \frac{(1+\sqrt{2}\, g_1R\langle a_1\rangle e^{i\theta})}{R\mathcal{E}_o} \equiv \tilde{z}_1$$

and

$$\vec{d}_{-g}\cdot\vec{\mathcal{E}}_T = R\mathcal{E}_o\, e^{i\theta}\, \frac{(1+\sqrt{2}\, g_2R\langle a_2\rangle e^{-i\theta})}{R\mathcal{E}_o} \equiv \tilde{z}_2 \ . \qquad (5.1.14)$$

A new set of equations of motion for the $\tilde{\sigma}_{ij}$'s can now be written. We further make a transformation on these matrix elements to eliminate the θ - dependence.

$$\tilde{\tilde{\sigma}}_{+g} = -\tilde{\sigma}_{+g}\, e^{i\theta} \;,\; \tilde{\tilde{\sigma}}_{-g} = \tilde{\sigma}_{-g}\, e^{-i\theta} \;,\; \tilde{\tilde{\sigma}}_{+-} = -\tilde{\sigma}_{+-}\, e^{2i\theta} \;,$$

$$\tilde{\tilde{\sigma}}_{ii} = \tilde{\sigma}_{ii} \qquad (5.1.15)$$

and

$$z_1 = R\mathcal{E}_o \left[\frac{1 + \sqrt{2}\, g_1 \langle a_1 \rangle\, R\, e^{i\theta}}{R\mathcal{E}_o} \right]$$

$$z_2 = R\mathcal{E}_o \left[\frac{1 + \sqrt{2}\, g_2 \langle a_2 \rangle\, R\, e^{-i\theta}}{R\mathcal{E}_o} \right] . \qquad (5.1.16)$$

Let us further redefine z_1 and z_2 in a more simplified manner as

$$z_1 = |z_1|\, e^{i\Lambda_1} = \alpha_1\, e^{i\Lambda_1}$$

$$z_2 = |z_2|\, e^{i\Lambda_2} = \alpha_2\, e^{i\Lambda_2} \qquad (5.1.17)$$

and redefine the density matrix elements as

$$\tilde{\tilde{\sigma}}_{ii} = \bar{\sigma}_{ii} \;,\; \tilde{\tilde{\sigma}}_{+g} = \bar{\sigma}_{+g}\, e^{i\Lambda_1} \;,\; \tilde{\tilde{\sigma}}_{-g} = \bar{\sigma}_{-g}\, e^{i\Lambda_2}$$

$$\tilde{\tilde{\sigma}}_{+-} = \bar{\sigma}_{+-}\, e^{i(\Lambda_1 - \Lambda_2)} \;,\; \tilde{\tilde{\sigma}}_{ii} = \bar{\sigma}_{ii} \qquad (5.1.18)$$

The equations of motion for the new set of density matrix elements $\bar{\sigma}_{ij}$'s are obtained as

$$\dot{\bar{\sigma}}_{++} = i\alpha_1 (\bar{\sigma}_{g+} - \bar{\sigma}_{+g}) - 2\gamma\, \bar{\sigma}_{++} + 2\gamma_u\, \bar{\sigma}_{gg} \;,$$

$$\dot{\bar{\sigma}}_{--} = i\alpha_2 (\bar{\sigma}_{g-} - \bar{\sigma}_{-g}) - 2\gamma \bar{\sigma}_{--} + 2\gamma_u \bar{\sigma}_{gg} ,$$

$$\dot{\bar{\sigma}}_{gg} = - (\dot{\bar{\sigma}}_{++} + \dot{\bar{\sigma}}_{--}) ,$$

$$\dot{\bar{\sigma}}_{+-} = i\alpha_1 \bar{\sigma}_{g-} - i\alpha_2 \bar{\sigma}_{+g} - (2\gamma + i\delta) \bar{\sigma}_{+-} , \qquad (5.1.19)$$

$$\dot{\bar{\sigma}}_{+g} = i\alpha_1 (\bar{\sigma}_{gg} - \bar{\sigma}_{++}) - i\alpha_2 \bar{\sigma}_{+-} - (2\gamma_u + \gamma + 2i\delta) \bar{\sigma}_{+g} ,$$

$$\dot{\bar{\sigma}}_{-g} = i\alpha_2 (\bar{\sigma}_{gg} - \bar{\sigma}_{--}) - i\alpha_1 \bar{\sigma}_{-+} - (2\gamma_u + \gamma + i\delta) \bar{\sigma}_{-g} .$$

Since the measurements are made at times much larger than the decay constants involved in the problem, the atomic density matrix elements have to be evaluated in the steady state limit. The steady state solutions of the density matrix elements are presented in the next section.

5.2 Steady state solutions of the density matrix elements

The steady state solutions of the set of linear differential equations (5.1.19) can be obtained by equating the left hand side to zero and solving them. We briefly outline the steps in solving the set of equations (5.1.19) at steady state. From the equation for $\bar{\sigma}_{++}$, we obtain

$$\gamma \bar{\sigma}_{++} - \gamma_u \bar{\sigma}_{gg} = \alpha_1 \, \mathrm{Im} \, \bar{\sigma}_{+g} \qquad (5.2.1)$$

and from the equation for $\bar{\sigma}_{--}$, we have

$$\gamma\ \bar{\sigma}_{--} - \gamma_u \bar{\sigma}_{gg} = \alpha_2\ \mathrm{Im}\ \bar{\sigma}_{-g}\ . \qquad (5.2.2)$$

Simplifying these two equations by using the relation $\bar{\sigma}_{++} + \bar{\sigma}_{--} + \bar{\sigma}_{gg} = 1$, we obtain for $\bar{\sigma}_{++}$ and $\bar{\sigma}_{--}$, the following

$$\bar{\sigma}_{++} = \frac{\gamma_u}{(2\gamma_u+\gamma)} + \frac{\alpha_1(\gamma+\gamma_u)}{(2\gamma_u+\gamma)\gamma}\ \mathrm{Im}\ \bar{\sigma}_{+g} - \frac{\alpha_2\ \gamma_u}{(2\gamma_u+\gamma)\gamma}\ \mathrm{Im}\ \bar{\sigma}_{-g}\ . \qquad (5.2.3)$$

and

$$\bar{\sigma}_{--} = \frac{\gamma_u}{(2\gamma_u+\gamma)} + \frac{\alpha_2(\gamma+\gamma_u)}{(2\gamma_u+\gamma)\gamma}\ \mathrm{Im}\ \bar{\sigma}_{-g} - \frac{\alpha_1\gamma_u}{(2\gamma_u+\gamma)\gamma}\ \mathrm{Im}\ \bar{\sigma}_{+g}\ . \qquad (5.2.4)$$

The real parts of the off-diagonal elements $\bar{\sigma}_{+g}$, $\bar{\sigma}_{-g}$ and $\bar{\sigma}_{+-}$ are obtained as

$$\mathrm{Re}\ \bar{\sigma}_{+g} = \frac{2\delta}{(2\gamma_u+\gamma)}\ \mathrm{Im}\ \bar{\sigma}_{+g} + \frac{\alpha_2}{(2\gamma_u+\gamma)}\ \mathrm{Im}\ \bar{\sigma}_{+-}\ , \qquad (5.2.5)$$

$$\mathrm{Re}\ \bar{\sigma}_{-g} = \frac{\delta}{(2\gamma_u+\gamma)}\ \mathrm{Im}\ \bar{\sigma}_{-g} - \frac{\alpha_1}{(2\gamma_u+\gamma)}\ \mathrm{Im}\ \bar{\sigma}_{+-} \qquad (5.2.6)$$

and

$$\mathrm{Re}\ \bar{\sigma}_{+-} = \frac{1}{2\gamma}\ [\ \delta\ \mathrm{Im}\ \bar{\sigma}_{+-} + \alpha_1\ \mathrm{Im}\ \bar{\sigma}_{-g} + \alpha_2\ \mathrm{Im}\ \bar{\sigma}_{+g}\ ]\ . \qquad (5.2.7)$$

Taking the imaginary part of $\bar{\sigma}_{+-}$ equation and simplifying, we have

$$\text{Im } \bar{\sigma}_{+-} = -\delta[\alpha_2(2\gamma_u+5\gamma)\text{Im } \bar{\sigma}_{+g}+\alpha_1(2\gamma_u-\gamma) \text{ Im } \bar{\sigma}_{-g}]D^{-1} \tag{5.2.8}$$

where

$$D = (4\gamma^2+\delta^2)\ (2\gamma_u+\gamma) + (\alpha_1^2 + \alpha_2^2)\ 2\gamma\ . \tag{5.2.9}$$

The imaginary parts of $\bar{\sigma}_{+g}$ and $\bar{\sigma}_{-g}$ equations respectively are given by

$$2\delta \text{ Re } \bar{\sigma}_{+g} + (2\gamma_u+\gamma)\text{Im } \bar{\sigma}_{+g}+\alpha_2 \text{ Re } \bar{\sigma}_{+-}+\alpha_1(2\bar{\sigma}_{++}+\bar{\sigma}_{--})-\alpha_1=0, \tag{5.2.10}$$

$$\delta \text{ Re } \bar{\sigma}_{-g} + (2\gamma_u+\gamma)\text{Im } \bar{\sigma}_{-g}+\alpha_1 \text{ Re } \bar{\sigma}_{+-}+\alpha_2(2\bar{\sigma}_{--}+\bar{\sigma}_{++})-\alpha_2=0\ . \tag{5.2.11}$$

Using equations (5.2.3) to (5.2.8) in (5.2.10) and (5.2.11) and simplifying, we obtain two equations in Im $\bar{\sigma}_{+g}$ and Im $\bar{\sigma}_{-g}$ which are of the form

$$\text{Im } \bar{\sigma}_{+g}\left[\frac{4\delta^2+(2\gamma_u+\gamma)^2}{(2\gamma_u+\gamma)} + \frac{\alpha_2^2}{2\gamma} + \frac{\alpha_1^2(2\gamma+\gamma_u)}{\gamma(2\gamma_u+\gamma)} - \frac{\delta^2\alpha_2^2(2\gamma_u+5\gamma)^2}{2\gamma(2\gamma_u+\gamma)\ D}\right] +$$

$$\text{Im } \bar{\sigma}_{-g}\left[\frac{3}{2(2\gamma_u+\gamma)} - \frac{\delta^2(2\gamma_u+5\gamma)(2\gamma_u-\gamma)}{2\gamma(2\gamma_u+\gamma)D}\right]\alpha_1\alpha_2 + \frac{\alpha_1(\gamma_u-\gamma)}{(2\gamma_u+\gamma)} = 0, \tag{5.2.12}$$

$$\text{Im}\ \bar{\sigma}_{+g}\left[\frac{3}{2(2\gamma_u+\gamma)} - \frac{\delta^2(2\gamma_u+5\gamma)(2\gamma_u-\gamma)}{2\gamma(2\gamma_u+\gamma)}\right]\alpha_1\alpha_2 + \frac{\alpha_2(\gamma_u-\gamma)}{(2\gamma_u+\gamma)} +$$

$$\text{Im}.\ \bar{\sigma}_{-g}\left[\frac{\delta^2+(2\gamma_u+\gamma)^2}{(2\gamma_u+\gamma)} + \frac{\alpha_1^2}{2\gamma} + \frac{\alpha_2^2(2\gamma+\gamma_u)}{\gamma(2\gamma_u+\gamma)} -\right.$$

$$\left.\frac{\delta^2\alpha_1^2(2\gamma_u-\gamma)^2}{2\gamma(2\gamma_u+\gamma)D}\right] = 0 \quad . \qquad (5.2.13)$$

From (5.1.12), the steady state solutions of $\langle a_i\rangle$'s are obtained as

$$\langle a_1\rangle = \frac{-\,i\ R\sqrt{2}\ g_1 N\ \langle\tilde{A}_{g+}\rangle}{\kappa} = \frac{-i\ R\sqrt{2}\ g_1\tilde{\sigma}_{+g}}{\kappa} \qquad (5.2.14)$$

and

$$\langle a_2\rangle = \frac{i\ R\sqrt{2}\ g_2 N\ \langle\tilde{A}_{g-}\rangle}{\kappa} = \frac{i\ R\sqrt{2}\ g_2\tilde{\sigma}_{-g}}{\kappa} \qquad (5.2.15)$$

The density matrix elements in the tilde '~' frame are related to those in '-' frame by

$$\tilde{\sigma}_{+g} = -\bar{\sigma}_{+g}\ e^{-i(\theta-\Lambda_1)}$$

$$\tilde{\sigma}_{-g} = \bar{\sigma}_{-g}\ e^{i(\theta+\Lambda_2)} \qquad (5.2.16)$$

Substituting for $\langle a_1\rangle$ and $\langle a_2\rangle$ in equations (5.1.16), we have

$$z_1 = \alpha_1 e^{i\Lambda_1} = \alpha_o + \frac{2i\, Ng_1^2 R^2}{\kappa} \bar{\sigma}_{+g} e^{i\Lambda_1} , \qquad (5.2.17a)$$

$$z_2 = \alpha_2 e^{i\Lambda_2} = \alpha_o + \frac{2i\, Ng_2^2 R^2}{\kappa} \bar{\sigma}_{-g} e^{i\Lambda_2} , \qquad (5.2.17b)$$

where $\alpha_o = R\,\mathcal{E}_o$.

Rewriting these two equations, we obtain

$$\alpha_o = \left(\alpha_1 - \frac{2i\, Ng_1^2 R^2}{\kappa} \bar{\sigma}_{+g} \right) e^{i\Lambda_1} \qquad (5.2.18a)$$

$$\alpha_o = \left(\alpha_2 - \frac{2i\, Ng_2^2 R^2}{\kappa} \bar{\sigma}_{-g} \right) e^{i\Lambda_2} . \qquad (5.2.18b)$$

Taking the modulus on either side of the equations (5.2.18a and b) and defining

$$\nu_i = 2Ng_i^2 R^2/\kappa\gamma , \qquad (5.2.19)$$

we obtain the following pair of transcendental equations.

$$\alpha_o = \alpha_1 \left| 1 - \frac{i\gamma\nu_1}{\alpha_1} \bar{\sigma}_{+g} \right| , \qquad (5.2.20)$$

$$\alpha_o = \alpha_2 \left| 1 - \frac{i\gamma\nu_2}{\alpha_2} \bar{\sigma}_{-g} \right| . \qquad (5.2.21)$$

The solution of these two equations appears very difficult and hence we studied a simplified situation when the

intensities of both the cavity modes are equal namely when $\alpha_1 = \alpha_2 = \alpha$.

For the case when $\gamma_u=0$ and $\delta=0$ the equations (5.2.12) and (5.2.13) simplify to

$$(2\gamma^2+4\alpha_1^2+\alpha_2^2)\ \mathrm{Im}\ \bar{\sigma}_{+g} + 3\alpha_1\alpha_2\ \mathrm{Im}\ \bar{\sigma}_{-g} - 2\gamma\alpha_1 = 0 \qquad (5.2.22)$$

$$(2\gamma^2+\alpha_1^2+4\alpha_2^2)\ \mathrm{Im}\ \bar{\sigma}_{-g} + 3\alpha_1\alpha_2\ \mathrm{Im}\ \bar{\sigma}_{+g} - 2\gamma\alpha_2 = 0\ . \qquad (5.2.23)$$

Solving these two equations and by substituting for these in (5.2.5) to (5.2.8) we obtain the relevant quantities that occur in (5.2.18a) and (5.2.18b). After simplification, the pair of transcendental equations (5.2.18a and b) will reduce to the following

$$\alpha_o = \alpha_1\, e^{i\Lambda_1} \left[\, 1 + \frac{2\,\nu_1}{\left(\, 1+\frac{2I}{\gamma^2}\,\right)}\,\right] \qquad (5.2.24)$$

and

$$\alpha_o = \alpha_2\, e^{i\Lambda_2} \left[\, 1 + \frac{2\,\nu_2}{\left(\, 1+\frac{2I}{\gamma^2}\,\right)}\,\right]\ . \qquad (5.2.25)$$

where

$$I = \left(\, \alpha_1^2 + \alpha_2^2 \,\right)\ .$$

Using (5.1.17) these can be rewritten as

$$\alpha_o = z_1 \left(\, 1 + \frac{2\nu_1}{1+\frac{2I}{\gamma^2}}\,\right) \qquad (5.2.26)$$

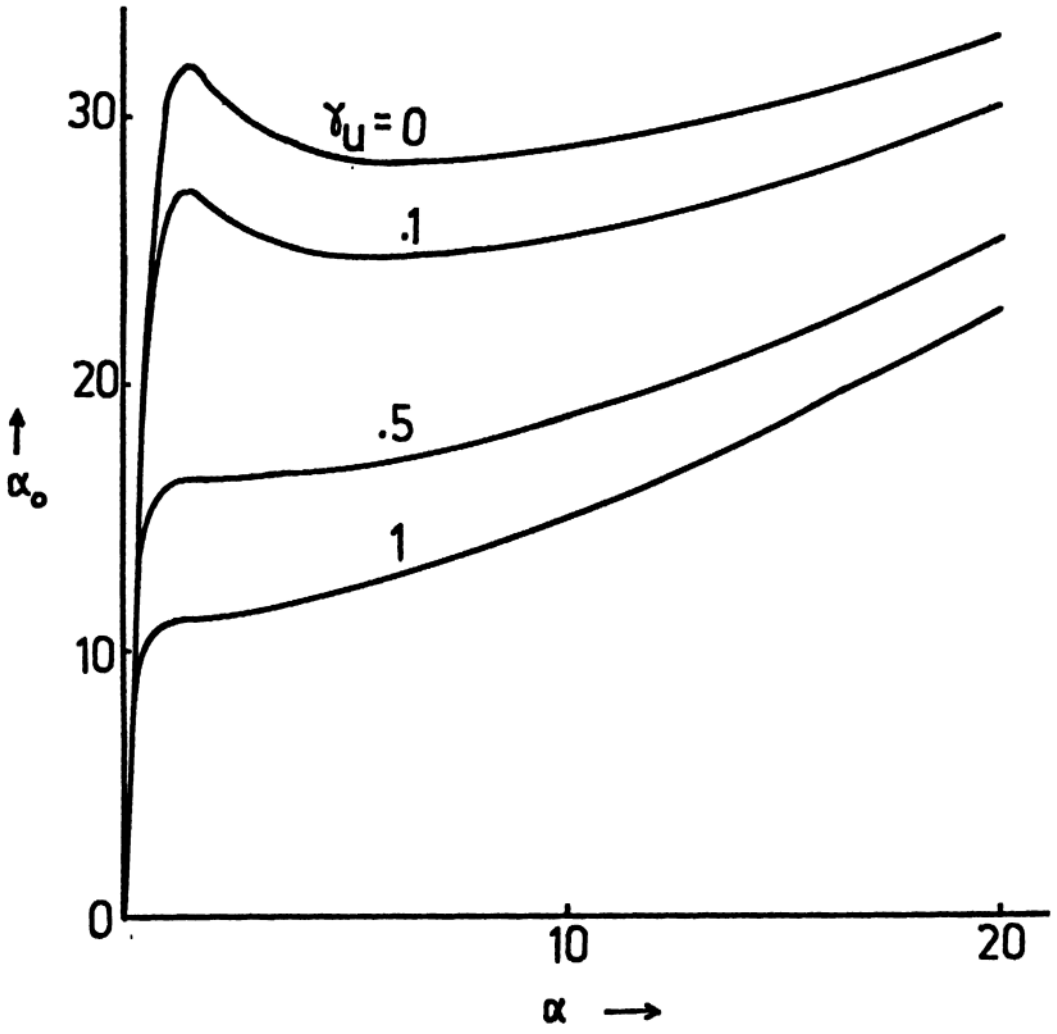

Fig.17 Input field α_o vs output field α for different values of relaxation parameter γ_u (indicated in the figure) for the values of the parameters $\nu = 50$, $\delta = 1$ and $\gamma = 1$.

$$\alpha_o = z_2 \left(1 + \frac{2\nu_2}{1+\frac{2I}{\gamma^2}} \right) \qquad (5.2.27)$$

which are nothing but the bistability equations for a two mode cavity field containing two level atoms. For the single mode case when $z_1=z_2$ and $\nu_1= \nu_2$ equations (5.2.26) and (5.2.27) will reduce to a single equation namely the standard bistability equation for a two-level atom[53].

We now present some of the numerical results of our calculations for the single mode cavity field case. Figure 17 shows the behaviour of the input field α_o vs the output field α for different values of the relaxation parameter γ_u for the parameter $\nu = 50$, light shift $\delta = 1$ and the relaxation rate $\gamma = 1$. The system exhibits bistable behaviour throughout, for the choice of parameters chosen here. Thus the transmission characteristics of the system are seen to be strongly dependent on the choice of the relaxation parameters.

5.3 Cooperative behaviour of optical Hanle system under external pumping

We now consider the situation when there are additional relaxation mechanisms in the system. We allow the excited states to decay at a rate $2\gamma_1$ and the ground state at a rate $2\gamma_o$ (see fig.18). Due to these additional decay channels, the atomic states will be

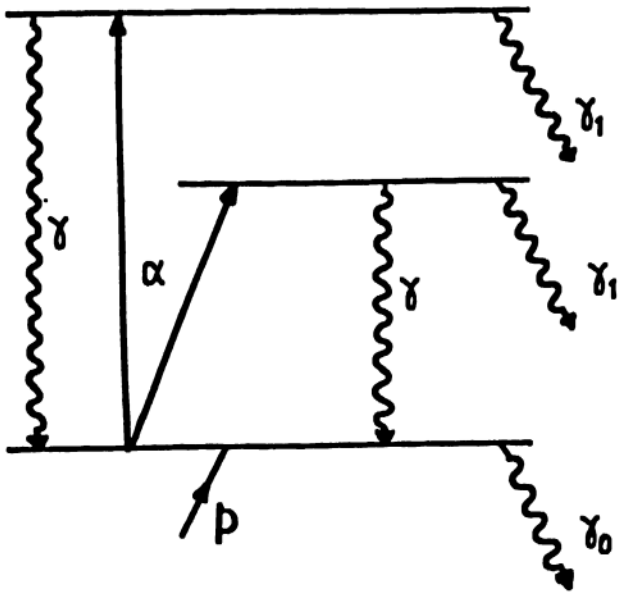

Fig.18 Schematic representation of the energy level diagram for optical Hanle geometry with additional relaxations and under external pumping

depleted after a certain time. In order to maintain a steady state population in the levels of the system, the ground state has to be pumped with atoms by an external source. We therefore introduce a parameter p which is the rate at which atoms are pumped into the ground state. We simplify the analysis by considering the cavity field to comprise of a single mode and we consider the cavity frequency to be detuned from the frequency of the driving field. The total electric field which is a sum of the pump field and the cavity field therefore is given by

$$\vec{E}_T = (\hat{x}\cos\Theta + \hat{y}\sin\Theta)\,\mathcal{E}_o e^{-i\Omega t} + c.c. + g\,a\,\hat{\epsilon}\,e^{-i\Omega_c t} + g\,a^+\,\hat{\epsilon}^*\,e^{i\Omega_c t} \qquad (5.3.1)$$

where $\hat{\epsilon}$ is the polarization of the cavity field given by

$$= (\hat{x}\cos\phi + \hat{y}\sin\phi) \quad . \qquad (5.3.2)$$

The equation for the cavity operator a therefore is given by

$$\langle a\rangle = iRgN\,[e^{-i(\Theta-\phi)}\langle\tilde{A}_{g+}\rangle + e^{i(\Theta-\phi)}\langle\tilde{A}_{g-}\rangle] - [i(\Omega_c-\Omega)+\kappa]\langle a\rangle \qquad (5.3.3)$$

where '~' denotes the operators in the frame rotating with the frequency of the driving field.

For the simplified situation when the cavity field has the same polarization as the applied field, we have

$$\langle a \rangle = \frac{iRNg}{\kappa(1+i\eta)} \left[\langle \tilde{A}_{g+} \rangle + \langle \tilde{A}_{g-} \rangle \right] \qquad (5.3.4)$$

where $\eta = (\Omega_c - \Omega)/\kappa$ and

$$z = \alpha\, e^{i\Lambda} = \alpha_o = RNg \langle a \rangle \qquad (5.3.5)$$

where $\alpha_o = R\,\mathcal{E}_o$. Let us further define

$$\langle \tilde{A}_{g+} \rangle = \langle \bar{A}_{g+} \rangle\, e^{i\Lambda}, \langle \tilde{A}_{g-} \rangle = \langle \bar{A}_{g-} \rangle\, e^{i\Lambda}\,.$$

Substituting for $\langle a \rangle$ in (5.3.5), we obtain

$$\alpha_o = \left[\alpha - \frac{i\nu\gamma}{1+i\eta} (\bar{\sigma}_{+g} + \bar{\sigma}_{-g})\right] e^{i\Lambda} \qquad (5.3.6)$$

where

$$\nu = \frac{Ng^2R^2}{\kappa\gamma}\,.$$

Taking the modulus on either side of (5.3.6) and simplifying we obtain

$$|\alpha_o| = \left| \alpha - \frac{\gamma(\eta+i)}{(1+\eta^2)} (\bar{\sigma}_{+g} + \bar{\sigma}_{-g}) \right|\,. \qquad (5.3.7)$$

We now proceed forth to calculate the density matrix elements under steady state conditions. The equations of

of motion for the density matrix elements $\bar{\sigma}_{ij}$ for the above system are given by

$$\dot{\bar{\sigma}}_{++} = -(2\gamma_1+2\gamma)\ \bar{\sigma}_{++} + i\alpha\ (\bar{\sigma}_{g+} - \bar{\sigma}_{+g}), \tag{5.3.8}$$

$$\dot{\bar{\sigma}}_{--} = -(2\gamma_1+2\gamma)\ \bar{\sigma}_{--} + i\alpha\ (\bar{\sigma}_{g-} - \bar{\sigma}_{-g}), \tag{5.3.9}$$

$$\dot{\bar{\sigma}}_{+-} = -(2\gamma_1+2\gamma+i\delta)\ \bar{\sigma}_{+-} + i\alpha\ (\bar{\sigma}_{g-} - \bar{\sigma}_{+g}), \tag{5.3.10}$$

$$\dot{\bar{\sigma}}_{+g} = -(\gamma_o+\gamma_1+\gamma+i\ (2\delta-\Delta))\ \bar{\sigma}_{+g}+i\alpha(\bar{\sigma}_{gg}-\bar{\sigma}_{++}-\bar{\sigma}_{+-}), \tag{5.3.11}$$

$$\dot{\bar{\sigma}}_{-g} = -(\gamma_o+\gamma_1+\gamma+i(\delta-\Delta))\bar{\sigma}_{-g}+i\alpha(\bar{\sigma}_{gg}-\bar{\sigma}_{--}-\bar{\sigma}_{-+}) \tag{5.3.12}$$

and

$$\dot{\bar{\sigma}}_{gg} = 2\gamma(\bar{\sigma}_{++}+\bar{\sigma}_{--})-i\alpha(\bar{\sigma}_{g+}-\bar{\sigma}_{+g}+\bar{\sigma}_{g-}-\bar{\sigma}_{-g})+p-2\gamma_o\bar{\sigma}_{gg}. \tag{5.3.13}$$

We now obtain the steady state solutions of the density matrix elements from the set of equations (5.3.8) to (5.3.13) in the following. From (5.3.8) and (5.3.9) we obtain

$$\text{Im}\ \bar{\sigma}_{+g} = \frac{\gamma_1+\gamma}{\alpha}\ \bar{\sigma}_{++} \tag{5.3.14}$$

and

$$\text{Im}\ \bar{\sigma}_{-g} = \frac{\gamma_1+\gamma}{\alpha}\ \bar{\sigma}_{--} \tag{5.3.15}$$

respectively.

Adding equations (5.3.8) and (5.3.9) and subtracting from (5.3.13), we have

$$\bar{\sigma}_{gg} = p/2\gamma_o - \frac{\gamma_1}{\gamma_o} (\bar{\sigma}_{++} + \bar{\sigma}_{--}) \ . \qquad (5.3.16)$$

Taking the real part of (5.3.10) and simplifying, we obtain

$$\text{Re } \bar{\sigma}_{+-} = \frac{\delta \text{ Im } \bar{\sigma}_{+-}}{2(\gamma+\gamma_1)} + \frac{1}{2} (\bar{\sigma}_{++} + \bar{\sigma}_{--}) \ . \qquad (5.3.17)$$

The real part of (5.3.11) and (5.3.12) are obtained as

$$\text{Re } \bar{\sigma}_{+g} = [\ (2\delta-\Delta \ ) \frac{(\gamma_1+\gamma)}{\alpha} \bar{\sigma}_{++} + \alpha \text{ Im } \bar{\sigma}_{+-} \ ] \frac{1}{(\gamma+\gamma_1+\gamma_o)} \qquad (5.3.18)$$

and

$$\text{Re } \bar{\sigma}_{-g} = [\ (\delta- \Delta) \frac{(\gamma_1+\gamma)}{\alpha} \bar{\sigma}_{--} - \alpha \text{ Im } \bar{\sigma}_{+-} \ ] \frac{1}{(\gamma+\gamma_1+\gamma_o)} \ . \qquad (5.3.19)$$

Taking the imaginary part of (5.3.10) and simplifying will yield the following expression for Im $\bar{\sigma}_{+-}$.

$$\text{Im } \bar{\sigma}_{+-} = \frac{\delta(\gamma+\gamma_1)[\bar{\sigma}_{--}(\gamma_1+\gamma+\gamma_o-2\frac{\Delta}{\delta}(\gamma+\gamma_1)-\bar{\sigma}_{++}(\gamma_o+5\gamma_1+5\gamma-2(\gamma+\gamma_1}{[4(\gamma+\gamma_1)^2 + \delta^2] \ (\gamma_o+\gamma+\gamma_1)+4\alpha^2(\gamma+\gamma_1)} \qquad (5.3.20)$$

Taking the imaginary parts of (5.3.11) and (5.3.12) and on making use of the equations (5.3.14) to (5.3.20) and simplifying, two equations in $\bar{\sigma}_{++}$ and $\bar{\sigma}_{--}$ are obtained which are of the form

$$\left\{ \frac{2\gamma_o(\gamma+\gamma_1)}{(\gamma+\gamma_1+\gamma_o)} \left[(\gamma+\gamma_1+\gamma_o)^2+(2\delta-\Delta)^2\right] + \alpha^2(3\gamma_o+2\gamma_1) \right.$$

$$\left. - \frac{\alpha^2\delta^2\gamma_o}{D} \left[(\gamma_o+5\gamma+5\gamma_1) - \frac{2\Delta}{\delta}(\gamma+\gamma_1)\right]^2 \right\} \bar{\sigma}_{++}$$

$$+ \left\{ \frac{\alpha^2\delta^2\gamma_o}{D} \left[\gamma_o+5\gamma+5\gamma_1 - \frac{2\Delta}{\delta}(\gamma+\gamma_1)\right]\left[\gamma_1+\gamma-\gamma_o - \frac{2\Delta}{\delta}(\gamma+\gamma_1)\right] + \right.$$

$$\left. \alpha^2(\gamma_o+2\gamma_1) \right\} \sigma_{--} - \alpha^2 p = 0 , \qquad (5.3.21)$$

$$\left\{ \frac{\alpha^2\delta^2\gamma_o}{D} \left[\gamma_o+5\gamma+5\gamma_1 - \frac{2\Delta}{\delta}(\gamma+\gamma_1)\right]\left[\gamma_1+\gamma-\gamma_o - \frac{2\Delta}{\delta}(\gamma+\gamma_1)\right] \right.$$

$$\left. + \alpha^2(\gamma_o+2\gamma_1) \right\} \sigma_{++} + \left\{ \frac{2\gamma_o(\gamma+\gamma_1)}{(\gamma+\gamma_1+\gamma_o)} \left[(\gamma_o+\gamma_1+\gamma)^2+(\delta-\Delta)^2\right] \right.$$

$$\left. + \alpha^2(2\gamma_1+3\gamma_o) - (\alpha^2\delta^2\gamma_o/D) \left[\gamma_1+\gamma-\gamma_o - \frac{2\Delta}{\delta}(\gamma+\gamma_1)\right]^2 \right\} \sigma_{--}$$

$$- \alpha^2 p = 0 \qquad (5.3.22)$$

where D is given by

$$D = (\gamma_1+\gamma_o+\gamma) \left[(4(\gamma+\gamma_1)^2+\delta^2)(\gamma_o+\gamma_1+\gamma) + 4\alpha^2(\gamma+\gamma_1)\right]. \qquad (5.3.23)$$

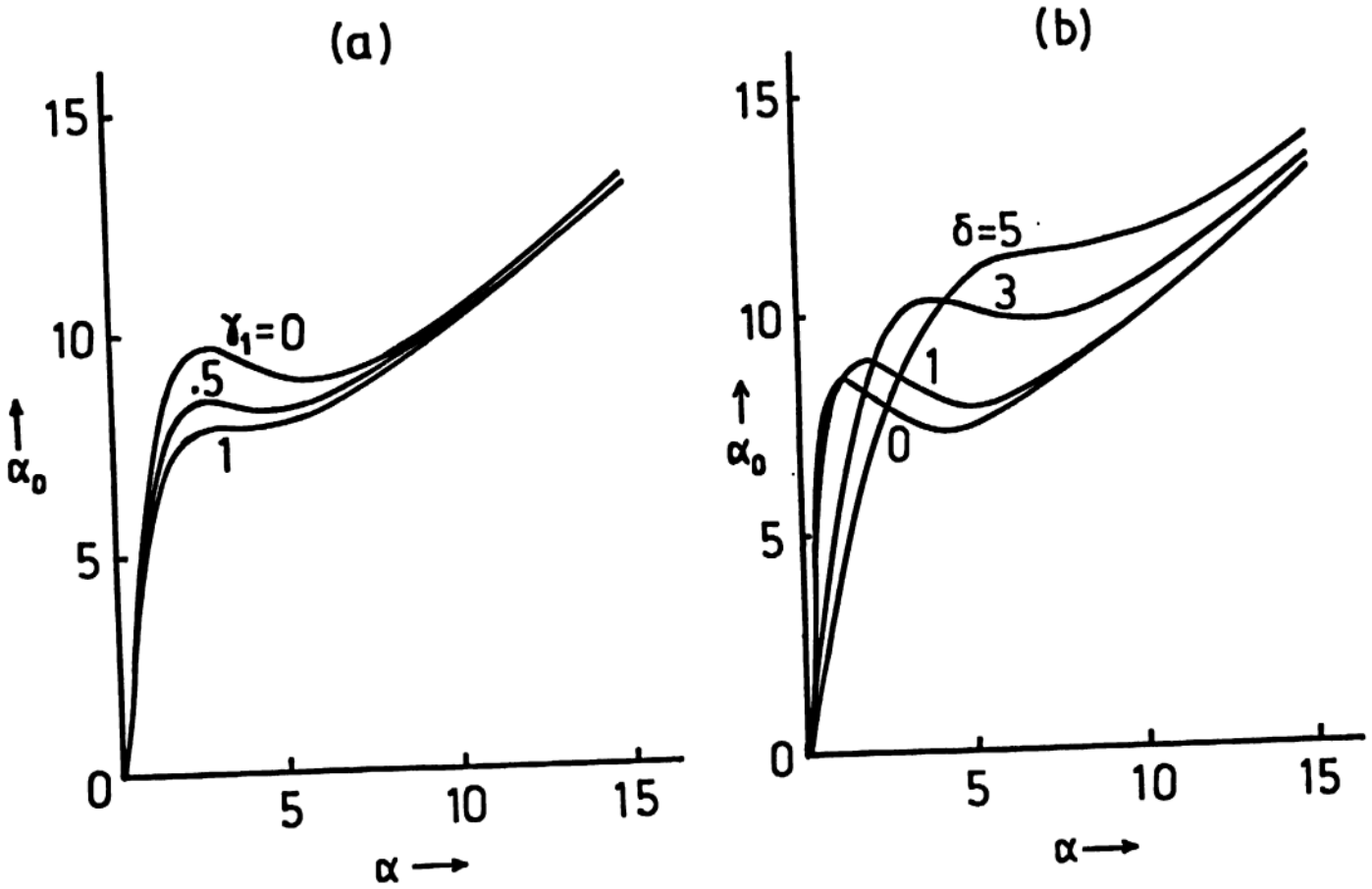

Fig.19 (a) α_o vs α for optical Hanle system under external pumping for different values of the excited state decay rate γ_1 (shown in figure) and for the values of the parameters $\delta = 2$, $\gamma = \gamma_1 = 1$, $\nu = 30$ and the pumping rate $p = 1$. (b) α_o vs α for different values of the light shift δ for $\gamma = \gamma_o = 1$, $\gamma_1 = 0$, $\nu = 30$ and $p = 1$

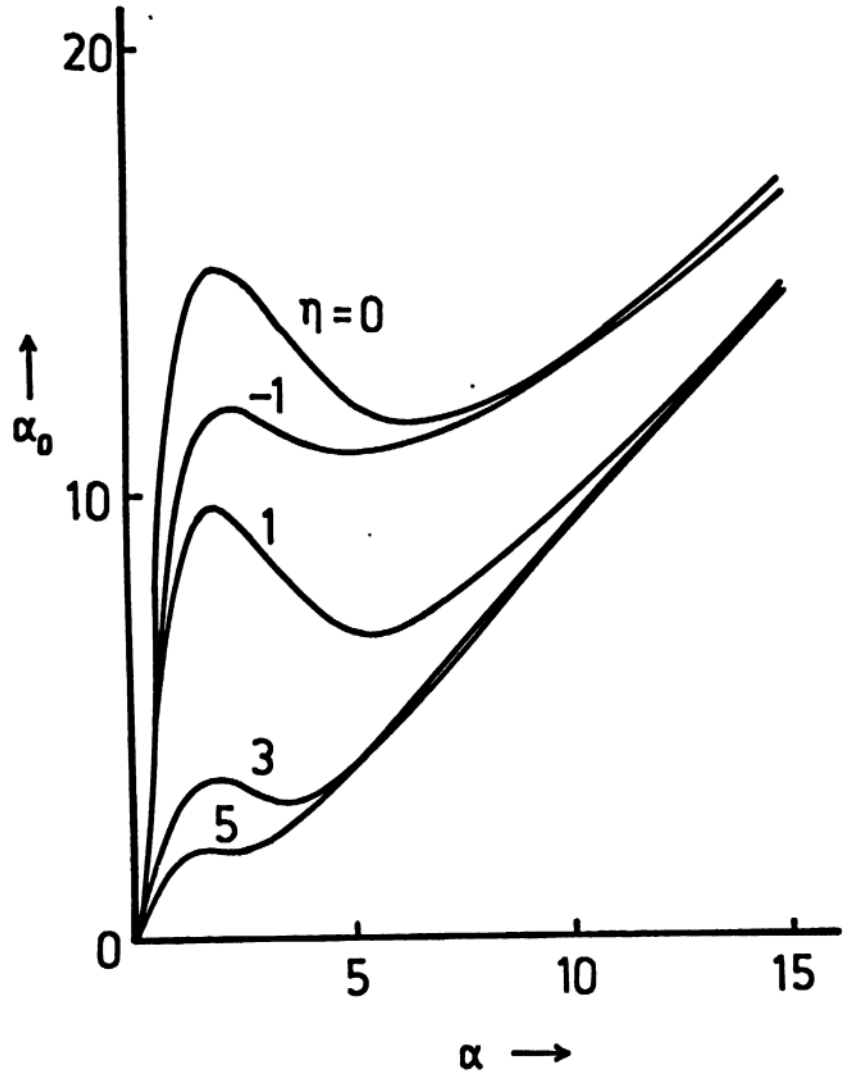

Fig.20 α_o vs α for optical Hanle case under external pumping for different values of the cavity detuning parameter η for the values of the parameters $\gamma = \gamma_o = p = 1$, $\gamma_1 = 0$ and $\nu = 50$

Thus, by solving the set of equations (5.3.21) and (5.3.22) and substituting in the earlier expressions, we can obtain the density matrix elements which can be substituted in (5.3.7) to obtain the transmission characteristics of the atomic system under consideration.

We now present some of our numerical results of (5.3.7) as functions of various parameters such as the light shift, cavity detuning, relaxation parameters etc. Figure 19a shows the behaviour of α_o vs α for different values of the excited state relaxation rate γ_1 for fixed values of δ, γ, γ_o and the pumping rate $p = 1$ and the cavity detuning parameter $\eta = 0$. Here the system exhibits bistable behaviour. It is also seen that the region over which the system exhibits bistability decreases with increase in γ_1. Figure 19b shows the transmission characteristics for different values of the light shift parameter δ. In this case also, the region over which bistability is observed is seen to be a function of the light shift parameter. In Fig. 20 α_o is plotted as a function of α for different values of the cavity detuning parameter η. The extent of bistable region depends strongly on the cavity detuning.

Thus, our studies show that the bistable behaviour of the system depends in an important way on each of the parameters such as light shift, cavity detuning, various relaxation parameters.

CHAPTER VI

SQUEEZED STATES IN RADIATION - MATTER INTERACTIONS

So far, we have studied the steady state intensities, fluorescence spectra of an atomic system in interaction with a strong resonant radiation field. It would also be of interest to study the higher order correlation properties of the scattered radiation field. For example, a study of the intensity correlation function will yield information about the antibunching properties of the radiation field. Similarly, squeezing of the scattered radiation[69-72] field

can also be studied by measuring such correlations. Squeezed states[69-72], which have fluctuations in one quadrature reduced below that of the coherent states, at the expense of enhanced fluctuations in a second quadrature, have recently become very important in connection with the quantum limits on a measurement process[73]. Various methods of producing such states have been shown to be theoretically possible but experimental detection of such states has several problems. Mandel[75], in a remarkable study has shown the feasibility of experimental detection of such states by photon counting techniques. In particular, he has shown that the quantity $S(T) = \langle n^{[2]} \rangle - \langle n \rangle^2$ related to the second factorial moment $\langle n^{[2]} \rangle$ of the photon counting distribution for a superposition of an external coherent radiation and the radiation scattered by a two level atom exhibits squeezing of the scattered radiation by such an atom. However, Mandel[75] has treated the case when the counting time T is much smaller than the correlation time τ_c of the scattered radiation. In order to aid the experimentalist interested in such studies, it is very important to know the behaviour of the system when $T > \tau_c$. This is even more critical in view of the dependence of the second factorial moment on $\langle I(t+\tau)\, I(t) \rangle$ rather than on $\langle I(t)\, I(t) \rangle$. A calculation of this intensity correlation function of the mixture of the scattered

radiation field with an external coherent radiation field will involve, in addition to the usual correlation functions like $\langle E_i^-(\tau)\, E_j^+(o) \rangle$, the correlators of the complex amplitudes of the type $\langle E_i^+(\tau)\, E_j^+(o) \rangle$, which are called the anomalous correlators[74]. These anomalous correlators are nonzero only in the presence of an external coherent driving field. These anomalous correlators are becoming important in the radiation - matter interaction problems as they have been shown to provide information on the space as well as spectral properties of the medium. Kazantsev et al.[74] have discussed the anomalous correlators of a two level atom in the presence of thermal motion. Thus, the anomalous correlators, squeezing properties etc., can be studied only by mixing the scattered radiation with an external coherent field of definite phase.

As the study of photon counting distribution corresponding to a three level system is quite complex, we will first show what can be learnt from a similar study on a two level model system. In this chapter, we provide a general expression for the second factorial moment of the photon counting distribution p(n) for a two level case. Our investigations show that sub-poissonian nature of p(n) is very sensitive to the range of system parameters. Squeezing, i.e., negative value of the quantity S(T)

may only persist for very short intervals T in most cases. We also derive the conditions for squeezing in atomic operators, which are related to the scattered radiation field, for the three level Hanle case.

6.1 Equations of motion for the two level atom

The equations of motion for the density matrix elements of a two level atom driven with a coherent field are obtained from the well known master equation[76] used to describe the resonance fluorescence[47]

$$\frac{\partial \sigma}{\partial t} = -\gamma(S^+S^-\sigma - 2S^-\sigma S^+ + \sigma S^+S^-) - i\alpha[S^+ + S^-, \sigma] - i\Delta[S^z, \sigma] \quad . \qquad (6.1.1)$$

Here the atomic operators are defined by $S^+ = |1\rangle\langle 2|$, $S^- = |2\rangle\langle 1|$, $S^z = \frac{1}{2}(|1\rangle\langle 1| - |2\rangle\langle 2|)$ where $|1\rangle$ and $|2\rangle$ are the excited and ground states respectively. The equations of motion therefore are given by

$$\langle \dot{S}^+ \rangle = (i\Delta - \gamma)\langle S^+ \rangle + 2i\alpha \langle S^z \rangle$$

$$\langle \dot{S}^- \rangle = -(i\Delta + \gamma)\langle S^- \rangle - 2i\alpha \langle S^z \rangle$$

$$\langle \dot{S}^z \rangle = i\alpha(\langle S^+ \rangle - \langle S^- \rangle) - 2\gamma(\langle S^z \rangle - \langle S^z_{eq} \rangle) \qquad (6.1.2$$

where Δ is the detuning of the atomic frequency from the driving field frequency, 2γ is the spontaneous decay rat and 2α is the Rabi frequency of the transition. These

equations can be cast into the form

$$\dot{\psi} = M\,\psi + \phi \tag{6.1.3}$$

where

$$M = \begin{bmatrix} i\Delta - \gamma & 0 & 2i\alpha \\ 0 & -(i\Delta + \gamma) & -2i\alpha \\ i\alpha & -i\alpha & -2\gamma \end{bmatrix} \tag{6.1.4}$$

and

$$\phi = \begin{bmatrix} 0 \\ 0 \\ 2\gamma\langle S^{z}_{eq}\rangle \end{bmatrix} \tag{6.1.5}$$

The Laplace transform of (6.1.3) can be written as

$$\hat{\psi}(z) = (z-M)^{-1}\,\psi(o) + z^{-1}(z-M)^{-1}\,\phi \tag{6.1.6}$$

and the steady state solution of ψ is given by

$$\psi(\infty) = \lim_{z \to o} z\,\hat{\psi}(z) = (-M)^{-1}\,\phi \tag{6.1.7}$$

The inverse of $(z-M)$ is obtained as

$$(z-M)^{-1} = \frac{1}{P(z)} \begin{bmatrix} (z+i\Delta+\gamma)(z+2\gamma)+2\alpha^2 & 2\alpha^2 & 2i\alpha(z+i\Delta+\gamma) \\ 2\alpha^2 & (z-i\Delta+\gamma)(z+2\gamma)+2\alpha^2 & -2i\alpha(z-i\Delta+\gamma) \\ i\alpha(z+i\Delta+\gamma) & -i\alpha(z-i\Delta+\gamma) & (z-i\Delta+\gamma)(z+i\Delta+\gamma) \end{bmatrix}$$

(6.1.8)

where

$$P(z) = 4\alpha^2(z+\gamma) + (z+2\gamma)\left[(z+\gamma)^2 + \Delta^2\right] . \qquad (6.1.9)$$

From (6.1.6), the Laplace transforms of the ensemble averages of the atomic operators can be written as

$$\langle \hat{S}^+(z) \rangle = \frac{1}{P(z)} \{ [2\alpha^2 + (z+i\Delta+\gamma)(z+2\gamma)] \langle S^+(o) \rangle + 2\alpha^2 \langle S^-(o) \rangle + 2i\alpha(z+i\Delta+\gamma) (\langle S^z(o) \rangle - \frac{\gamma}{z}) \}$$

$$\langle \hat{S}^-(z) \rangle = \frac{1}{P(z)} \{ [2\alpha^2 + (z-i\Delta+\gamma)(z+2\gamma)] \langle S^-(o) \rangle + 2\alpha^2 \langle S^+(o) \rangle - 2i\alpha(z-i\Delta+\gamma) (\langle S^z(o) \rangle - \frac{\gamma}{z}) \}$$

and

$$\langle \hat{S}^z(z) \rangle = \frac{1}{P(z)} [i\alpha(z+i\Delta+\gamma)\langle S^+(o) \rangle - i\alpha(z-i\Delta+\gamma)\langle S^-(o) \rangle + (z+i\Delta+\gamma)(z-i\Delta+\gamma)(\langle S^z(o) \rangle - \frac{\gamma}{z})] \qquad (6.1.10)$$

where the steady state solutions occuring in (6.1.10) are obtained from (6.1.7) as

$$\langle S^+\rangle_{st} = \frac{-i\alpha(\gamma+i\Delta)}{(\gamma^2+\Delta^2+2\alpha^2)} \quad , \quad \langle S^-\rangle_{st} = \frac{i\alpha(\gamma-i\Delta)}{(\gamma^2+\Delta^2+2\alpha^2)}$$

and

$$\langle S^z\rangle_{st} = \frac{-(\gamma^2+\Delta^2)}{2(\gamma^2+\Delta^2+2\alpha^2)} \quad . \qquad (6.1.11)$$

6.2 Intensity Correlation function and the squeezing parameter S(T)

The radiation field scattered by a two-level atom in the radiation zone is defined by

$$\vec{E}_s^-(r,t) = \hat{r}x(\hat{r}x\vec{d})\, e^{ikr} \quad \frac{\omega^2}{rc^2} \; S^+(t-r/c)$$

and

$$\vec{E}_s^+(r,t) = \hat{r}x(\hat{r}x\vec{d})\, e^{-ikr} \quad \frac{\omega^2}{rc^2} \; S^-(t-r/c) \qquad (6.2.1)$$

where by proper choice of phases, the dipole moment has been made real. The electric field detected at the detector after mixing the scattered radiation field with an external coherent field therefore is

$$E = E^+ + E^- \qquad (6.2.2)$$

where

$$E^+ = E_s^+ + E_c^+ \qquad (6.2.3)$$

The external coherent driving field E_c is defined by

$$E_c^+ = |E_c|\, e^{-i\theta} \tag{6.2.4}$$

where θ is the phase angle of the external coherent field E_c. The quantity of interest will be $\langle n^{[2]} \rangle - \langle n \rangle^2 \equiv S(T)$ which in other words is given by the difference between the variance and mean of the photo electron counting distribution namely $S(T) \equiv \langle (\Delta n)^2 \rangle - \langle n \rangle$ is related to the intensity correlations by

$$S(T) = \lim_{t\to\infty} \int_t^{t+T} dt_1 \int_t^{t+T} dt_2 \, [\langle I(t_1)I(t_2)\rangle - \langle I(t_1)\rangle\langle I(t_2)\rangle] \tag{6.2.5}$$

where T is the counting interval. Let us call the function

$$\lim_{t\to\infty} \int_t^{t+T} dt_1 \int_t^{t+T} dt_2 \, \langle I(t_1)I(t_2)\rangle = \int_0^T dt_1 \int_0^T dt_2 \, \langle I(t_1)I(t_2)\rangle$$

$$\equiv f(T) \tag{6.2.6}$$

Taking the time derivative of this function, we obtain

$$\frac{df}{dT} = \int_0^T dt_2 \, \langle I(T)I(t_2)\rangle + \int_0^T dt_1 \langle I(t_1)I(T)\rangle = 2\int_0^T dt \, \langle I(T)I(t)\rangle$$

$$= 2\int_0^T d\tau \, \langle I(\tau)\, I(o)\rangle \tag{6.2.7}$$

Taking the Laplace transform of (6.2.7) and using the

convolution theorem, we obtain

$$f(T) = 2 \int_0^T d\tau \, (T-\tau) \, \langle I(\tau) \, I(0) \rangle \qquad (6.2.8)$$

Therefore S(T) can be rewritten as

$$S(T) = 2 \int_0^T d\tau \, (T-\tau) \, [\, \langle I(\tau) I(0) \rangle - \langle I \rangle^2 \,] \qquad (6.2.9)$$

The correlation functions occuring in (6.2.7) to (6.2.9) are all evaluated at steady state.

The intensity correlation function $\langle I(\tau)I(0) \rangle$ is defined by

$$\langle I(\tau)I(0) \rangle = \langle E^-(0) \, E^-(\tau) \, E^+(\tau) \, E^+(0) \rangle \, . \qquad (6.2.10)$$

If the coherent light beam E_c is made sufficiently intense, the term in $|E_c|^2$ will dominate over those in E_c and those without E_c which will henceforth be discarded. Therefore, considering terms to order $|E_c|^2$ and more, the intensity correlation function (6.2.10) can be expanded as

$$\begin{aligned} \langle E^-(0)E^-(\tau)E^+(\tau)E^+(0) \rangle &= \langle E_s^-(0)E_s^-(\tau) \rangle E_c^{+2} + \langle E_s^+(\tau)E_s^+(0) \rangle E_c^{-2} \\ &+ |E_c|^2 \, [\langle E_s^-(0)E_s^+(\tau) \rangle + \langle E_s^-(\tau)E_s^+(0) \rangle + \langle E_s^-(0)E_s^+(0) \rangle \\ &+ \langle E_s^-(\tau)E_s^+(\tau) \rangle] + |E_c|^4 + 2 \, |E_c|^2 \, [E_c^- \langle E_s^+(\tau) \rangle \\ &+ E_c^+ \, \langle E_s^-(\tau) \rangle] \end{aligned} \qquad (6.2.11)$$

and the steady state intensity $\langle I \rangle$ is given by

$$\langle I \rangle = [\langle E_s^- \rangle E_c^+ + \langle E_s^+ \rangle E_c^- + |E_c|^2 + \langle E_s^- E_s^+ \rangle] \ . \qquad (6.2.12)$$

Therefore

$$\langle I(\tau)I(o) \rangle - \langle I \rangle^2 = E_c^{+2}[\langle E_s^-(o)E_s^-(\tau) - \langle E_s^- \rangle^2] +$$

$$E_c^{-2} [\langle E_s^+(\tau)E_s^+(o) \rangle - \langle E_s^+ \rangle^2] + |E_c|^2[\langle E_s^-(o)E_s^+(\tau) \rangle +$$

$$\langle E_s^-(\tau)E_s^+(o) \rangle - 2\langle E_s^- \rangle \langle E_s^+ \rangle] \ . \qquad (6.2.13)$$

The quantity $S(T)$[77] therefore is given by

$$S(T) = 2\beta^2\mu \int_o^T d\tau \ (T-\tau) \{ e^{-2i\theta} (\langle S^+(o)S^+(\tau) \rangle - \langle S^+ \rangle^2 +$$

$$e^{2i\theta} (\langle S^-(\tau)S^-(o) \rangle - \langle S^- \rangle^2) + \langle S^+(o)S^-(\tau) \rangle -$$

$$2\langle S^+ \rangle \langle S^- \rangle + \langle S^+(\tau) \ S^-(o) \rangle \} \ . \qquad (6.2.14)$$

As has already been mentioned, all the correlation functions appearing in (6.2.14) are at the steady state. The parameter μ depends on the geometrical factors and β is related to the quantum efficiency of the detector. One can see the appearance of anomalous correlators like $\langle S^+(o) \ S^+(\tau) \rangle$ in $S(T)$. Thus, the θ - dependent contribu-

tion to S(T) arises solely from the anomalous correlators. S(T) can now be calculated using the solution of the master equation (6.1.1) which is given by (6.1.10) and the quantum regression theorem.[35] Thus, the Laplace transform of each of the correlations occuring in (6.2.14) is obtained as

$$\langle \hat{S^+}(o)S^+(z)\rangle = \frac{1}{P(z)}\left[\frac{2\alpha^4}{(\gamma^2+\Delta^2+2\alpha^2)} - \frac{\alpha^2(\gamma+i\Delta)}{(\gamma^2+\Delta^2+2\alpha^2)}\,\frac{(z+i\Delta+\gamma)(z+2\gamma)}{z}\right]$$

$$\langle \hat{S^-}(z)S^-(o)\rangle = \frac{1}{P(z)}\left[\frac{2\alpha^4}{(\gamma^2+\Delta^2+2\alpha^2)} - \frac{\alpha^2(\gamma-i\Delta)}{(\gamma^2+\Delta^2+2\alpha^2)}\,\frac{(z-i\Delta+\gamma)(z+2\gamma)}{z}\right]$$

$$\langle \hat{S^+}(o)S^-(z)\rangle = \frac{1}{P(z)}\left[(2\alpha^2+(z-i\Delta+\gamma)(z+2\gamma))\,\frac{\alpha^2}{\gamma^2+\Delta^2+2\alpha^2} + \frac{\alpha^2(z-i\Delta+\gamma)(z+2\gamma)(\gamma+i\Delta)}{z(\gamma^2+\Delta^2+2\alpha^2)}\right]$$

and

$$\langle \hat{S^+}(z)S^-(o)\rangle = \frac{1}{P(z)}\left[\frac{\alpha^2[2\alpha^2+(z+i\Delta+\gamma)(z+2\gamma)]}{(\gamma^2+\Delta^2+2\alpha^2)} + \frac{\alpha^2(z+i\Delta+\gamma)(z+2\gamma)(\gamma-i\Delta)}{z(\gamma^2+\Delta^2+2\alpha^2)}\right] \qquad (6.2.15)$$

The Laplace transform of (6.2.14) can therefore be written as

$$[\langle \hat{I}(z)\hat{I}(o)\rangle - \langle \hat{I}\rangle^2] = \beta^2\mu \{ e^{-2i\theta} [\frac{1}{P(z)} (\frac{2\alpha^4}{\gamma^2+\Delta^2+2\alpha^2}$$

$$- \frac{\alpha^2(\gamma+i\Delta)(z+\gamma+i\Delta)(z+2\gamma)}{z(\gamma^2+\Delta^2+2\alpha^2)} + \frac{\alpha^2(\gamma+i\Delta)^2}{z(\gamma^2+\Delta^2+2\alpha^2)^2}]$$

$$+ \frac{1}{P(z)} [[2\alpha^2+(z-i\Delta+\gamma)(z+2\gamma)] \frac{\alpha^2}{\gamma^2+\Delta^2+2\alpha^2}$$

$$+ \frac{\alpha^2(z-i\Delta+\gamma)(\gamma+i\Delta)(z+2\gamma)}{z(\gamma^2+\Delta^2+2\alpha^2)}] - \frac{\alpha^2(\gamma^2+\Delta^2)}{z(\gamma^2+\Delta^2+2\alpha^2)} \} + c.c.$$

(6.2.16)

The inverse Laplace transform of (6.2.14) is obtained as

$$\langle I(\tau)I(o)\rangle - \langle I\rangle^2 = 4\beta^2\mu \frac{\alpha^2}{\gamma^2+\Delta^2+2\alpha^2} \; Re \{ \frac{e^{z_1\tau}}{(z_1-z_2)(z_1-z_3)} \times$$

$$[e^{-2i\theta}(2\alpha^2-(\gamma+i\Delta)(z_1+2\gamma) - \frac{(\gamma+i\Delta)^2(z_1+2\gamma)}{z_1})$$

$$+ 2\alpha^2+(z_1+2\gamma)^2 + \frac{(z_1+2\gamma)(\gamma^2+\Delta^2)}{z_1}] + \frac{e^{z_2\tau}}{(z_2-z_1)(z_2-z_3)} \times$$

$$[e^{-2i\theta}(2\alpha^2-(\gamma+i\Delta)(z_2+2\gamma) - \frac{(\gamma+i\Delta)^2(z_2+2\gamma)}{z_2}) + 2\alpha^2+(z_2+2\gamma)^2+$$

$$\frac{(z_2+2\gamma)(\gamma^2+\Delta^2)}{z_2}] + \frac{e^{z_3\tau}}{(z_3-z_1)(z_3-z_2)} [e^{-2i\theta}(2\alpha^2-(\gamma+i\Delta)(z_3+2\gamma)$$

$$- \frac{(\gamma+i\Delta)^2(z_3+2\gamma)}{z_3}) + 2\alpha^2+(z_3+2\gamma)^2 + \frac{(z_3+2\gamma)(\gamma^2+\Delta^2)}{z_3}] +$$

$$e^{-2i\theta}(\gamma+i\Delta)^2\left(\frac{1}{\gamma^2+\Delta^2+2\alpha^2}+\frac{2\gamma}{z_1z_2z_3}\right)-(\gamma^2+\Delta^2)\times$$

$$\left(\frac{1}{\gamma^2+\Delta^2+2\alpha^2}+\frac{2\gamma}{z_1z_2z_3}\right)\} \qquad (6.2.17)$$

where z_1, z_2 and z_3 are the complex roots of the polynomia P(z). After carrying out the time integration in (6.2.9) S(T) can be obtained as[89]

$$S(T)=4\beta^2\mu\frac{\alpha^2}{(\gamma^2+\Delta^2+2\alpha^2)}\,\mathrm{Re}\{\left(\frac{(e^{z_1T}-1)}{z_1^2}-\frac{T}{z_1}\right)\frac{1}{(z_1-z_2)(z_1-z_3}$$

$$[e^{-2i\theta}(2\alpha^2-(\gamma+i\Delta)(z_1+2\gamma)-\frac{(\gamma+i\Delta)^2(z_1+2\gamma)}{z_1})+2\alpha^2+(z_1+2\gamma)^2+$$

$$\frac{(z_1+2\gamma)(\gamma^2+\Delta^2)}{z_1}]+\left(\frac{e^{z_2T}-1}{z_2^2}-\frac{T}{z_2}\right)\frac{1}{(z_2-z_1)(z_2-z_3)}\times$$

$$[e^{-2i\theta}(2\alpha^2-(\gamma+i\Delta)(z_2+2\gamma)-\frac{(\gamma+i\Delta)^2(z_2+2\gamma)}{z_2})+2\alpha^2+(z_2+2\gamma)^2+$$

$$\frac{(z_2+2\gamma)(\gamma^2+\Delta^2)}{z_2}]+\left(\frac{e^{z_3T}-1}{z_3^2}-\frac{T}{z_3}\right)\frac{1}{(z_3-z_1)(z_3-z_2)}\;[\,e^{-2i\theta}\times$$

$$(2\alpha^2-(\gamma+i\Delta)(z_3+2\gamma)-\frac{(\gamma+i\Delta)^2(z_3+2\gamma)}{z_3})+2\alpha^2+(z_3+2\gamma)^2+$$

$$\frac{(z_3+2\gamma)(\gamma^2+\Delta^2)}{z_3}\,]+\frac{T^2}{2}\,[\,e^{-2i\theta}(\gamma+i\Delta)^2\left(\frac{1}{\gamma^2+\Delta^2+2\alpha^2}+\frac{2\gamma}{z_1z_2z_3}\right.$$

$$- (\gamma^2+\Delta^2) \left(\frac{1}{\gamma^2+\Delta^2+2\alpha^2} + \frac{2\gamma}{z_1 z_2 z_3} \right)] \} \quad . \qquad (6.2.18)$$

In the next section we present the numerical results for S(T) as a function of the counting time T for various values of α,γ,Δ and the phase angle θ.

6.3 Numerical results and discussion

In this section, we present some of the numerical results for the quantity S(T), which is a measure of squeezing, as a function of the counting time T for various values of the parameters α, γ,Δ and θ. The results of our numerical calculations are shown in Figs. 21 and 22. The parameters of Fig. 21 have been chosen such that $\Delta^2 > \gamma^2 + 2\alpha^2$ so that the x-component of the scattered field shows squeezing[69] whereas the parameters of Fig. 22 correspond to the squeezing in the y-component of the scattered field i.e., $\gamma^2 > \Delta^2 + 2\alpha^2$. For small counting intervals $\gamma T \ll 1$, Figs. 21a and 22c indeed show respectively the squeezing characteristics[69,75] of the x and y components of the scattered field. For arbitrary θ, S(T) for $\gamma T \ll 1$ will show squeezing characteristics of $S_x \cos\theta + S_y \sin\theta$ and thus the conditions on the field strength α and the detuning Δ to exhibit squeezing in such a case can be obtained from the condition that

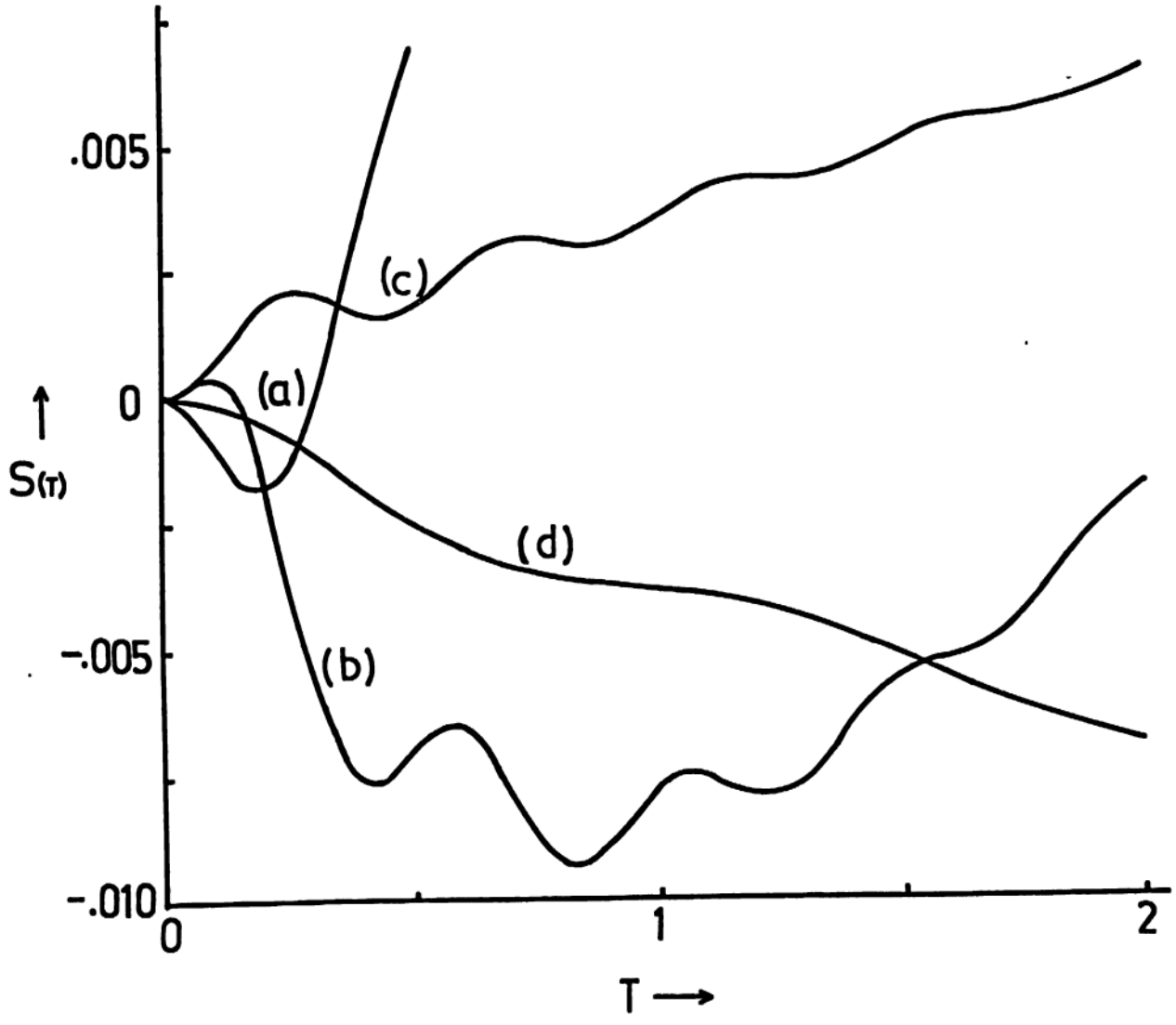

Fig.21 S(T) in units of $\mu\beta^2 |E_c|^2$ as a function of the counting time T in units of γ^{-1} for the parameters $\alpha/\gamma = 5$, $\Delta/\gamma = 10$ (a) $\theta = 0$, (b) $\theta = \pi/4$, (c) $\theta = \pi/2$. The curve (d) corresponds to a different set of parameters $\alpha/\gamma = 1$, $\Delta/\gamma = 5$ and $\theta = 0$. The function S(T) has been multiplied by a factor of .25 in (c) and (d)

$$\langle (S_x \cos\theta + S_y \sin\theta)^2 \rangle - \langle S_x \cos\theta + S_y \sin\theta \rangle^2 < 0 . \qquad (6.3.1)$$

Substituting for S_x and S_y in terms of S^+ and S^-, we obtain

$$\left\langle \left[\frac{(S^+ + S^-)}{2} \cos\theta + \frac{(S^+ - S^-)}{2i} \sin\theta \right]^2 \right\rangle - \left\langle \frac{(S^+ + S^-)}{2} \cos\theta + \frac{(S^+ - S^-)}{2i} \sin\theta \right\rangle^2 < 0. \qquad (6.3.2)$$

On making use of (6.1.11) and simplifying this expression we obtain

$$\frac{\langle S^+ S^- \rangle}{2} - \alpha^2 \frac{(\Delta \cos\theta - \gamma \sin\theta)^2}{(\gamma^2 + \Delta^2 + 2\alpha^2)^2} < 0 \longrightarrow$$

$$\frac{\alpha^2}{2(\gamma^2 + \Delta^2 + 2\alpha^2)} - \frac{\alpha^2 (\Delta \cos\theta - \gamma \sin\theta)^2}{(\gamma^2 + \Delta^2 + 2\alpha^2)^2} < 0 \qquad (6.3.3)$$

which on further simplification will yield the condition for squeezing in $S_x \cos\theta + S_y \sin\theta$ to be

$$2 (\Delta \cos\theta - \gamma \sin\theta)^2 > (\gamma^2 + \Delta^2 + 2\alpha^2) . \qquad (6.3.4)$$

Equation (6.3.4) shows the impossibility of squeezing for $\theta = \pi/4$ which is confirmed by the small time behaviour of Fig. 21b. However, in this case, S(T) becomes negative

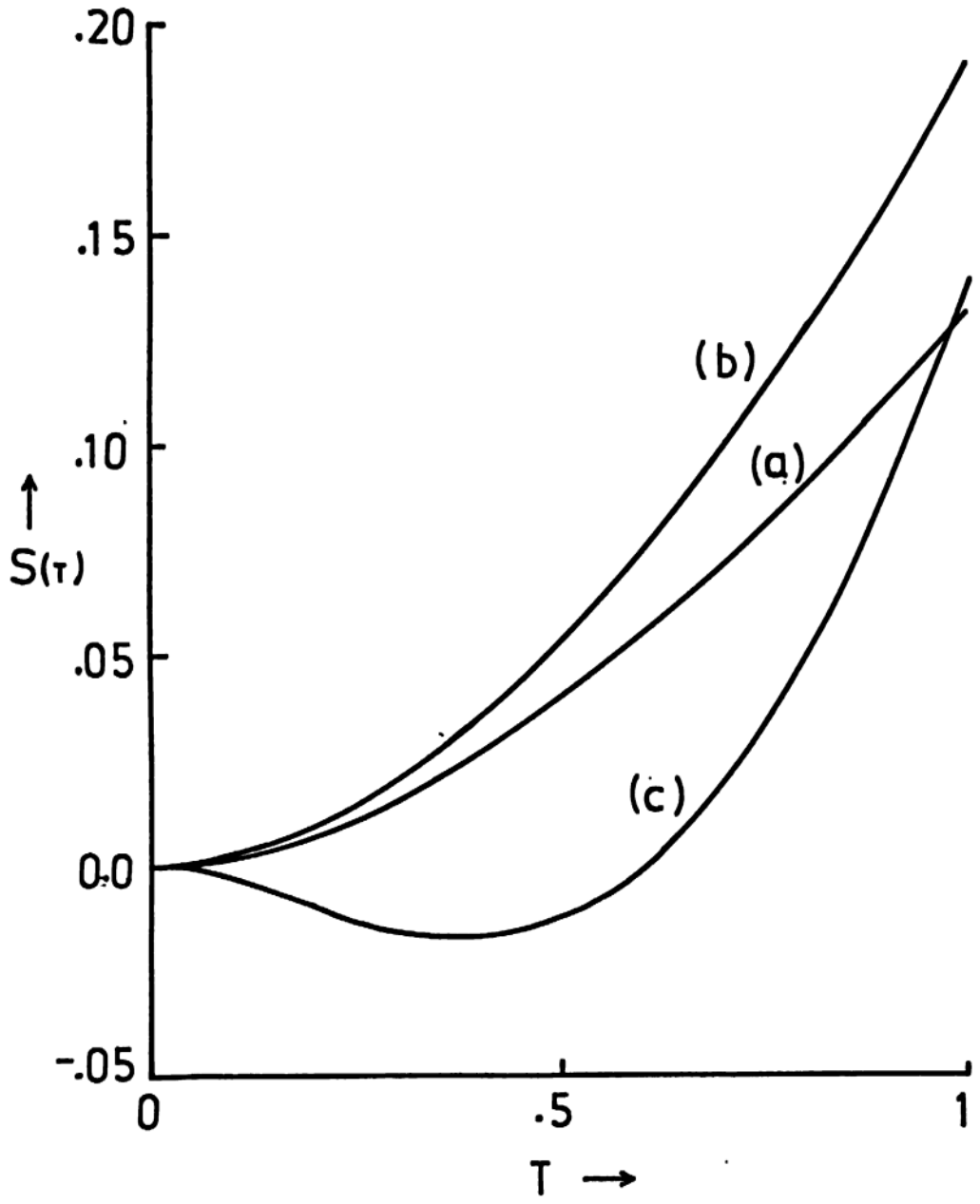

Fig.22 S(T) vs T f0r $\alpha/\gamma = .5$ $\Delta/\gamma = .5$ (a) $\Theta = 0$, (b) $\Theta = \pi/4$ (c) $\Theta = \pi/2$. The function S(T) has been multiplied by a factor 10 in (c)

for moderate values of γT. A remarkable feature that emerges from our present study is that S(T) becomes positive when $\gamma T \geq \frac{1}{2}$, suggesting that if the squeezing were to be seen using this method, then the counting interval must be chosen to be much smaller than the radiative lifetime. For the range of parameters chosen here, the behaviour for large T ($\gamma T \sim 10$) is dominated by the term proportional to T in S(T). Fig. 21d suggests that it is possible to choose the parameters α and Δ so that S(T) will remain negative over long counting intervals. Such a situation obviously corresponds to choosing the parameters α and Δ so that the term linear in (6.2.18) is negative. Note that the coefficient of the linear term in T is positive for the parameters of Fig. 21a. Thus, our studies here suggest that a judicious choice of the parameters can be made to see the squeezing characteristics of the scattered radiation.

6.4 Conditions for squeezing in the radiation field scattered by a $J=0 \rightarrow J=1$ atomic system in the optical Hanle geometry.

In this section, we derive conditions for reduced quantum fluctuations in the atomic operators, for the optical Hanle case, which in turn are related to the radiation field scattered by such a system. For simplicity of analysis, we consider the case of narrowband excitation ($\gamma_c=0$).

For the case of a two-level atom we have already seen that the squeezing in the scattered radiation field is related to the variance in the dimensionless operators S_x and S_y. Similarly for the three level optical Hanle case the squeezing in the scattered electric field is related to the variance in linear combinations of the atomic operators A_{+g}, A_{-g} etc. We define the relevant operators that have to be considered for the same purpose as follows.

$$A'_{+g} = \frac{A_{+g}+A_{g+}}{2} \quad , \quad A''_{+g} = \frac{A_{+g}-A_{g+}}{2i}$$

$$A'_{-g} = \frac{A_{-g}+A_{g-}}{2} \quad , \quad A''_{-g} = \frac{A_{-g}-A_{g-}}{2i} \qquad (6.4.1)$$

The squeezing for arbitrary operators can be defined as follows. Consider two dimensionless operators A and B which obey the commutation relation

$$[A,B] = C \qquad (6.4.2)$$

The product of the uncertainties in their measurement obeys the inequality

$$\Delta A \, \Delta B \geq \frac{1}{2} |\langle C \rangle| \qquad (6.4.3)$$

Squeezing is said to occur when the uncertainty in one observable is less than that for a minimum uncertainty state i.e.,

$$\Delta A^2 < \tfrac{1}{2}\,|\langle C\rangle| \qquad \text{(for squeezing in A)}$$
$$\Delta B^2 < \tfrac{1}{2}\,|\langle C\rangle| \qquad \text{(for squeezing in B)} \tag{6.4.4}$$

Thus a measure of variance in an observable will directly give information about its squeezing properties. The variances in the dimensionless operators A'_{+g}, A''_{+g}, A'_{-g}, A''_{-g} respectively will result in the following four inequalities

$$\langle A_{++}\rangle+\langle A_{gg}\rangle - 4(\mathrm{Re}\langle A_{+g}\rangle)^2 < (\langle A_{gg}\rangle-\langle A_{++}\rangle)$$
$$\text{(for squeezing in } A'_{+g}) \tag{6.4.5}$$

$$\langle A_{++}\rangle+\langle A_{gg}\rangle - 4(\mathrm{Im}\langle A_{+g}\rangle)^2 < (\langle A_{gg}\rangle-\langle A_{++}\rangle)$$
$$\text{(for squeezing in } A''_{+g}) \tag{6.4.6}$$

$$\langle A_{--}\rangle+\langle A_{gg}\rangle - 4(\mathrm{Re}\langle A_{-g}\rangle)^2 < (\langle A_{gg}\rangle-\langle A_{--}\rangle)$$
$$\text{(for squeezing in } A'_{-g}) \tag{6.4.7}$$

$$\langle A_{--}\rangle+\langle A_{gg}\rangle - 4(\mathrm{Im}\langle A_{-g}\rangle)^2 < (\langle A_{gg}\rangle-\langle A_{--}\rangle)$$
$$\text{(for squeezing in } A''_{-g}) \tag{6.4.8}$$

The analytical steady state solutions of different density matrix elements ψ_{ij}'s ($\psi_{ij} = \langle A_{ji}\rangle$) occuring in (6.4.5) to (6.4.8) are given by [cf. Sec. 3.2]

$$\psi_{++} + \psi_{--} = \Phi_1 = 2\alpha^2[9\delta^2(\delta^2+4\gamma^2)+(\delta^2+4\gamma^2+4\alpha^2)^2]D_1^{-1} \tag{6.4.9}$$

$$\psi_{++} - \psi_{--} = \Phi_2 = \frac{-6\delta^2(\delta^2+4\gamma^2)}{[(\delta^2+4\gamma^2+4\alpha^2)^2 + 9\delta^2(\delta^2+4\gamma^2)]}\ \Phi_1 \tag{6.4.10}$$

where

$$D_1 = (\gamma^2+4\alpha^2+\tfrac{3}{2}\delta^2)\ [9\delta^2(\delta^2+4\gamma^2) + (\delta^2+4\gamma^2+4\alpha^2)^2] \ + \ \delta^2(\delta^2+4\gamma^2+4\alpha^2)(\delta^2+4\gamma^2)] \tag{6.4.11}$$

We further have the following relations from the solution of the set of equations (3.1.17)

$$\text{Re}\ \psi_{+g} = \frac{\delta}{2\alpha}\ \Phi_1 + \frac{(\delta^2-2\gamma^2-2\alpha^2)}{6\delta\alpha}\ \Phi_2 \ , \tag{6.4.12}$$

$$\text{Im}\ \psi_{+g} = \frac{\gamma}{2\alpha}\ (\Phi_1 + \Phi_2) \ , \tag{6.4.13}$$

$$\text{Re}\ \psi_{-g} = \frac{\delta}{\alpha}\ \Phi_1 + \frac{(\gamma^2+\delta^2+\alpha^2)}{3\delta\alpha}\ \Phi_2 \ , \tag{6.4.14}$$

$$\text{Im}\ \psi_{-g} = \frac{\gamma}{2\alpha}\ (\Phi_1 - \Phi_2) \ . \tag{6.4.15}$$

By making use of the equations (6.4.9) to (6.4.15) in (6.4.5) to (6.4.8) we obtain the following inequalities.

$$(2+\Phi_2-\Phi_1) - \frac{2}{9\delta^2\alpha^2}\ [3\delta^2\ \Phi_1 + (\delta^2-2\gamma^2-2\alpha^2)\ \Phi_2]^2 < (2-3\Phi_1-\Phi_2), \tag{6.4.16}$$

$$(2+\Phi_2-\Phi_1) - \frac{2\gamma^2}{\alpha^2}(\Phi_1+\Phi_2)^2 < (2-3\Phi_1-\Phi_2), \quad (6.4.17)$$

$$(2-\Phi_1-\Phi_2) - \frac{8}{9\delta^2\alpha^2}[3\delta^2\Phi_1+(\delta^2+\gamma^2+\alpha^2)\Phi_2]^2 < (2-3\Phi_1+\Phi_2), \quad (6.4.18)$$

$$(2-\Phi_1-\Phi_2) - \frac{2\gamma^2}{\alpha^2}(\Phi_1-\Phi_2)^2 < (2-3\Phi_1+\Phi_2) \quad . \quad (6.4.19)$$

The above set of equations (6.4.16) to (6.4.18) correspond respectively to (6.4.5) to (6.4.8). Substituting for Φ_1 and Φ_2 in these inequalities will result in very complicated expressions for the same and we therefore study the set of inequalities (6.4.16) to (6.4.19) for some special cases. For the simplified situation when $\delta=0$, the problem will reduce to a two-level case. The two pairs of inequalities (6.4.16), (6.4.18) and (6.4.17), (6.4.19) will result in identical conditions and they are given by

$$\alpha^2 < 0 \quad \text{(for squeezing in } A'_{+g} \text{ or } A'_{-g}) \quad , \quad (6.4.20)$$

$$4\alpha^2 < \gamma^2 \quad \text{(for squeezing in } A''_{+g} \text{ or } A''_{-g}) \quad . \quad (6.4.21)$$

Condition (6.4.20) suggests that squeezing is not possible in the observables A'_{+g} and A'_{-g} for $\delta=0$.

For the case of a weak monochromatic pump field, we obtain the conditions for squeezing as

$$4\delta^2 > \gamma^2 \qquad (\text{for } A'_{+g}) \qquad (6.4.22)$$

$$4\delta^2 < \gamma^2 \qquad (\text{for } A''_{+g}) \qquad (6.4.23)$$

$$\gamma^2 < 0 \qquad (\text{for } A'_{-g}) \qquad (6.4.24)$$

$$\gamma^2 > \delta^2 \qquad (\text{for } A''_{-g}) \qquad (6.4.25)$$

Inequality (6.4.24) again shows that for the weak field case, it is not possible to obtain squeezing in the operator A'_{-g}. Using these relations, we can obtain the conditions under which squeezing of the scattered radiation field can be obtained.

CHAPTER VII

EXCITED STATE COHERENCES UNDER INTENSE FIELD ILLUMINATION

The question of the existence of coherence between the excited states of atoms has been of great importance in connection with a number of new spectroscopic techniques such as quantum beats[79-86], Hanle resonances[16] and Raman beats[90]. Therefore, one should examine how effectively the coherence between the excited states can be produced. Normally, one examines the coherence produced by a weak light pulse whose dura-

tion and/or correlation time has a specific relation with the relaxation times in the system[86]. One may also ask whether the intense field can be used to prepare a coherent superposition of the excited states. It may be added that some novel applications of the intense fields in atomic spectroscopy have also appeared recently[16,28,79-86], eg., it has been shown how the saturating fields could be used to compensate for the Doppler widths.

In this chapter, we investigate how the excitation of atoms and molecules by intense laser fields could lead to strong coherence between the excited states. In fact, one finds a type of complete coherence. The calculations are performed for a three level model system consisting of two excited states $|1\rangle$ and $|2\rangle$ which are not connected to each other by a dipole transition but are connected to the ground state $|3\rangle$ by a dipole transition. Therefore, radiative transitions $|1\rangle \longrightarrow |3\rangle$ (at the rate $2\gamma_1$), $|2\rangle \longrightarrow |3\rangle$ (at the rate $2\gamma_2$) take place. These two transition amplitudes interfere to produce the beat signals, provided that there is initially a nonzero coherence between the excited states $|1\rangle$ and $|2\rangle$, i.e., the initial state be such that $\sigma_{12} \neq 0$. This is the most common version of the three-level scheme used in the description of quantum beats[79-86] and Hanle experiments[16].

7.1 Mathematical formulation and the density matrix equations

We consider the interaction of the system with two resonant laser fields, resonant with the transitions $|1\rangle \longleftrightarrow |3\rangle$ (Rabi frequency G_1) and $|2\rangle \longleftrightarrow |3\rangle$ (Rabi frequency G_2) respectively. The master equation describing the atomic dynamics is

$$\dot{\sigma} = -i[H,\sigma] - \gamma_1(A_{13}A_{31}\sigma - A_{31}\sigma A_{13} + H.c.)$$

$$- \gamma_2(A_{23}A_{32}\sigma - A_{32}\sigma A_{23} + H.c.) \quad , \qquad (7.1.1)$$

$$H = A_{13}G_1 + A_{31}G_1^* + A_{23}G_2 + A_{32}G_2^* \quad , \qquad (7.1.2)$$

where σ is the density matrix in the interaction picture. The master equation (7.1.1) can be solved by working in a representation in which H is diagonal[91,92] and by ignoring all rapidly oscillating terms in such a representation[43]. This method has many features similar to the dressed atom approach of Cohen-Tannoudji and his coworkers[44]. The diagonalization of (7.1.2) leads to

$$S^{-1}HS = \begin{bmatrix} 0 & 0 & 0 \\ 0 & G_o & 0 \\ 0 & 0 & -G_o \end{bmatrix} = \Lambda \qquad (7.1.3)$$

$$S = \begin{bmatrix} -G_2/G_o & G_1/\sqrt{2}\,G_o & -G_1/\sqrt{2}\,G_o \\ G_1/G_o & G_2/\sqrt{2}\,G_o & -G_2/\sqrt{2}\,G_o \\ 0 & 1/\sqrt{2} & 1/\sqrt{2} \end{bmatrix} . \qquad (7.1.4)$$

where $G_o = \sqrt{G_1^2 + G_2^2}$.

On making the canonical transformation with S we obtain the equations

$$\tilde{\sigma} = S^{-1}\,\sigma\,S \qquad (7.1.5)$$

$$\dot{\tilde{\sigma}} = -i[\Lambda, \tilde{\sigma}] - [\gamma_1\ S^{-1}A_{13}A_{31}S\tilde{\sigma} - 2S^{-1}A_{31}S\tilde{\sigma}\,S^{-1}A_{13}S + \tilde{\sigma}\,S^{-1}A_{13}A_{31}S\ +\ \text{terms with } 1 \longrightarrow 2] . \qquad (7.1.6)$$

We now use the conditions that the fields are intense, i.e. $G_1, G_2 >> \gamma_1, \gamma_2$. In such a case, the approximate equations for σ can be obtained by ignoring all the rapidly oscillating terms in (7.1.6) and we find that

$$\dot{\tilde{\sigma}}_{11} = -[2\gamma_1 + 2\gamma_2 - 2\Gamma\,]\,\tilde{\sigma}_{11} ,$$

$$\dot{\tilde{\sigma}}_{22} = -\tfrac{1}{2}\Gamma\,(\tilde{\sigma}_{22} - \tilde{\sigma}_{33}) + \tfrac{1}{2}\,\tilde{\sigma}_{11}\,\frac{(\gamma_1 G_2^2 + \gamma_2 G_1^2)}{G_o^2} ,$$

$$\dot{\tilde{\sigma}}_{12} = [iG_o - (\gamma_1+\gamma_2) + \Gamma/2]\ \tilde{\sigma}_{12} ,$$

$$\dot{\tilde{\sigma}}_{13} = [-iG_o - (\gamma_1+\gamma_2) + \Gamma/2]\ \tilde{\sigma}_{13} ,$$

$$\dot{\tilde{\sigma}}_{23} = [-2iG_o - (3/2)\Gamma]\ \tilde{\sigma}_{23} , \qquad (7.1.7)$$

$$\dot{\tilde{\sigma}}_{33} = 1 - \tilde{\sigma}_{11} - \tilde{\sigma}_{22}$$

and

$$\Gamma = \frac{(\gamma_1 G_1^2 + \gamma_2 G_2^2)}{G_o^2}$$

Given the initial conditions for σ, one could use (7.1.5) and (7.1.6) to obtain the complete time dependence of $\sigma(t)$. Assuming that at time t=o, the system is in the state $|3\rangle$, we indicate how the time dependence of $\sigma(t)$ can be obtained. From the relation (7.1.5), we obtain for $\sigma(o)$

$$\tilde{\sigma}(o) = \begin{bmatrix} 0 & 0 & 0 \\ 0 & 1/2 & -1/2 \\ 0 & -1/2 & 1/2 \end{bmatrix} \qquad (7.1.8)$$

Using the initial conditions (7.1.8) and solving the set of equations (7.1.7), we obtain

$$\cdot) = \begin{bmatrix} 0 & 0 & 0 \\ 0 & 1/2 & -\frac{1}{2} e^{-(2iG_o+\frac{3}{2}\Gamma)t} \\ 0 & -1/2\, e^{(2iG_o-\frac{3}{2}\Gamma)t} & 1/2 \end{bmatrix} \quad (7.1.9)$$

But $\sigma(t)$ is given by

$$\sigma(t) = S\ \tilde{\sigma}(t)\ S^{-1} \quad . \quad (7.1.10)$$

Therefore multiplying (7.1.9) on the left by S and on the right by S^{-1} we obtain for $\sigma(t)$, the following

$$\begin{bmatrix} \frac{G_1^2}{2G_o^2}(1-e^{-\frac{3}{2}\Gamma t}\cos 2G_o t) & \frac{G_1G_2}{2G_o^2}(1-e^{-\frac{3}{2}\Gamma t}\cos 2G_o t) & \frac{-iG_1}{2G_o}e^{-\frac{3}{2}\Gamma t}\sin 2G_o t \\ \frac{G_1G_2}{2G_o^2}(1-e^{-\frac{3}{2}\Gamma t}\cos 2G_o t) & \frac{G_2^2}{2G_o^2}(1-e^{-\frac{3}{2}\Gamma t}\cos 2G_o t) & \frac{-iG_2}{2G_o}e^{-\frac{3}{2}\Gamma t}\sin 2G_o t \\ \frac{iG_1}{2G_o}e^{-\frac{3}{2}\Gamma t}\sin 2G_o t & \frac{iG_2}{2G_o}e^{-\frac{3}{2}\Gamma t}\sin 2G_o t & \frac{1}{2}(1+e^{-\frac{3}{2}\Gamma t}\cos 2G_o t) \end{bmatrix}$$

(7.1.11)

which can be rewritten as

$$\sigma_{11}(t) = \frac{G_1^2}{G_o^2} f(t) \quad , \quad \sigma_{22}(t) = \frac{G_2^2}{G_o^2} f(t) \quad ,$$

$$\sigma_{12}(t) = \sigma_{21}(t) = \frac{G_1 G_2}{G_o^2} f(t) \quad , \qquad (7.1.12)$$

$$\sigma_{33}(t) = 1 - f(t) \quad ,$$

$$\sigma_{13}(t) = \sigma_{31}^*(t) = - \frac{iG_1}{2G_o} e^{-\frac{3}{2}\Gamma t} \sin (2G_o t)$$

and

$$\sigma_{23}(t) = \sigma_{32}^*(t) = - \frac{iG_2}{2G_o} e^{-\frac{3}{2}\Gamma t} \sin (2G_o t)$$

where the function f(t) is given by

$$f(t) = \tfrac{1}{2} [1 - e^{-\frac{3}{2}\Gamma t} \cos (2G_o t)]$$

$$f(o) = 0, \lim_{t \to \infty} f(t) = 1/2 \quad . \qquad (7.1.13)$$

From the above, it is clear that the density matrix of the system under steady state conditions will be

$$\sigma_{13} = \sigma_{31} = \sigma_{23} = \sigma_{32} = 0 \quad ,$$

$$\sigma_{33} = 1/2 \; ; \; \sigma_{11} = \frac{G_1^2}{2G_o^2} \quad , \quad \sigma_{22} = \frac{G_2^2}{2G_o^2} \quad , \qquad (7.1.14)$$

$$\sigma_{12} = \sigma_{21} = \frac{G_1 G_2}{2G_o^2} \quad .$$

Thus, from (7.1.14), we see that there is no coherence between the ground and excited levels. However, the reduced density matrix for the excited states alone could be written in a superposition form

$$\sigma^{ex} \longrightarrow |\psi\rangle \langle\psi| \qquad (7.1.15)$$

$$|\psi\rangle = \frac{G_1}{G_o}\sqrt{f(t)}\,|1\rangle + \frac{G_2}{G_o}\sqrt{f(t)}\,|2\rangle \qquad (7.1.16)$$

and thus the coherence between $|1\rangle$ and $|2\rangle$ depends on the relative magnitudes of the two fields and it is obvious that for $G_1 \sim G_2$, the coherence between the two excited states $|1\rangle$ and $|2\rangle$ is very strong.

In the above discussion, it was assumed that the excited levels $|1\rangle$ and $|2\rangle$ are well separated from each other so that the laser 1 does not interact with level $|2\rangle$ and laser 2 has no influence on level $|1\rangle$ i.e., the coupling of laser 1 (2) with level $|2\rangle$ ($|1\rangle$) was neglected. But when these levels $|1\rangle$ and $|2\rangle$ are very close to each other, these interactions can no longer be neglected. However, when such a situation arises, we need not excite the atomic system with two different lasers, instead it is sufficient to excite both the levels $|1\rangle$ and $|2\rangle$ with a single laser. But, for such a case the analytical

results are too complicated and a better understanding can be obtained by numerical computation. For comparison we have also carried out the numerical calculations on this model when only one laser is used for excitation of both the excited states $|1\rangle$ and $|2\rangle$. We present such a study in the next section.

7.2 Excited state coherences for a system excited with a single laser field

In this section, we consider a model where both the excited levels $|1\rangle$ and $|2\rangle$ are excited by a single broadband laser field. This laser may be resonant with the transition $|2\rangle \longrightarrow |3\rangle$, but will be off-resonant with the transition $|1\rangle \longrightarrow |3\rangle$ by an amount equal to ω_{12} which will be denoted by Δ. Since the excitation is usually done with a broadband laser, we have taken into account the laser fluctuations for the description of which we adopt the phase diffusion model[38] described in chapter III. This model results in a finite bandwidth γ_c of the pump laser. The equations of motion for the density matrix elements of such a system are given by

$$\dot{\bar{\sigma}}_{11} = i\alpha\,(\bar{\sigma}_{31} - \bar{\sigma}_{13}) - 2\gamma_1\,\bar{\sigma}_{11}\,,$$

$$\dot{\bar{\sigma}}_{22} = i\alpha\,(\bar{\sigma}_{32} - \bar{\sigma}_{23}) - 2\gamma_2\,\bar{\sigma}_{22}\,,$$

$$\dot{\bar{\sigma}}_{33} = -(\dot{\bar{\sigma}}_{11} + \dot{\bar{\sigma}}_{22}) ,$$

$$\dot{\bar{\sigma}}_{12} = i\alpha(\bar{\sigma}_{32} - \bar{\sigma}_{13}) - (\gamma_1+\gamma_2+i\Delta)\bar{\sigma}_{12} , \qquad (7.2.1)$$

$$\dot{\bar{\sigma}}_{13} = i\alpha(\bar{\sigma}_{33} - \bar{\sigma}_{11} - \bar{\sigma}_{12}) - (\gamma_1+\gamma_c+i\Delta)\bar{\sigma}_{13}$$

and

$$\dot{\bar{\sigma}}_{23} = i\alpha(\bar{\sigma}_{33} - \bar{\sigma}_{22} - \bar{\sigma}_{21}) - (\gamma_2+\gamma_c)\bar{\sigma}_{23} .$$

Here Δ is the detuning of the laser frequency, from the atomic frequency ω_{13}, which is equal to ω_{12} and α is the Rabi frequency of the transition. The density matrix elements in the '-' frame are related to the initial density matrix elements by

$$\bar{\sigma}_{12} = \sigma_{12} , \quad \bar{\sigma}_{13} = -\sigma_{13} e^{i(\phi(t)+\Omega t)}$$

$$\bar{\sigma}_{23} = \sigma_{23} e^{i(\phi(t)+\Omega t)} , \quad \bar{\sigma}_{ii} = \sigma_{ii} \qquad (7.2.2)$$

where $\phi(t)$ is the phase of the exciting laser.

Using the theory of the type developed in chapter III, we have evaluated the excited state population $\bar{\sigma}_{11}$ and the coherence $\bar{\sigma}_{12}$ (averaged over the ensemble of the temporal fluctuations of the laser), both for moderate fields and strong fields. The results for $\bar{\sigma}_{11}$ and $\bar{\sigma}_{12}$ are shown in Fig. 23. The imaginary part of $\bar{\sigma}_{12}$ (for the choice of parameters) is found to be rather small compared

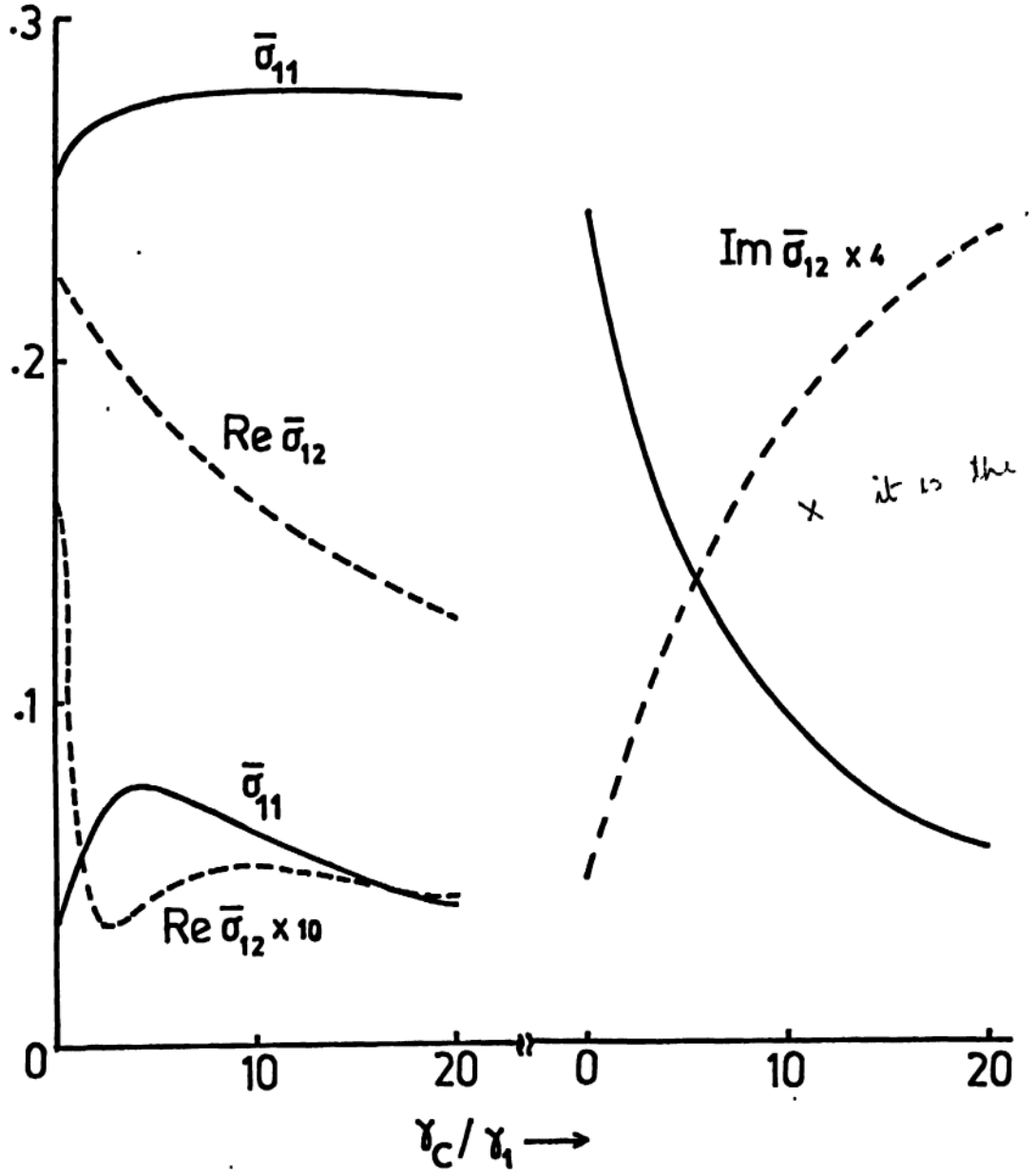

Fig.23 Excited state characteristics i.e. the variation of $\bar{\sigma}_{11}$, Re $\bar{\sigma}_{12}$ and Im $\bar{\sigma}_{12}$ as a function of the exciting laser bandwidth for both moderate and strong fields. The values of the parameters are $\Delta = 5\gamma_1$, $\gamma_2 = \gamma_1$, $|G_1| = |G_2| = \alpha = 10\gamma_1$ (solid curves) and $\alpha = \gamma_1$ (dashed curves)

to $\bar{\sigma}_{11}$. It however increases as the laser bandwidth γ_c increases. As mentioned earlier in the beginning of this chapter, the coherence $\bar{\sigma}_{12}$ is very small even in moderate fields $|G_1| = |G_2| = \alpha \sim \gamma_1$. We see that only in strong fields $\alpha >> \gamma_1$, the coherence is of the same order as the diagonal element $\bar{\sigma}_{11}$.

FOOT NOTES

1. Lord Rayleigh, Proc. Royal Soc. Lond. 102, 190 (1922).
2. R.W. Wood and A. Ellett, Phys. Rev. 24, 243 (1924).
3. R.W. Wood, Physical Optics, Macmillan, New York.
4. A.C.G. Mitchell and M.W. Zemansky, Resonance radiation and excited atoms, Cambridge University Press, London.
5. J. Brossel and A. Kastler, C.r. hebd. Séanc. Acad. Sci. Paris 229, 1213 (1949).
6. W. Hanle, Z. Phys. 30, 93 (1924); ibid. 35, 346 (1926).
7. B. Decomps, M. Dumont and M.Ducloy, in " Laser Spectroscopy" edited by H. Walther (Springer-Verlag, New York, 1976), Vol. 2, p. 283.
8. H. Walther in " Laser Spectroscopy" edited by H.Walther (Springer-Verlag, New York, 1976) Vol. 2, p. 1.
9. C.G. Carrington and A. Corney, Opt. Commun. 1, 115 (1969); J. Phys. B4, 849 (1971); C.G. Carrington, J. Phys. B5, 1572 (1972).
10. I. Colomb, M. Gorlicki and M. Dumont, Opt. Commun. 21, 289 (1977); M. Gorlicki and M. Dumont, Opt. Commun. 11, 166 (1974).
11. W. Rasmussen, R. Schieder and H. Walther, Opt. Commun. 12, 315 (1974).
12. D. Lecler, R. Ostermann, W. Lange and J. Luther, Jr. de Physique 36, 647 (1975).
13. S.J. Silvers and M.R. McKeever, Chem. Phys. 27, 27 (1978).
14. A. Corney, in " Atomic and Laser Spectroscopy" (Oxford University Press, 1977) chap. 15.

15. R.C. Hilborn and R.L. de Zafra, Jr., Opt. Soc. Am. 62, 1492 (1972).

16. P. Avan and C. Cohen Tannoudji, J. Phys. B10, 171 (1977).

17. C.G. Carrington and A. Corney, Opt. Commun. 7, 30 (1973); M. Ducloy, Opt. Commun. 8, 17 (1973).

18. J.N. Dodd and G.W. Series, Proc. Roy. Soc. Lond. 263, 353 (1961); J.N. Dodd, R.D. Kaul and D.M. Warrington, Proc. Phys. Soc. Lond. 84, 176 (1964).

19. A. Corney and G.W. Series, Proc. Phys. Soc. Lond. 83, 207 (1964); ibid. 83, 213 (1964).

20. B.P. Kibble and G.W. Series, Proc. Phys. Soc. Lond. 78, 70 (1961).

21. J.L. Picque, J. Phys. B11, L59 (1978).

22. A. Corney, J. Phys. B1, 458 (1968).

23. V.P. Kaftandjian, L. Klein, Phys. Lett. 62A, 317 (1977).

24. V.P. Kaftandjian, L. Klein and W. Hanle, ibid. 65A, 188 (1978).

25. C. Delsart, J.C. Keller and V.P. Kaftandjian, Proc. Fourth International Conference on Laser Spectroscopy (1979); edited by H. Walther and K.W. Rothe (Springer New York, 1979) p. 618.

26. V.S. Letokhov and V.P. Chebotayev, in "Nonlinear Laser Spectroscopy" (Springer-Verlag, New York, 1977) Sec. 4, Vol. 4, p. 169.

27. J.E. Bjorkholm and P.F. Liao, in "Laser Spectroscopy" edited by S. Haroche et al. (Springer-Verlag, New York, 1975), Vol. 43, p. 176.

28. S. Reynaud, M. Himbert, J. Dupont - Roc, H.H. Stroke and C. Cohen Tannoudji, Phys. Rev. Lett.42, 756 (1979).

C. Delsart, J.C. Keller and V.P. Kaftandjian, Opt. Commun. 32, 406 (1980).

V.P. Kaftandjian, C. Delsart and J.C. Keller, Phys. Rev. A23, 1365 (1981).

G.S. Agarwal in 'Springer Tracts in Modern Physics', edited by G. Höhler et al. (Springer-Verlag, New York, 1974) Sec. 6, Vol. 70.

F. Haake in 'Springer Tracts in Modern Physics', (Springer-Verlag, New York, 1973) Vol. 66, p. 98.

G.S. Agarwal in 'Progress in Optics', edited by E. Wolf (North-Holland, Amsterdam, 1973), Vol. 11, p. 1.

R.W. Zwanzig in 'Lectures in Theoretical Physics', edited by W.E. Brittin (John Wyley, New York 1961), Vol. III; Physica (33, 119) (1964).

M. Lax in 'Statistical Physics, Phase transitions and Superfluidity' edited by Chretien et al. (Gordon and Breach, New York 1968), Vol. 2, p. 269 ; Phys. Rev. 172, 350 (1968); H. Haken and W. Weidlich, Z. Physik 205, 96 (1967).

N.N. Bogoliubov and J.A. Mitropolsky, in 'Asymptotic methods in the theory of non-linear oscillations' (Hindustan Publishing Co., Delhi, 1961), Chap. 5.

Reference 31, Appendix A.

G.S. Agarwal, Phys. Rev. A18, 1490 (1978); and the references cited therein.

G.S. Agarwal, Phys. Rev. A1, 1445 (1970).

P. Anantha Lakshmi and G.S. Agarwal, Phys. Rev. A23, 2553 (1981).

P. Anantha Lakshmi and G.S. Agarwal, Phys. Rev. A25, 3379 (1982).

C. Mavroyannis, Opt.Commun. 29, 80 (1979).

G.S. Agarwal and S.S. Jha, J. Phys. B12, 2655 (1979).

C. Cohen Tannoudji and S. Reynaud, ibid. 10, 345, 2511 (1977).

J. Cooper, R.J. Ballagh and K. Burnett, Phys. Rev. A22, 535 (1980).

R. Kornblith and J.H. Eberly, J. Phys. B11, 1545 (1978).

B.R. Mollow, Phys. Rev. 188, 1969 (1969); Phys. Rev. A12, 1919 (1975).

G.S. Agarwal, Z. Physik B33, 111 (1979).

G.S. Agarwal, Phys. Rev. Lett. 37, 1383 (1976).

J.H. Eberly, Phys. Rev. Lett. 37, 1387 (1976); in 'Laser Spectroscopy IV' edited by H. Walther and K.W. Rothe (Springer 1979), p. 80.

P.Zoller, J. Phys. B10, L321 (1977); ibid. 11, 805 (1978).

P. Avan and C. Cohen Tannoudji, J. Phys. B10, 155 (1977).

R. Bonifacio and L.A. Lugiato, Opt. Commun. 19, 172 (1976); Phys. Rev. A18, 1129 (1978) and the references therein.

H.M. Gibbs, S.L. McCall and T.N.C. Venkatesan, Phys. Rev. Lett. 36, 1135 (1976).

G.S. Agarwal, L.M. Narducci, R. Gilmore, D.H. Feng, Phys. Rev. A18, 620 (1978) and the references therein ; L.M. Narducci, R. Gilmore, D.H. Feng and G.S. Agarwal, Opt. Lett. 4, 88 (1978).

G.S. Agarwal, L.M. Narducci, D.H. Feng and R. Gilmore, 'Coherence and Quantum Optics IV' edited by L. Mandel and E. Wolf,(Plenum Publishing Co., New York 1978) p. 281.

G.S. Agarwal, A.C. Brown, L.M. Narducci and G. Vetri, Phys. Rev. A15, 1613 (1977).

A. Schenzle and H. Brand, Opt. Commun. 31, 401 (1979).

K.G. Weyer, H. Wiedermann, M. Rateike, W.R. Mac Gillivray, P. Meystre and H. Walther, Opt. Commun. 37, 426 (1981).

D.E. Grant and H.J. Kimble, Opt. Lett. 7, 353 (1982); Opt. Commun. 44, 415 (1983).

A. Giacobino, M. Devaud, F. Biraben and G. Grynberg, Phys. Rev. Lett. 45, 434 (1980).

G.S. Agarwal, Opt. Commun. 35, 149 (1980).

A. Flusberg, M. Mossberg and S.R. Hartmann, 'Coherence and Quantum Optics IV', edited by L. Mandel and E. Wolf, (Plenum Publishing Co., New York 1978) p. 695.

D.F. Walls, P. Zoller and M.L. Steÿn-Ross, IEEE Jr. Qntm. Elec. V.QE-17, 380 (1981).

C. Parigger, P. Zoller and D.F. Walls, Opt. Commun. 44, 213 (1983).

F.T. Arecchi, J. Kurmann and A. Politi, Opt. Commun. 44, 421 (1983).

D.F. Walls and P. Zoller, Opt. Commun. 34, 260 (1980).

M. Kitano, T. Yabuzaki and T. Ugawa, Phys. Rev. Lett. 46, 926 (1981).

D.F. Walls and P. Zoller, Phys. Rev. Lett. 47, 709 (1981).

D.F. Walls and G.T. Milburn in 'Quantum Optics and Experimental General Relativity', Lectures at the NATO Summer School, Bad Windsheim (to be published).

W. Becker, M.O. Scully and M.S. Zubairy, Phys. Rev. Lett. 48, 475 (1982).

H.P. Yuen, Phys. Rev. A13, 2226 (1976); H.P. Yuen and J.H. Shapiro, Opt. Lett. 4, 334 (1979).

C.M. Caves, K.S. Thorne, P.W.P. Drever, V.D. Sandberg and M. Zimmermann, Rev. Mod. Phys. 52, 341 (1980).

A.P. Kazantsev,V.S. Smirnov and V.P. Sokolov, Opt. Commun. 35, 209 (1980); A.P. Kazantsev, V.S. Smirnov V.P. Sokolov and A.W. Tumaikin, Appl. Phys. B27, 83 (1982).

L. Mandel, Phys. Rev. Lett. 49, 136 (1982).

G.S. Agarwal, 'Quantum Optics', Springer Tracts in Modern Physics, Vol. 70, edited by G. Höhler (Springer-Verlag, Berlin 1974) chap. 18.

When no mixing with coherent radiation is considered, then S(T) for the radiation scattered by a two-level atom has been calculated by L. Mandel, Opt. Lett. 4, 205 (1979).

D.F. Walls, G.J. Milburn and H.J. Carmichael, Optica Acta 29, 1179 (1982).

H.P. Silvermann, S. Haroche and M. Griss, Phys. Rev. A18, 1507, 1517 (1978).

W.W. Chow, M.O. Scully and J.O. Stoner, Phys. Rev. A11, 1380 (1975).

R.M. Hermann, H. Grotch, R. Kornblith and J.H. Eberly, Phys. Rev. A11, 1389 (1975).

G.S. Agarwal, Phys. Rev. A15, 2380 (1977).

S. Haroche, J.A. Paisner and A.L. Schawlow, Phys. Rev. Lett. 30, 948 (1973).

T.W. Ducas, M.G. Littman and M.L. Zimmermann, Phys. Rev. Lett. 35, 1752 (1975).

W. Lange and J. Mlynek, Phys. Rev. Lett. 40, 1373 (1978).

S. Haroche in 'Laser Spectroscopy of atoms and molecules', edited by H. Walther (Springer - Verlag, Berlin, 1976) p. 253.

It would perhaps be interesting to study the optical Hanle signals with the pump laser off the resonance frequency corresponding to the J=0 to J=1 transition. The magnetic field Hanle signals in this situation for zero bandwidth of the field have been reported by P. Avan and C. Cohen Tannoudji [J. de Physique Lettres 36, L85 (1975)].

M. Ducloy, Phys. Rev. A8, 1844 (1973); ibid. A9 1319 (1973).

P. Anantha Lakshmi and G.S. Agarwal, Phys. Rev. A (in press).

R. Brewer and E.L. Hahn, Phys. Rev. A11, 1641 (1975).

K. Shimoda, Z. Phys. 234, 293 (1970).

D.F. Walls, Z. Phys. 244, 117 (1971).